A Study of Air Flow Effects on the Cushioning Characteristics of Multi Layered Pre-Compressed Fibreboard

Mervyn W Minett

2006

A thesis submitted in fulfillment of the requirement of the Degree of Doctor of Philosophy

School of Architectural, Civil and Mechanical Engineering

Victoria University

Melbourne, Australia

Student Declaration

"I, Mervyn W Minett, declare that the PHD thesis entitled A Study of Air Flow Effects on the Cushioning Characteristics of Multi Layered Pre-Compressed Fibreboard is no more than 100,000 words in length, exclusive of tables, figures, appendices, references and footnotes. This thesis contains no material that has been submitted previously, in whole or in part, for the award of any other academic degree or diploma. Except where otherwise indicated, this thesis is my own work".

Signature Date 8 - 12 - 2005

Acknowledgements

The author would like to acknowledge guidance and encouragement given by his principal supervisor Dr Michael Sek during the course of the research culminating in this thesis.

The author would also like to acknowledge the following:
Mr Vincent Rouillard for his technical help and advice
Dr Jun-de Li for assistance in model development
My co-supervisor Dr Danh Tran for his help and encouragement
Dr G Lleonart for his advice and encouragement
Mr Laslo Knovacs for his help in electronics
Technical staff of the School Architectural Civil and Mechanical Engineering, for their assistance.
Successive HOS of the School Architectural, Civil and Mechanical Engineering for their help from a workload prospective

I would sincerely like to thank my wife Pauline for her patience and encouragement sometimes under trying circumstances for which I will always appreciate.

Abstract

Multi-layered corrugated fibreboard, has in recent years been gaining attention as a replacement for polymeric materials for protective packaging for environmental reasons. The properties of pre-compressed multi-layered corrugated fibreboard make it a sustainable replacement for poly-foam and polystyrene. Pre-compressed multi-layered fibreboard cushions have most of the structural resistance and damping removed, and the properties of air-flow through the flutes becomes a more predominant, they behave more like a soft spring.

Artificially restricting the exiting airflow or prudently choosing the direction of flutes in the case of rectangular cushions, allows for the differing design situations that may be required. A mathematical model is developed, to describe the pre-compressing process. Mathematical models and software are developed, based on the airflow characteristics, that allow for the prediction of peak acceleration for differing end conditions or sizes providing the friction component can be estimated using iterative methods.

The models were verified by a static compression test for the pre-compression and by dropping a mass, or platen and recording the resistive acceleration, or dynamic behaviour, over a time range.

There exists an acceleration component prior to platen contact, which is also modelled and should be considered in the interpretation of test results. The study has presented three models to allow for the prediction of the behaviour of multi-layered corrugated fibreboard for the use as protective cushions. The main thrust has been the behaviour of the airflow during and prior to impact whilst testing. The models developed will assist in the design of protective packaging and produce predictive tools for the use in the packaging industry.

List of Abbreviations

Static and Pre-Compression

k = cushion stiffness (k/m)
δ = deflection (m)
F = instantaneous force (N)
F_m = mean force (N)
F_a = alternating force (N)
SF = slope factor
N = the number of cushion layers
y = displacement record (m)
ε = strain - ratio of deflection to unloaded thickness
ε_0 = maximum strain
b = multiplier in equation (3.2)

Air-Flow Models

a = platen total acceleration (m/sec^2)
F = forcing function (N)
IF = impact factor
h = platen-cushion air space (m)
$\dot{h}$ = platen velocity (m/sec)
$\ddot{h}$ = platen acceleration (m/sec^2)
k = cushion static stiffness (N/m)
m = platen mass (kg)
D = cushion width (m)
L = the flute length (m)
h_t = cushion height at time t (m)
A_t = exit area of cushion cross section at time t (m^2)
F_f = frictional resisting force (N)
P_0 = average air pressure (kPa)
P_x = air pressure at point x (k)Pa
ρ = air density (kg/m^3)

A Study of Air Flow Effects on the Cushioning Characteristics of Multi Layered Pre-Compressed Fibreboard

Table of Contents

Chapter 1 Introduction

Traditionally package cushioning has been manufactured from Polymeric materials such as expanded polystyrene or polyurethane. In recent years the environmental impact of using polymeric materials for protective cushions has stimulated interest in a replacement. It is a common occurence to use corrugated fibreboard for the construction of shipping and storage containers, however it is also gaining attention as an alternative to the polymeric materials for protective cushions. It has some major advantages when compared with some of the traditional materials such as polymeric foams, these include its ability to be easily recycled, and it has a significantly lower cost on a volume basis.

Expanded polystyrene is a typical closed cell material where polyurethane and polyethylene can be open or closed cell. Closed cell materials allow air to be trapped during impact having a different effect to that of an open cell material. Closed cell increases the pressure effect and sharp resistance to impact occurs, whereas open cell materials allow passages for air to escape during impact thus causing a steady resistance to impact. Multi-layered corrugated fibreboard cushions can be likened to open cell materials in the sense their ends are opened such that the air can flow (exhausted) during impact. If the ends were closed then they would behave in a similar manner to closed cell materials.

Regardless of the material being used, protective cushions are required to protect goods against shock and vibration. It is therefore necessary to possess an understanding of how their underlying physical properties behave under the conditions of shock loading and vibration. This is the basis for testing of materials in the sense that they are subjected to impact loading in special purpose cushion and vibration testing machines to replicate the real life situation. Figure 1.1 shows a typical cushion-testing machine.

It has been generally accepted that the shock absorbing performance information for cushioning materials be presented as curves or graphs of deceleration versus static loads. The standard ASTM D 1596 *Standard Test Method for Shock Absorbing Characteristics of Package Cushioning Materials* was developed for materials of a high degree of compressibility and bulk recovery. The method requires an extensive test program based on a mass that is dropped from a given height and the peak acceleration measured for a sample of cushioning material. The aim is to determine the effect of static load and the drop height on the level of shock to which the mass is subjected. By either changing the mass and the cushion area the value of the static load can be varied.

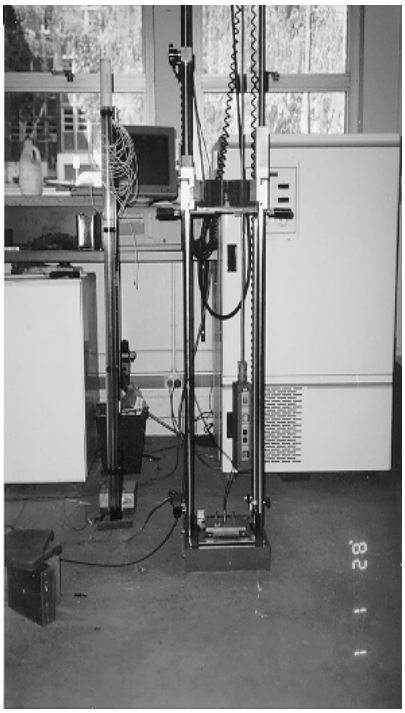

Figure 1.1 Lansmont Cushion Testing Machine

The shock absorbing characteristics, or peak accelerations plotted against static loads, are presented as a family of 'performance cushion curves' produced by curve fitting

techniques from experimental data. These curves require a large number of data points and as a consequence this method is very time consuming and costly. For corrugated fibreboard, each test is destructive the number of samples required is also a major cost associated with this test procedure.

Victoria University (VU) in Melbourne has been actively involved in research on the application of corrugated fibreboard as cushioning materials for several years. The main focus has been on the shock attenuation or cushioning characteristics and methods to produce cushion curves using simple compression data and to understand the physical behaviour of multi-layered corrugated fibreboard protective cushions. This work began as a collaborative research project between VU and AMCOR Research and Technology Centre funded by the Australian Research Council.

The literature is reviewed in chapter 2 and is divided into two parts, the current research into the simplification of determining of peak accelerations and the nature of the transient effects of corrugated fibreboard. The concept of pre-compressed multi-layered corrugated fibreboard is introduced as a replacement for poly-foam materials. A hypothesis is presented, that suggests that the acceleration of multi-layered corrugated fibreboard protective cushion when tested is influenced by the flow of air through the flutes.

In chapter 3 a model is developed to describe how the acceleration is affected by the flow of air through the flutes of multi-layered corrugated fibreboard with experimental work in chapter 4 verifying the model.

The work presented in chapter 5 is a result of some unexpected results from the experimental work in chapter 4. There appears to be a pre-contact acceleration component during normal cushion testing. This chapter shows the development of a model to describe these phenomena with experimental work in chapter 6 verifying the model.

Conclusions and summarising remarks are presented in chapter 7. Extensive software has been written to perform the analysis of the experimental work and to test the models. This software written in the Matlab® environment and consists of a combination of m file scripts and Simulink® models. This software is presented in the appendices A and B.

Chapter 2 Protective Packaging

2.1 Protective Cushion Requirements

Like all materials to use multi-layered corrugated fibreboard as a cushioning material performance cushion curves or alternative information is required. The lack of cushion curves and other relevant characteristics for corrugated fibreboard has hampered its optimum use as a replacement material for polymeric materials. There has however, been a more active participation in research into the application of corrugated fibreboard as cushioning materials recently as materials that can be recycled are becoming a material of choice. The research has been concentrating on the dynamic effects when testing both virgin and pre-compressed multi-layered corrugated fibreboard to be used as a cushioning material. Although in the subsequent discussion there is reference to other materials, the intent is to concentrate on corrugated fibreboard.

2.1.1 Standard Performance Requirements for Protective Cushions

Before discussing the literature on the behaviour of corrugated fibreboard it is virtuous to review the current cushion testing methods. It has been generally accepted that the shock absorbing performance information for cushioning materials be presented as curves or graphs of deceleration versus static loads. The standard ASTM D 1596 *Standard Test Method for Shock Absorbing Characteristics of Package Cushioning Materials* was developed for materials of a high degree of compressibility and bulk recovery. The method requires an extensive test program based on a mass **m** that is dropped from a height **h** and the peak acceleration, or more correctly de-acceleration, measured for a sample of cushioning material of area **A** as shown in Figure 2.1. The aim is to determine the effect of static load and the drop height on the level of shock to which the mass is subjected. This method is designed to

replicate the event of a package falling to a surface and to determine whether the cushion protects the package content. The static load is obtained from equation (2.1)

$$\sigma_0 = \frac{mg}{A} \qquad (2.1)$$

By either changing the mass **m** the area **A** the value of the static load $\boldsymbol{\sigma_0}$ can be varied.

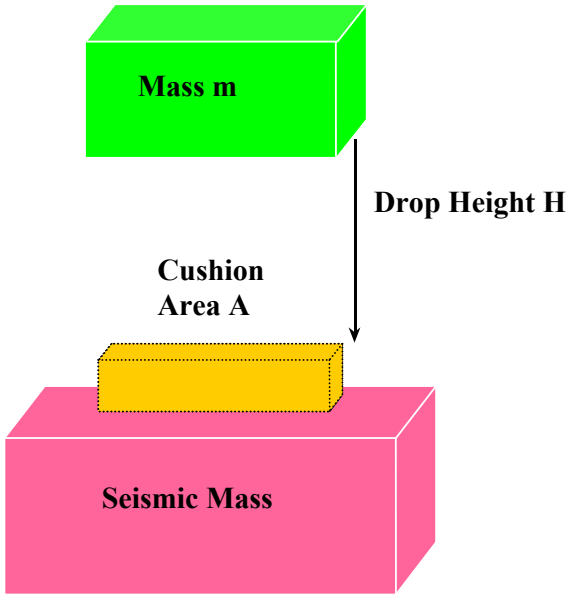

Figure 2.1 Standard Testing procedure

The shock absorbing characteristics of the material being tested, are presented as a family of 'performance cushion curves' in which the experimental peak accelerations during impact are plotted for a range of static loads for several drop heights. The curves are typically produced from the experimental data, using curve-fitting techniques. These curves require a large number of data points and as a consequence this method is a very time consuming and costly methodology and considerable inaccuracy in methods in construction of cushion curves from discrete experimental data have been a major difficulty. For corrugated fibreboard, each test is destructive so the number of samples required is also a major cost associated with this test procedure.

2.1.2 Simplification of the Determining Cushion Performance Data

There have been numerous attempts to describe the performance of cushioning materials, Woolam (1968) used research based on earlier work by Soper and Dove (1961) to study the dynamics of low energy cushioning materials. A scaling technique was developed that enabled large packaged items to be modeled and tested to determine the dynamic performance under shock loading.

More recently there have been many attempts to simplify the process of obtaining performance cushion curves or cushion data and some are presented here:
Wiskida and McDaniel (1980) proposed a complicated curve fitting equation to obtain de-acceleration G by linking the thickness T, drop height h and static load σ_o, and comprising 15 coefficients C_n.

$$
\begin{aligned}
G = {} & C_1 \frac{1}{\sqrt{T}} + C_2 \frac{1}{\sqrt{T}} \ln(\sigma_o - 0.145) + C_3 \frac{1}{\sqrt{T}} \left(\ln(\sigma_o - 0.145)\right)^2 + \\
& + C_4 \sqrt{h} \frac{1}{\sqrt{T^3}} + C_5 \sqrt{h} \frac{1}{\sqrt{T^3}} \ln(\sigma_o - 0.145) + C_6 \sqrt{h} \frac{1}{\sqrt{T^3}} \left(\ln(\sigma_o - 0.145)\right)^2 + \\
& + C_7 \sqrt{h} \frac{1}{\sqrt{T}} + C_8 \sqrt{h} \frac{1}{\sqrt{T}} \ln(\sigma_o - 0.145) + C_9 \sqrt{h} \frac{1}{\sqrt{T}} \left(\ln(\sigma_o - 0.145)\right)^2 + \\
& + C_{10} \frac{1}{\sqrt{T^3}} + C_{11} \frac{1}{\sqrt{T^3}} \ln(\sigma_o - 0.145) + C_{12} \frac{1}{\sqrt{T^3}} \left(\ln(\sigma_o - 0.145)\right)^2 + \\
& + C_{13} + C_{14} \ln(\sigma_o - 0.145) + C_{15} \left(\ln(\sigma_o - 0.145)\right)^2
\end{aligned}
\qquad \textbf{(2.2)}
$$

Henriksson (1994) used fourth order polynomials (five coefficients) with some but arguable effect. Teragashi et al (1993), Thakur and McDougall (1996) have proposed methods of simplifying the testing procedure for polymeric materials.

Ansorge and Nendel (1998) investigated a method of pre-calculating cushion curves by developing a system of equations from the conservation of energy and material laws. The results of these developments were compared with measured values of peak acceleration versus static loads. They used a Kelvin model to describe the material properties. They had limited success in predicting peak accelerations in open cell materials.

Burgess (1994) reiterated from a previous paper and research by Wenger (1994) demonstrated a method of generating cushion curves of polymeric materials based on knowing the dynamic stress and the energy density information which are determined by equations (2.3) and (2.4).

$$\text{Energy Density} = \frac{\text{Static Stress} \times \text{Drop height}}{\text{Cushion Thickness}} \qquad (2.3)$$

$$\text{Dynamic Stress} = \text{Peak Acceleration} \times \text{Static Stress} \qquad (2.4)$$

With this method a curve of dynamic stress determined using the measured peak accelerations taken from a small number of cushion tests, versus energy density, can be plotted. Peak acceleration values can be then interpolated or extrapolated for various energy densities. The author improved this method so the energy density information can be determined from a single cushion test using an accelerometer to measure acceleration. This was achieved by integrating the cushion curve over a time period (area under the curve) to obtain the velocity change Δv. The energy absorbed by the cushion is the change in kinetic energy, which can be obtained from the well-known energy equation.

$$KE = \frac{1}{2}mv^2$$

where

m = mass

v = velocity (2.5)

The initial impact velocity can be found by using

$$v_i = \sqrt{2gh}$$

where

v_i = the initial velocity

h = drop height

g = gravitational constant of acceleration (2.6)

Using the above equations the energy absorbed by the cushion would be

$$\text{Energy Density} = \frac{\sigma_0}{2gt}\Delta v\left(2v_i - \Delta v\right)$$

where

σ_0 = static stress

Δv = change in velocity

v_i = impact velocity

t = material thickness

g = gravitational constant of acceleration (2.7)

The dynamic stress at peak acceleration can then be determined by the use of equation (2.4). The author concluded that the methods proposed for determining peak accelerations and velocity were reasonably accurate when compared with the standard testing procedure. The author conceded that filtering required to eliminate noise during cushion testing could lead to inaccuracies in some cases. However this work leads to the thought that accelerated tests could result in considerable savings in testing time and costs, but still obtain appropriate accuracy.

Sek and Kirkpatrick (1996, 1997) investigated a relation between compression characteristics of corrugated fibreboard obtained during the static or quasi-dynamic compression (constant rate of deflection) and its behaviour under shock conditions. A property called the "dynamic factor" was proposed which showed that a single coefficient (factor) was sufficient to produce a family of cushion curves from static or quasi-dynamic data. In general, the dynamic factor can be a function of many variables caused by dynamic effects such as gas flow and compression, structural damping and buckling. According to the standard ASTM D 1596-91 a material increases its deformation when subjected to impact loading and can be described by equation (2.8).

$$m\ddot{x} - F(x, \dot{x}) = 0$$

and

$$m = \frac{\sigma_o A}{g}$$

where

m = mass

$F(x, \dot{x})$ = the dynamic loading during impact (2.8)

$x, \dot{x}, \ddot{x}$ = the instantaneous deflection, velocity and acceleration respectively

σ_o = the static loading or dead weight stress

A = the cushion contact area

g = the gravitational constant of acceleration

A part of the force F is static compression, which is a function of deflection and the remainder is due to the transient nature of dynamic effects. Therefore equation (2.8) can be broken up into two parts:

$$F = F_s + F_d$$

where

F_s = the static compression component (2.9)

F_d = the transient component

therefore using equation

$$F_d = m\ddot{x} - F_s$$

The authors used these equations to investigate the comparison of transient dynamics to static compression on a large number of shock pulses from tests on multi-layered corrugated fibreboard cushions. A typical example is shown in Figure 2.2.

The shock pulse has been converted to load in terms of deflection and velocity to make the comparison with static compression data, although there are significant fluctuations making the trend harder to detect.

The authors investigated this further by subjecting cushions to pseudo-dynamic compression tests in a dynamic universal testing machine (Instron). The deflection rate was ramped up at increasing values. The deflection rate was applied as a ramp up to rate varying from 1mm/sec to 1m/sec. Typical results with a least squares linear fit of the force versus deflection for various compression rates is shown in Figure 2.3. The force levels are greater as the deflection rate increases. In other words, the compression force increases as the ramping speed increases. It was hypothesized that the peak accelerations could be approximated by multiplying the static compression data with a property termed the dynamic-factor, which is shown in terms of the ramping velocity in Figure 2.4.

The method however required a set of data from quasi-dynamic compression tests under various high deflection rates. A drawback of that approach was that a dynamic compression-testing machine was required to determine cushion curves.

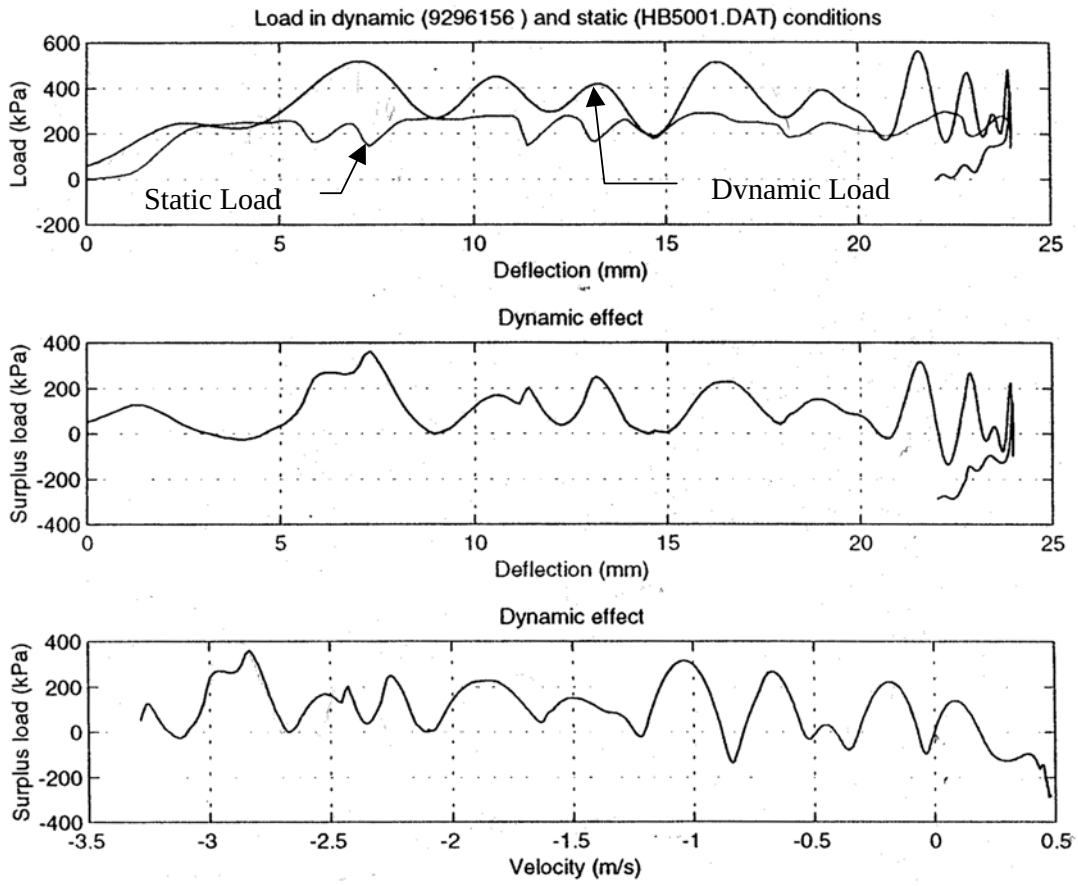

Figure 2.2 Comparison of static compression and transient data from cushion tests on a 50mm thick multi-layered fibreboard cushion using B-flute with a drop height 600mm. The first graph shows dynamic loading versus static loading. The subsequent graphs show the differences between dynamic and static.

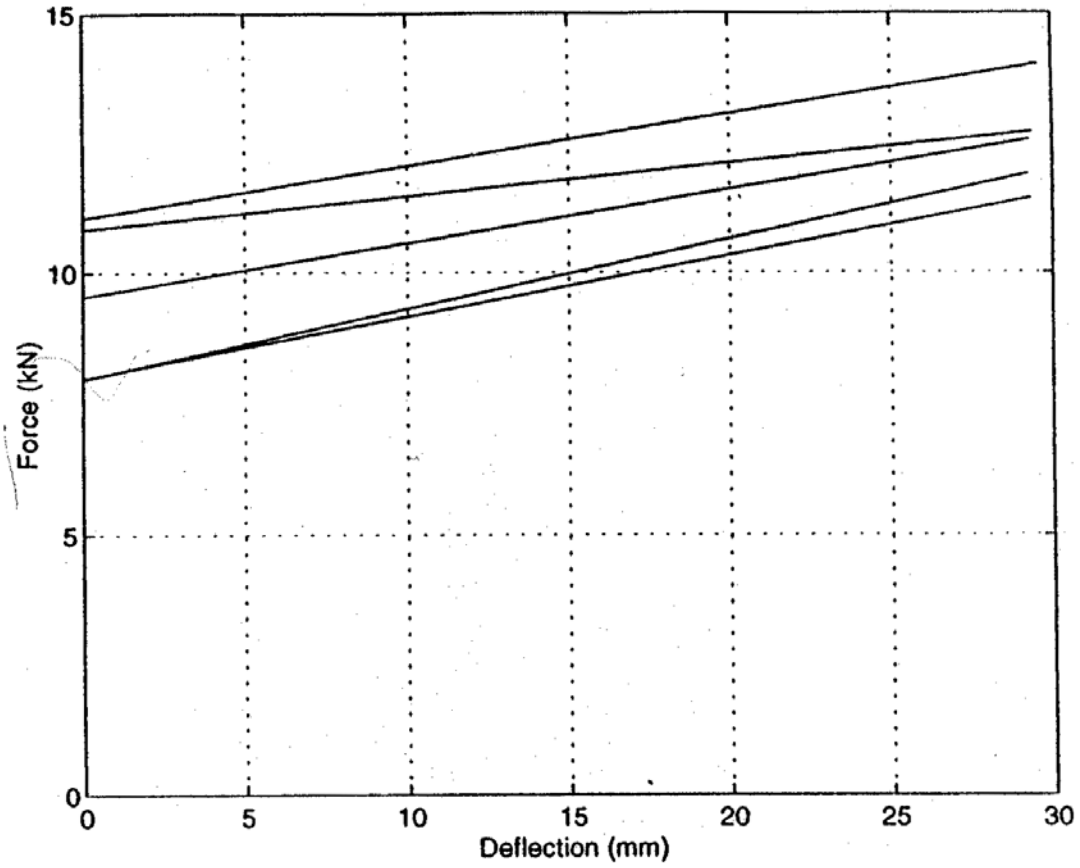

Figure 2.3 Effect of deflection rate on quasi-dynamic compression

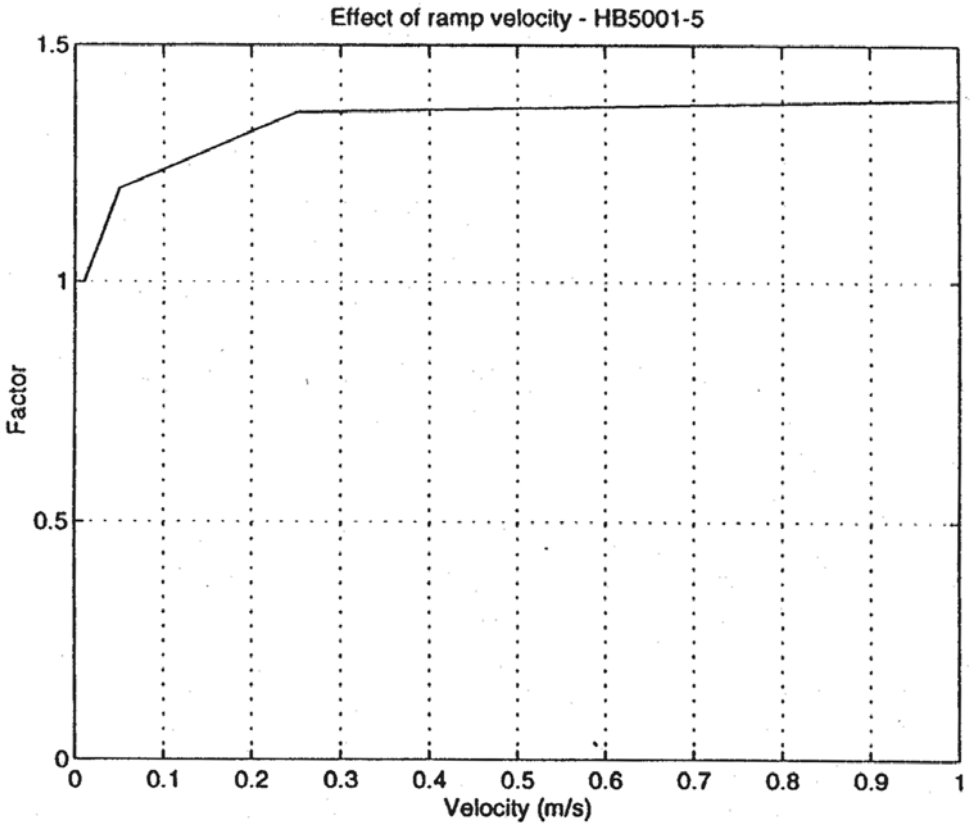

Figure 2.4 Dynamic Factor as a function of the deflection rate

Sek, *et al.* (2000) further investigated the dynamic effect of cushioning materials namely, expanded polystyrene, expanded polyurethane and multi layered corrugated fibreboard, and refined the 'dynamic factor' method.

As stated in equations (2.8) and (2.9) for any given deflection during impact the instantaneous resistive force produced by the cushioning material will have two components, one being that which would be present under static compression, F_s, and one that is attributed to transient nature and high velocity of impact, F_d. The total resistive force gives an acceleration $\ddot{x}$ of the mass m, as in equation (2.10).

$$m\ddot{x} - \left[F_s(x) + F_d(x, \dot{x}) \right] = 0 \qquad (2.10)$$

Dividing by the cushion area A yields:

$$\frac{\sigma_o}{g}\ddot{x} - \left[\sigma_s(x) + \sigma_d(x, \dot{x}) \right] = 0 \qquad (2.11)$$

Where the terms in the square bracket describe the total stress (dynamic stress) during impact. Extracting the static stress:

$$\frac{\sigma_o}{g}\ddot{x} - \left[1 + \frac{\sigma_d(x, \dot{x})}{\sigma_s(x)} \right] \sigma_s(x) = 0$$

Hence

$$\frac{\sigma_o}{g}\ddot{x} - c\sigma_s(x) = 0 \qquad (2.12)$$

where $\quad c = \left[1 + \frac{\sigma_d(x, \dot{x})}{\sigma_s(x)} \right]$

Equation (2.12) demonstrates that the dynamic effect can be accounted for by a function c named ‘dynamic factor function’. Taking the c as being constant produces a sufficiently accurate estimate of the dynamic stress giving particularly for corrugated fibreboard:

$$\sigma_d(x, \dot{x}) \approx c\,\sigma_s(x) \qquad (2.13)$$

Experimentally the dynamic factor can be found as the ratio of the dynamic stress to that of the static stress such that by multiplying the static stress by the factor the total stress can be obtained.

The authors developed a simple procedure to determine the dynamic factor by overlaying the equivalent stress-deflection or dynamic stress calculated from the acceleration pulse measured during an impact test onto the static stress measured from a compression test. They demonstrated this method for expanded polystyrene and polyurethane foam. The results for expanded polyurethane foam is shown in Figure 2.5.

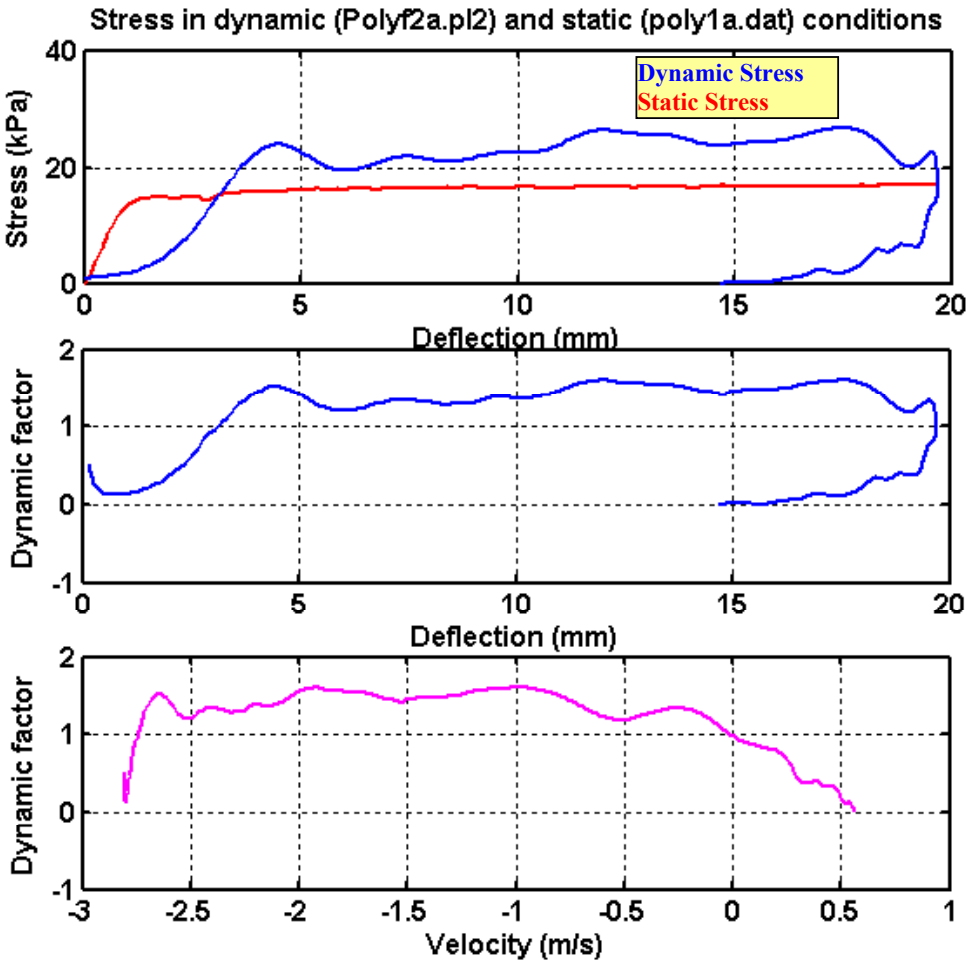

Figure 2.5 Dynamic to Compressive Stress and Dynamic effect for Expanded Poly-Urethane (EPU)

One important observation for EPU shown in Figure 2.5 is that with respect to deflection the dynamic factor can be considered constant for most deflections, (4 – 18 mm). This may lead to reasonable estimates of relationships between the dynamic and static properties. This would be more difficult to determine for multi-layered virgin corrugated fibreboard cushions due the layer collapsing mechanism. Figure 2.6 shows the dynamic and static conditions for a typical multi-layered virgin corrugated fibreboard cushion with the material specifications for this test is shown in Table 2-1. It can be seen that there are fluctuations in the curves that suggest sudden drops in the resistive force a phenomenon that is discussed fully in section 2.2.2.

Table 2-1 Specifications for a Typical Static-Dynamic Cushion Test

Material	Virgin Corrugated Fibreboard
Flute Type	B Type Flute
Cushion Size	100 x 100 mm
Thickness	50 mm
Conditioning	50% Relative Humidity
Temperature	20^{o} C
Static Load	14.2 kPa
Drop Height	600 mm

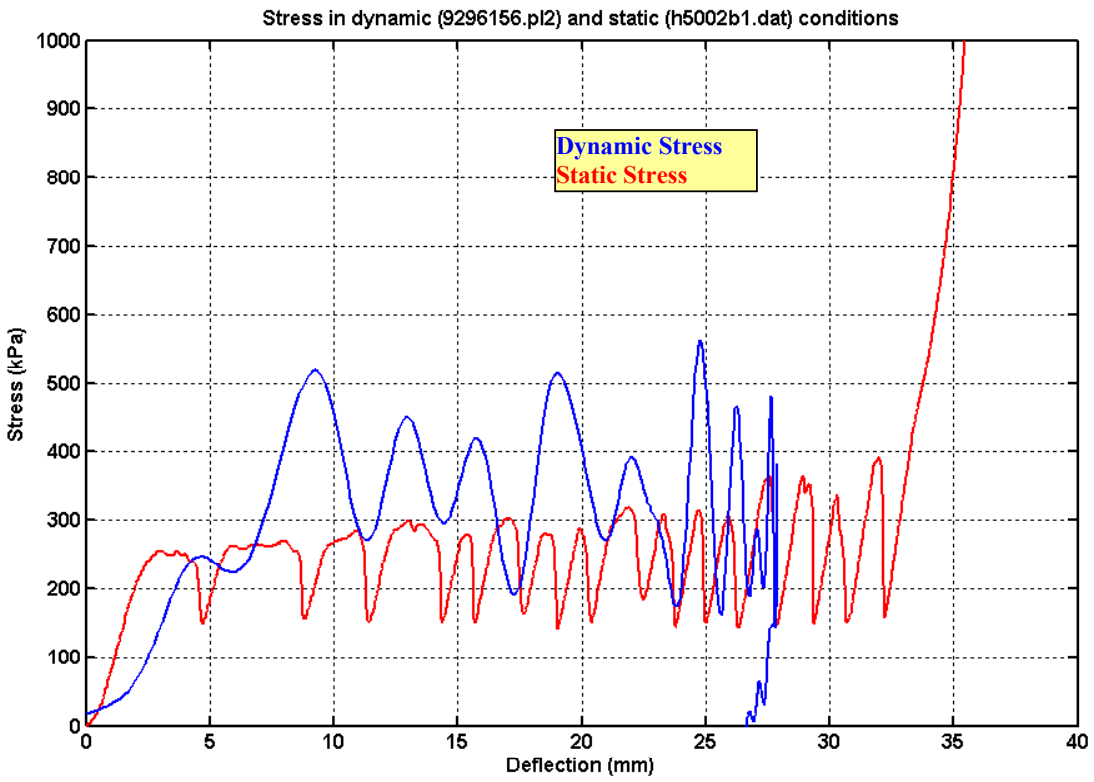

Figure 2.6 Overlayed Dynamic to Static Stress to Deflection for Corrugated Fibreboard the red curve being the the static compression and the blue curve the dynamic compression

2.1.3 Prediction of Peak Acceleration

Sek, *et al.* (2000) suggested that if the dynamic factor function is known, an estimate of the peak acceleration in an impact can be predicted from the corrected compression data and the deformation energy that is the kinetic energy of the mass m dropped from the height h. Considering the potential energy of the mass m at the drop height h, which by the laws of physics can be equated to the kinetic energy of the mass equation (2.14) was devised

$$\begin{aligned} &mgh = \sigma_o Ah \\ &\text{as} \\ &m = \frac{\sigma_o A}{g} \quad \text{from equation 2.1} \end{aligned} \tag{2.14}$$

The kinetic energy is also equal to the deformation energy represented by the area under the compression curve (neglecting other energy losses):

$$\begin{aligned} \text{Energy of deformation} &= \int_0^{x_{max}} F(x, \dot{x})\, dx \\ &= A \int_0^{x_{max}} \sigma(x, \dot{x})\, dx \end{aligned} \tag{2.15}$$

Equating (2.14) and (2.15) yielded

$$\int_0^{x_{max}} \sigma(x, \dot{x})\, dx = \sigma_o h \tag{2.16}$$

By introducing the dynamic factor the following equation can be used to determine the maximum deflection x_{max} during an impact:

$$\int_0^{x_{max}} c\,\sigma_s(x)\, dx \approx \sigma_o h \tag{2.17}$$

This maximum deflection is mapped on the compression data. The peak acceleration a_{max} occurs at the deflection for which the compression force/stress is the highest in the domain <0, x_{max}>. It is illustrated clearly in the enlarged section of the compression data for corrugated fibreboard as shown in Figure 2.7.

$$\ddot{x}_{max} = \frac{\max(F) \in x\left(0, x_{max}\right)}{m} = \frac{\max(\sigma) \in x\left(0, x_{max}\right)}{\sigma_o} g \qquad (2.18)$$

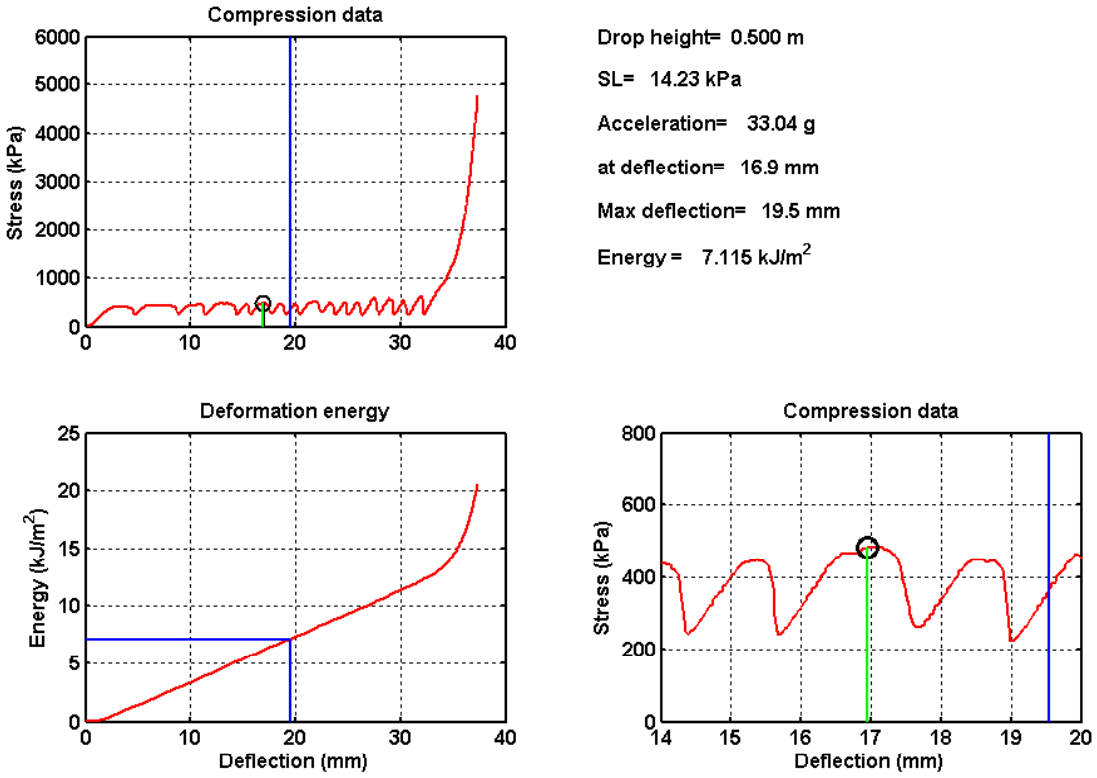

Figure 2.7 Prediction of peak acceleration from compression data for corrugated fibreboard

They also presented an algorithm for the iterative least squares optimization of the dynamic effect and the production of cushion curves from the static compression and dynamic characteristics. The algorithm for this method is shown Figure 2.8 and the results from a typical data set shown in Figure 2.9. With this method the discrepancies between predicted and experimental peak acceleration values are minimized

The discussion so far has developed methods to determine peak accelerations and cushion curves from a minimum number of experimental impact tests, which is generally all that is required. However aspects of the nature of how the material reacts to impact and what other influences affect the static and dynamic behaviour of multi-layered corrugated fibreboard is of interest, this will be the topic of discussion in the next section.

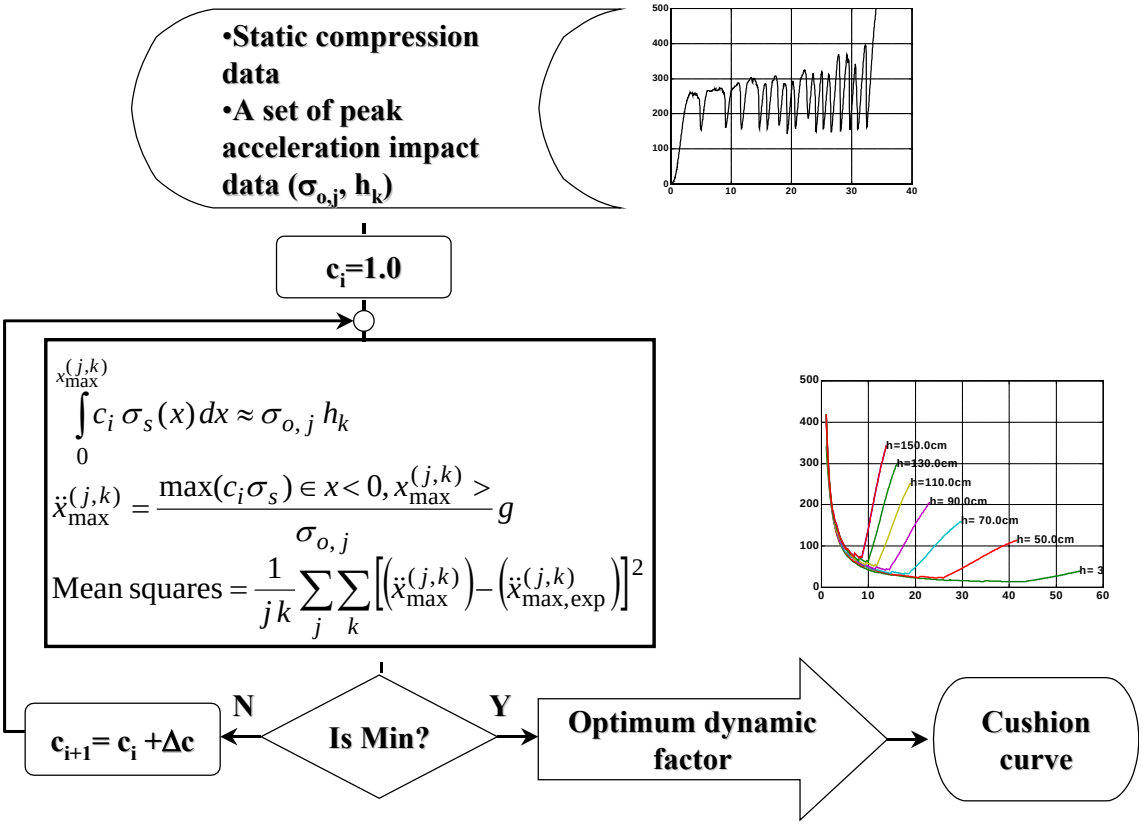

Figure 2.8 Algorithm for the Interative Least Mean Squares Optimization of the Dynamic Factor.

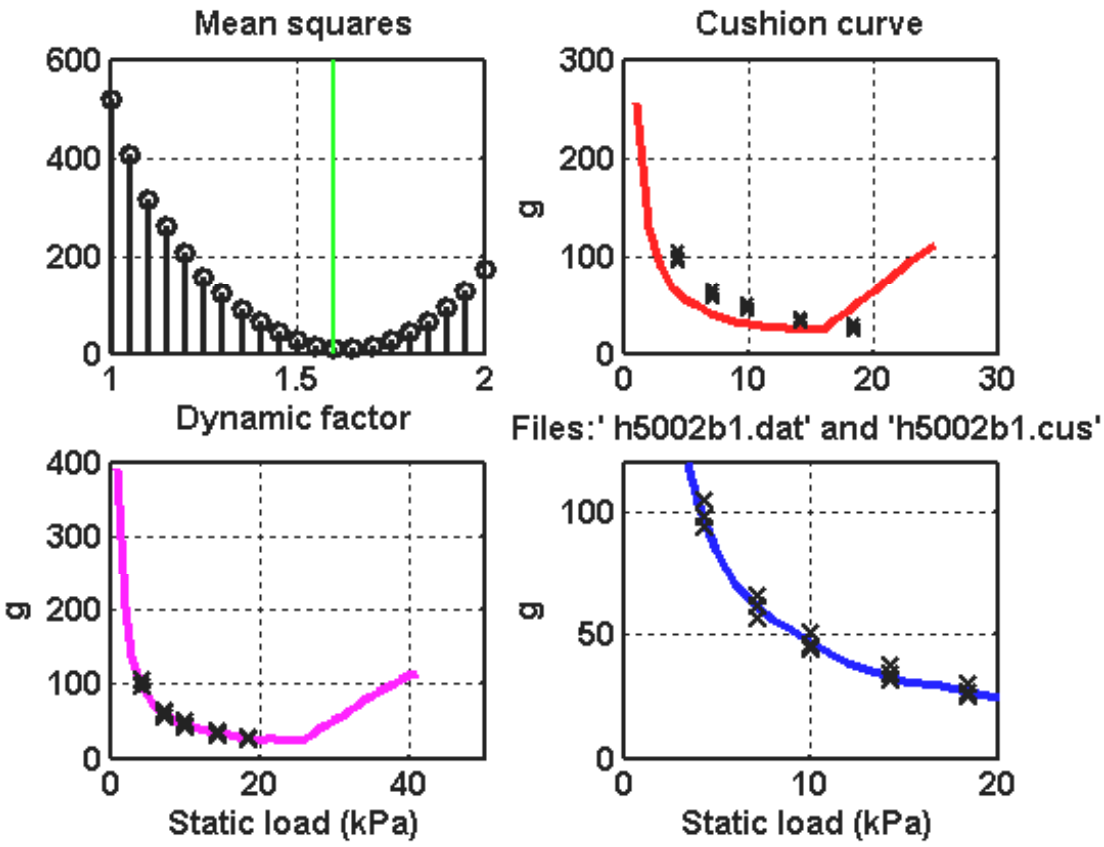

Figure 2.9 Application of the iterative Least Squares optimization for a Multi-layered corrugated fibreboard cushion with several impact test values

2.2 Other Behavioural Trends of Protectve Cushions

As was discussed in the previous section it is possible to determine the peak acceleration using the knowledge of how corrugated fibreboard behaves when being compressed statically. However it would be virtuous to discuss the literature on static behaviour.

2.2.1 Static Compression Behaviour

Thakur, K. and McDougall, A. (1996) investigated the mechanics of foam and considered, the first two phases of the stress-strain relationship. Phase one being the stiffer and linear section at the beginning of the stress-deflection curve which can be considered to obey Hooke's Law. The second phase being a softer more fluid phase or visco-elastic phase experiencing large strains due to the air trapped within cells being compressed.
They developed an expression to predict the static stress for this dual phase process and suggested that this approach could be used for corrugated fibreboard.

$$\sigma_s = \alpha_1\left[1-e^{-a\varepsilon}\right]+B\left(\frac{1}{x_0-\varepsilon}-\frac{1}{x_0}\right) \qquad (2.19)$$

For equation (2.19) to be applied to multi-layered corrugated fibreboard cushions, the layer collapsing mechanism would need to be taken into account.

Flexural stiffness is also an issue, Lee M., and Park J.,(2004) found that the flexural stiffness of corrugated fibreboard was higher in the machine direction than in the cross direction when tested in bending.

2.2.2 Collapsing Mechanism of Corrugated Fibreboard

Minett and Sek (2000) offered an explanation into how corrugated fibreboard collapsed during static compression. From Figure 2.6 and Figure 2.10 it can be noted that there are fluctuations on the compression data and the acceleration data respectively. Fluctuations on the acceleration pulse are often associated with noise. It can be seen that for similar displacement of say 25mm an identical number of fluctuations occurred with both the acceleration pulse and the compression curve.

This number of fluctuations has a correlation with the number of layers in the pad. It has also been observed that during both shock and static compression tests the individual layers do not necessarily collapse at the same time. They tend to roll over at a particular time followed by another layer at random intervals. These observed effects lead to the hypothesis that the fluctuating section of the compression and the shock pulse is due to the intrinsic behaviour of the individual layers of a multi-layered configuration of a cushion pad made from corrugated fibreboard.

The authors also suggested the following model to understand the buckling or collapsing effects. The model is that the dynamic behaviour can be described by considering compression springs in series and compressed. Each spring represents a layer in the cushion pad. The springs interact with each other in an elastic manner or failure due to visco-elasticity as shown in Figure 2.11

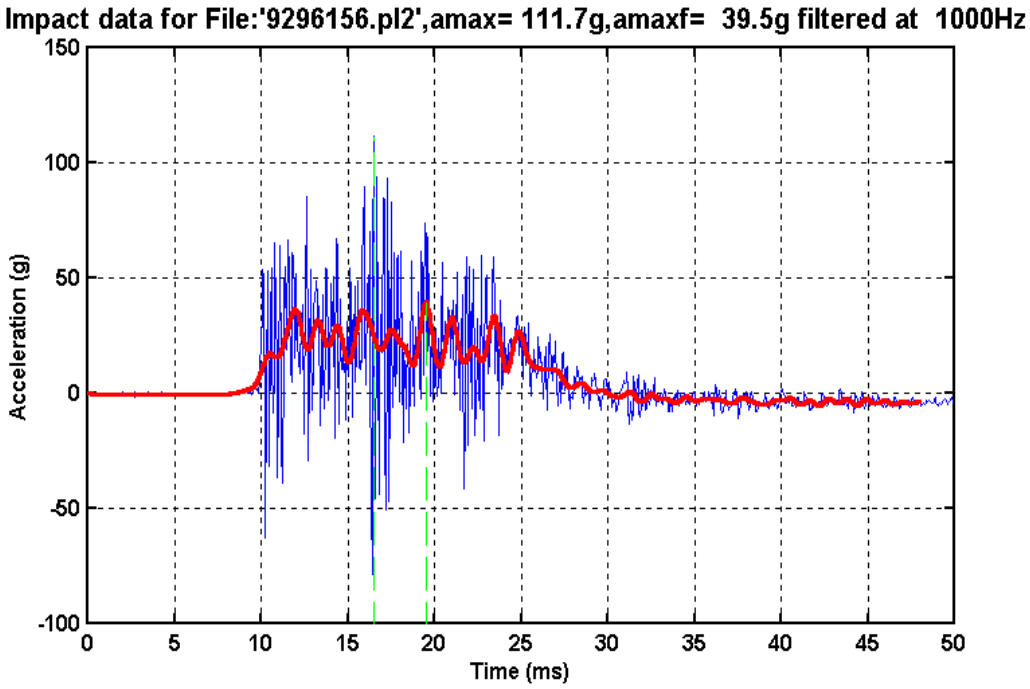

Figure 2.10 Typical acceleration pulse from an impact test on corrugated fibreboard.

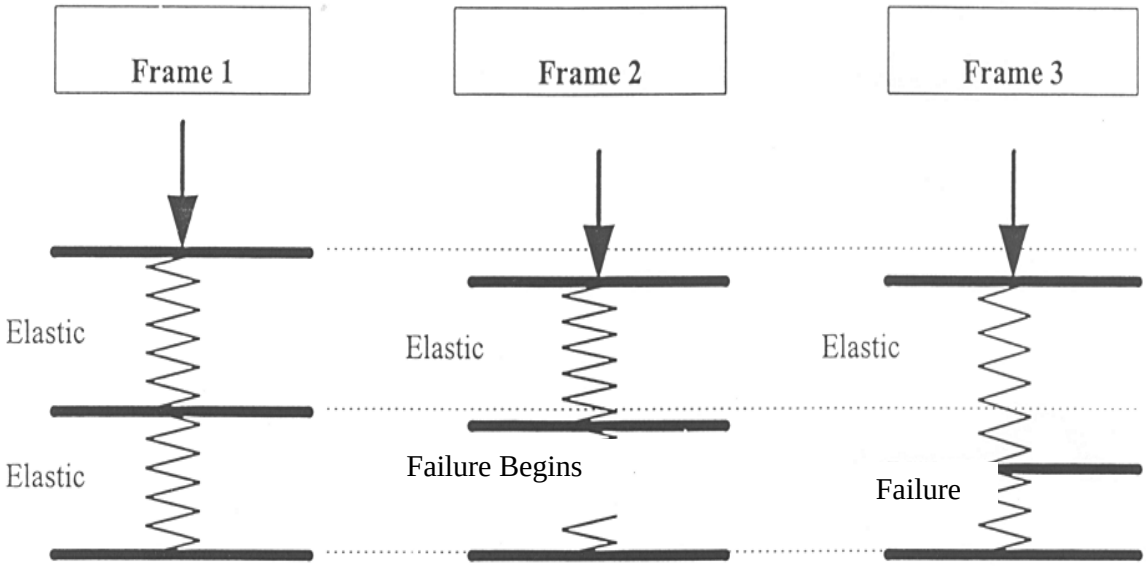

Figure 2.11 Spring model representing two layers of corrugated fibreboard

The first frame shows that the springs are under elastic deformation and the total deflection is the addition of the individual deflections. The second frame shows that the bottom spring has begun to fail (negative stiffness) and the spring offers no further resistance. The top spring will then expand as the force on the bottom spring is relaxed and the total deflection is dependent on the force in the bottom spring. Frame three shows the top spring expanding thus retaining its elastic behaviour. To understand the implications of this behaviour, a simple configuration of two linear springs in series subject to compression is constructed as shown in Figure 2.12.

The Figure 2.12 also shows compression characteristics of two springs a gradually increasing force is applied from O to point A the two springs are behaving in a linear fashion, thus the force and deflection of the system can be described by the following equation (2.20).

$$\text{Deflection } x = x_1 + x_2 \quad \text{and} \quad \text{Force } F = F_1 = F_2 \tag{2.20}$$

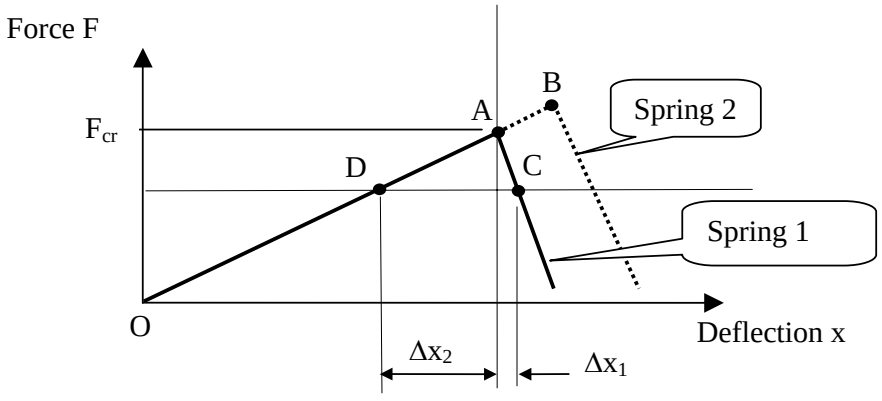

Figure 2.12 Representation of two springs compressed to failure

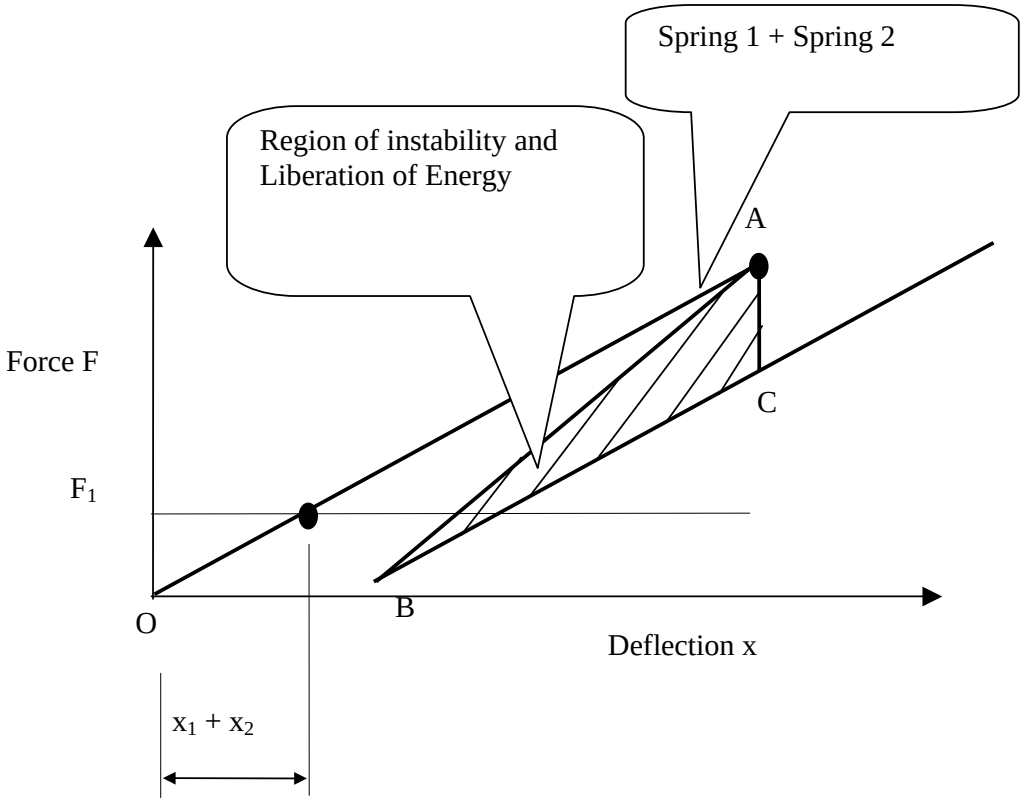

Figure 2.13 The resulting Force v Deflection after failure of spring 1

When the deformation reaches point A spring 1 starts to fail and its deformation requires less force. This spring is now independent and non-linear behaviour begins due to visco-elastic failure. Because there is equal force on both springs and as they are in series, then theoretically the spring 1 will continue to deform by Δx_1 and spring 2 will expand by Δx_2, to match the force of the independent spring the total deflection is reduced. This will continue until spring 1 is completely bottomed and spring 2 will begin to deform again with increasing deflection and force.

Figure 2.13 shows the resulting diagram of force versus deflection. Experimentally the overall deflection cannot diminish as the springs are locked between press platens and the shaded section in Figure 2.13 A,B,C, becomes a region of instability. The force will therefore decrease in an instant to a lower force at point C, in other words energy has been liberated and the springs try to find equilibrium in an instant and a fluctuation is produced. This process would be repeated, if more springs (pad layers) were added.

2.2.3 Pre-Compressed Multi-layered Corrugated Fibreboard

Minett M, Sek M. (1999) showed that after successive deformations of pads made of virgin corrugated fibreboard the cushioning characteristics are altered. Lower peak acceleration over a broader range of static loads was observed after successive stages of deformation shown in Figure 2.14. It stands to reason that subjecting a corrugated fibreboard cushion to a force profile as a pre-conditioning mechanism will improve the design qualities with respect to cushioning. For this state the mechanism of static compression is fairly simple

where the load deflection characteristics is similar to a linear spring up to the point of squashing.

Figure 2.15 shows peak accelerations calculated using similar techniques described earlier in section 2.2.2 for various static loads and at successive deformation levels. They showed that after the largest deformation level, which is fully pre-compressed, the lower the value of peak acceleration. It was thought that corrugated fibreboard in this pre-compressed state would make a sustainable replacement for poly-foam and polystyrene in protective packaging and its dynamic behaviour should be investigated. Pre-compressed fibreboard, Micor-Enviro-Cushion™, has been used as cushioning material for the packaging of such devices as smoke detectors and has been found to be a successful cushioning material, and research into its behaviour seems warranted.

When multi-layered fibreboard cushions are in this state the nature of airflow through the flutes becomes a more predominant property, as most of the effect of the structural properties are non-existent and the material have become more like a soft spring. Section 2.3.2 describes the acceleration pulses that are experienced when the material is this state.

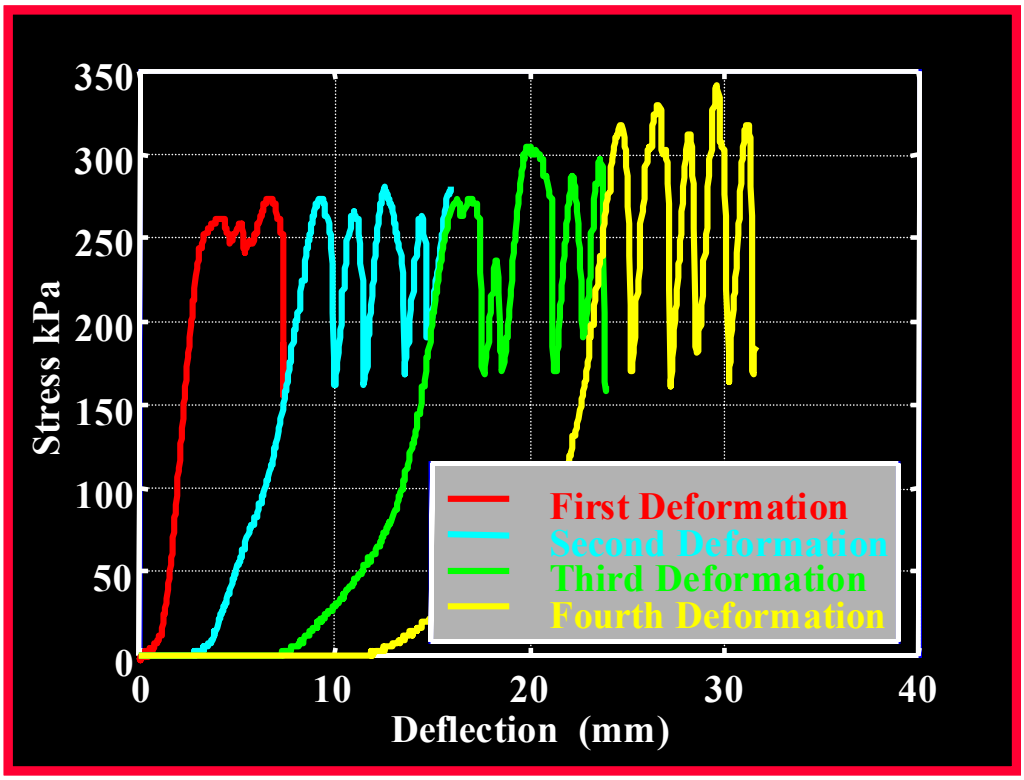

Figure 2.14 Progressive deformation of virgin corrugated fibreboard

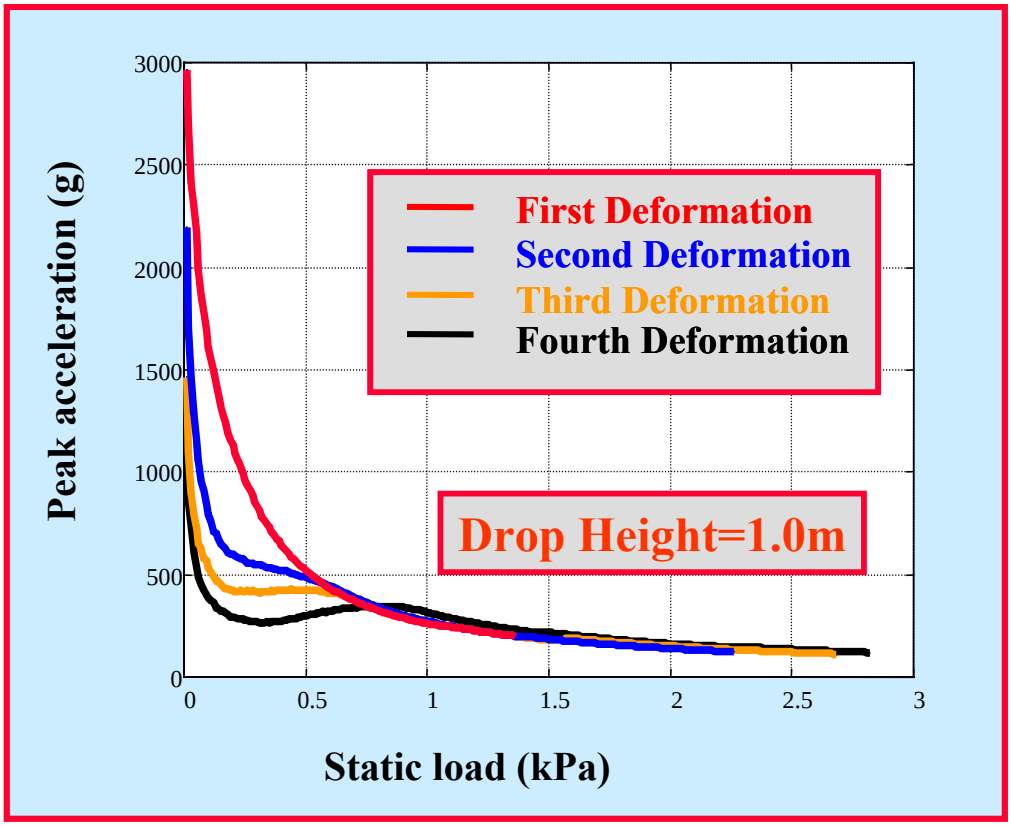

Figure 2.15 Peak accelelerations vs static loads for progressive deformations

2.3 Pre-Compressed Corrugated Fibreboard Behaviour

As was described earlier the force or acceleration is made up of two parts, that being the part due to static compression effects and that due to the dynamic effects. In general, the dynamic effects can be a function of many variables caused by dynamic effects such as gas flow and compression, structural damping and buckling. During testing protective cushions are subjected to impact at a relative fast rate, typically the time that the platen engages with the cushion is about 20ms. The shortness of time during impact leads to the thought that gas (air) flow considerations are important.

2.3.1 Air Compression Behaviour

Sasaki. H., Kaku Saito., and Kaname Abe., (1999) investigated the idea of using an airtight chamber filled with air together with a chamber filled with resilient urethane that allows restricted air flow. They also investigated the use of air discharge and intake ports which gives rise to the thought that air compression in corrugated fibreboard may be an important factor in that materials performance as a packaging material.

Naganathan P, He. J, Kirkpatrick J, (1999), investigated the effect of air compression, during static compression and impact tests. To further confirm the air effect, fibreboard cushions with taped and un-taped ends were tested in compression at constant rates. The tape did not completely seal and allowed the air to escape causing throttling. When multi-layered fibreboard cushions are subjected to compressive loads they tend to collapse by one layer rolling over at one time followed by another at random and creating a sudden drop off in compressive resistance as was discussed in section 2.1.3.

Compressive tests were carried out on 80mm square virgin cushions with six layers of ‘C’ type flute with ends taped and un-taped. The cushions were compressed at rates varying

from 1mm/s to 400mm/s. A comparison between resistive forces of un-taped to taped ends was insignificant at the lower compression rates, but at the higher rate the difference was more pronounced. Figure 2.16 shows the stress deflection curve for three taped and three open ended 80 x 80 six layered cushions compressed at 400mm/sec. The thicker lines being those cushions with taped ends.

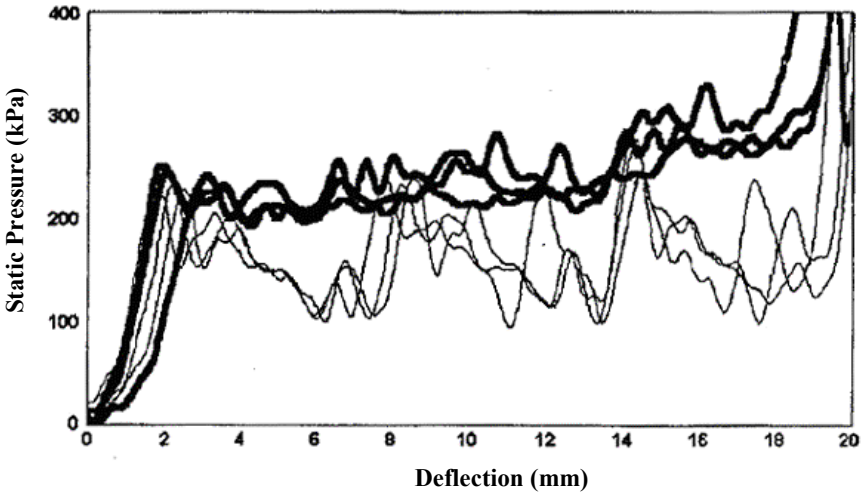

Figure 2.16 Stress Deflection curve for three taped and three un-taped six layered 80 x 80 mm, 'C' flute corrugated fibreboard cushion compressed at 400mm/s. The thicker lines are for the cushions with taped ends. Naganathan P, He. J, Kirkpatrick J, (1999).

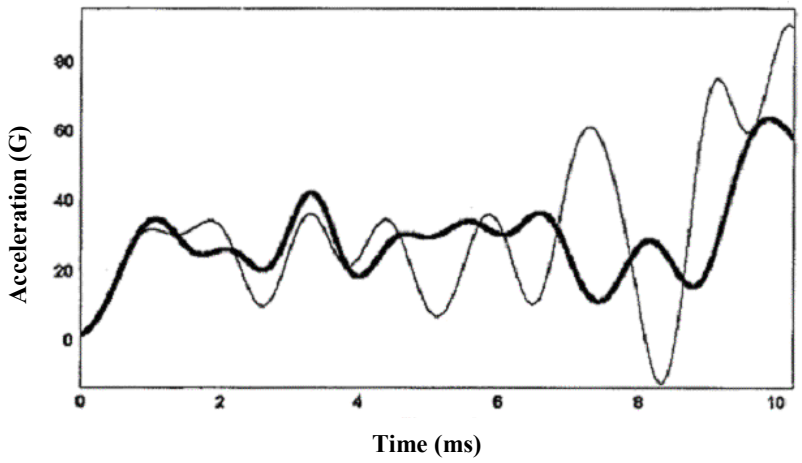

Figure 2.17 Comparison of impact signals from 600mm drop height and static load of 5.7kPa on 200 x 50mm rectangular six layered C type flute corrugated fibreboard cushion. Signals were filtered at 1000Hz. Naganathan P, He. J, Kirkpatrick J, (1999).

The authors also impact tested 200 x 50 rectangular cushions of virgin ‘C’ type flute at a drop height of 600mm and a static load of 5.7kPa. A comparison was made between the cushion being longer in the machine direction to being longer in the cross-machine direction, ie comparison of 200mm long to 50mm long flutes with identical contact area. The results are shown in Figure 2.17.

2.3.2 Air Behaviour of Pre-Compressed Corrugated Fibreboard

Minett, M. and Sek, M. (2002) investigated the differences in peak acceleration of long and short fluted pre-compressed corrugated fibreboard cushions of similar cushion area, when subjected to impact tests. Some interesting observations were made. Figure 2.18 and Figure 2.19 reveal that there is lower peak acceleration with the longer flutes. During testing it was found after multiple impacts a reduction of up to 30% in peak acceleration was achieved. It was suggested that the air pressure build-up, flute geometry and the frictional restriction to the flow of air through flutes can have an effect on the cushioning properties during impact on pre-compressed corrugated fibreboard. Comparisons of cushion pads with the same structural properties and same impact area but differing flute lengths have differing accelerations during impact. Longer flutes sizes exhibit lower peak accelerations. This is a similar finding by Naganathan. P, He. J, and Kirkpatrick. J, (1999), for virgin corrugated fibreboard, who did not consider pre-compressed fibreboard cushions in their deliberations.

Minett, M. and Sek, M. (2002) found that by restricting the flow of air by fully taping the ends, although not decreasing the stress levels, tended to lessen the dramatic drop off as the layers collapsed, thus allowing for more energy to be absorbed. They concluded that the effect of trapped air within the flutes, during impact, makes a significant contribution in the performance of corrugated fibreboard as a cushioning material, a similar conclusion reached by Naganathan. P, He. J, and Kirkpatrick. J, (1999). The authors also noticed that during

testing some unusual humps refer to Figure 2.18, occurred on the deceleration side of the acceleration pulse, which could lead to difficulty in determining exactly when the pulse begins.

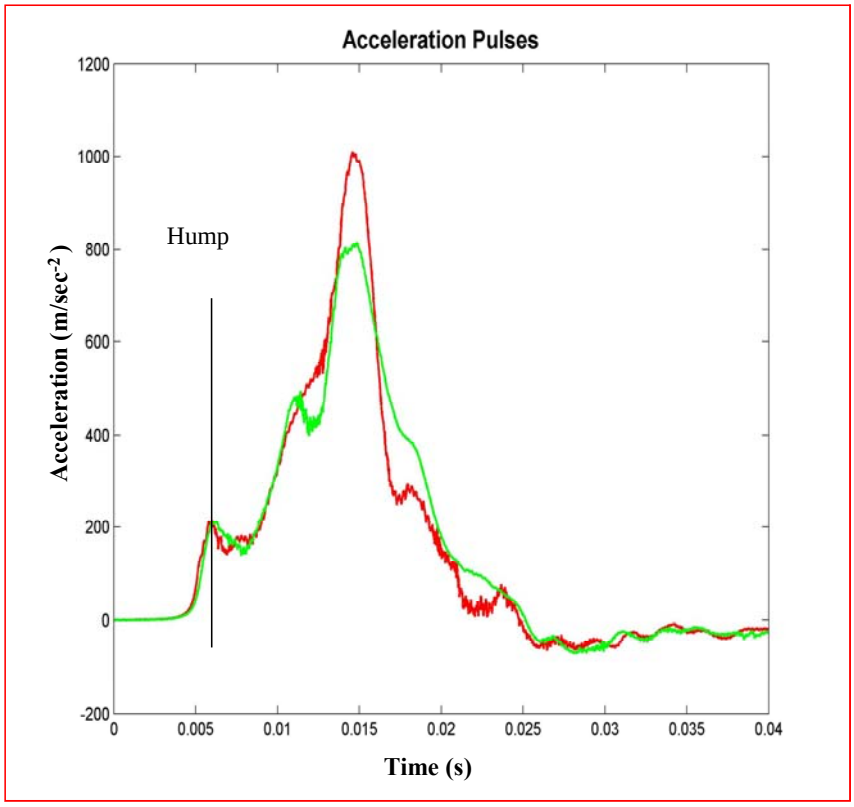

Figure 2.18 Differences of accelerations between short (red curve) and long flutes (green curve).

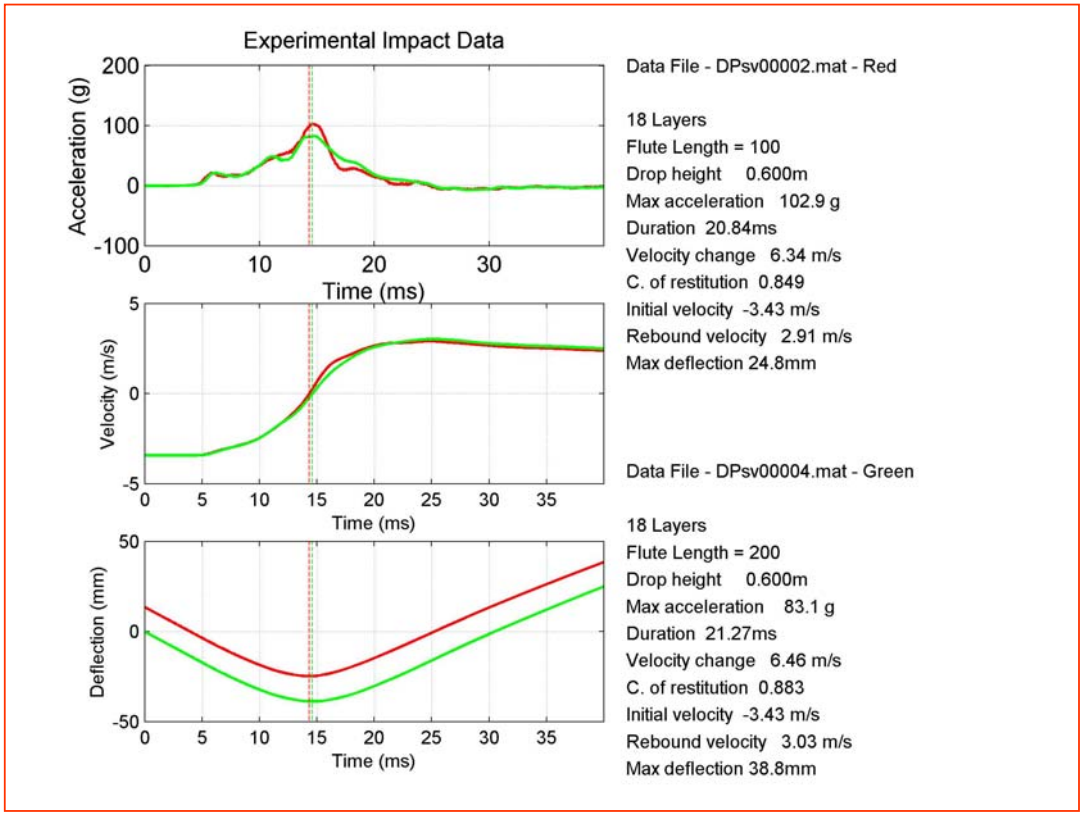

Figure 2.19 Differences of accelerations velocity and deflection between short (red curve) and long flutes (green curve).

2.4 Hypothesis

The literature reviewed suggests that it would be virtuous that research be carried out on at least other aspects of the cushion testing of corrugated fibreboard cushions rather than rely on peak acceleration for indications of a cushion's performance and to gain an understanding of what constitutes the dynamic factor suggested by Sek M., Kirkpatrick, J., (1996). It has also been indicated that the flow of air, plays a major role in the cushion performance, in particular for pre-compressed corrugated fibreboard as most of the structural resistance has been removed. The remainder of this study will mostly concentrate on the flow of air through pre-compressed multi-layered corrugated fibreboard cushions.

The impact on a multi-layered corrugated fibreboard cushion can be thought of as the well-known mass-spring damper system where the components of the system are the mass spring and a damper. It can be postulated that the airflow effects, or under some circumstances trapped air, play the damping role during dynamic compression. The static stiffness is still considered important as it influences the impact force and the resistive force.

To obtain a further understanding of these cushioning characteristics of pre-compressed corrugated fibreboard following questions should be investigated.

(a) How does corrugated fibreboard react when pre-compressed, and what is the resulting stiffness?

(b) When precisely does the acceleration pulse begin?

(c) What effect does the airflow and pressure within the flutes has on the acceleration pulse and deformation velocity under testing?

(d) What effect does the end conditions, namely pressure conditions, and flute configuration, will have on the acceleration pulse and deformation velocity?

(e) Can the effects be modeled mathematically?

It should be noted here that to call the resulting pulse of a cushion test as an acceleration pulse is slightly incorrect. The first section of the pulse up to the peak is in fact a de-acceleration and second section or recovery part is acceleration. However for simplicity the pulse is referred to an acceleration pulse for the rest of this study, with the maximum value being the peak acceleration.

Chapter 3 Pre-Compressing and Airflow Models

This chapter describes the development of mathematical models to determine the flow of air during impact when testing multi-layered pre-compressed corrugated fibreboard cushions. Static compression stress-strain data gives an indication of the resistive force, which is one of the components that affects the shock pulse however is not so important in the development of air-flow models. As was discussed in section 2.2 the airflow characteristics, is more of an issue for pre-compressed multi-layered corrugated fibreboard cushions than that of virgin cushions. This is largely due to the reduction in structural stiffness and is illustrated by comparison of virgin and pre-compressed states in Figure 3.1 and Figure 3.2. The mechanism for pre-compressing corrugated fibreboard is by static compression, which does not directly affect the airflow properties. A model termed the pre-compressing model is however presented.

3.1 Pre-Compressing Model for Corrugated Fibreboard

For the purposes of the discussion, deflection will be used rather than strain as this, is the usual measurement taken experimentally. As strain is deflection divided by the original length, deflection is really a measure of strain. Stress-deflection curves are not strictly static as they are measured at slow compression over a period of time. However results can be considered as static or compression at a slow rate.

As shown in Figure 3.1 multi-layered corrugated fibreboard has three stages of static compression the first stage or initial stiffening suggests that large peak accelerations will occur for small static loads in impact. Cushioning will improve when the central flatter section is reached. In this central region irreversible

deformations occur which reduces the cushions ability to resist multiple impacts. The final stage reflects full cushion squashing and is not suitable for cushioning.

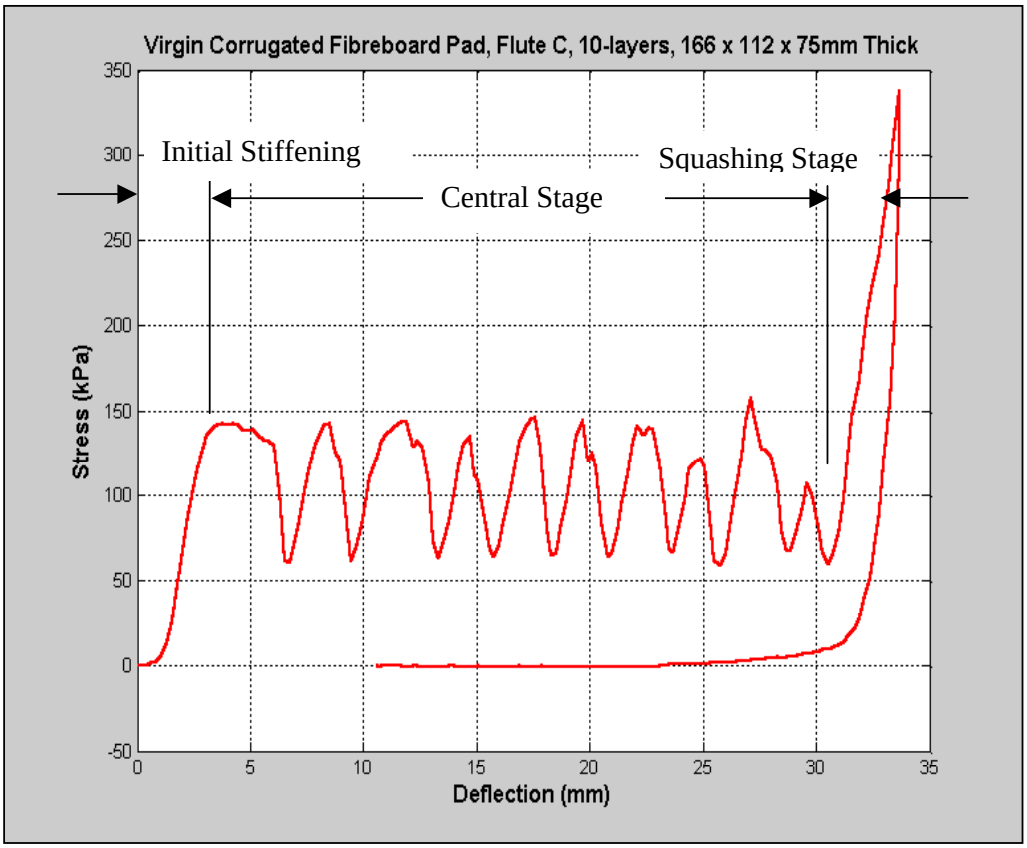

Figure 3.1 Stress – Deflection curve of Virgin Corrugated Fibreboard

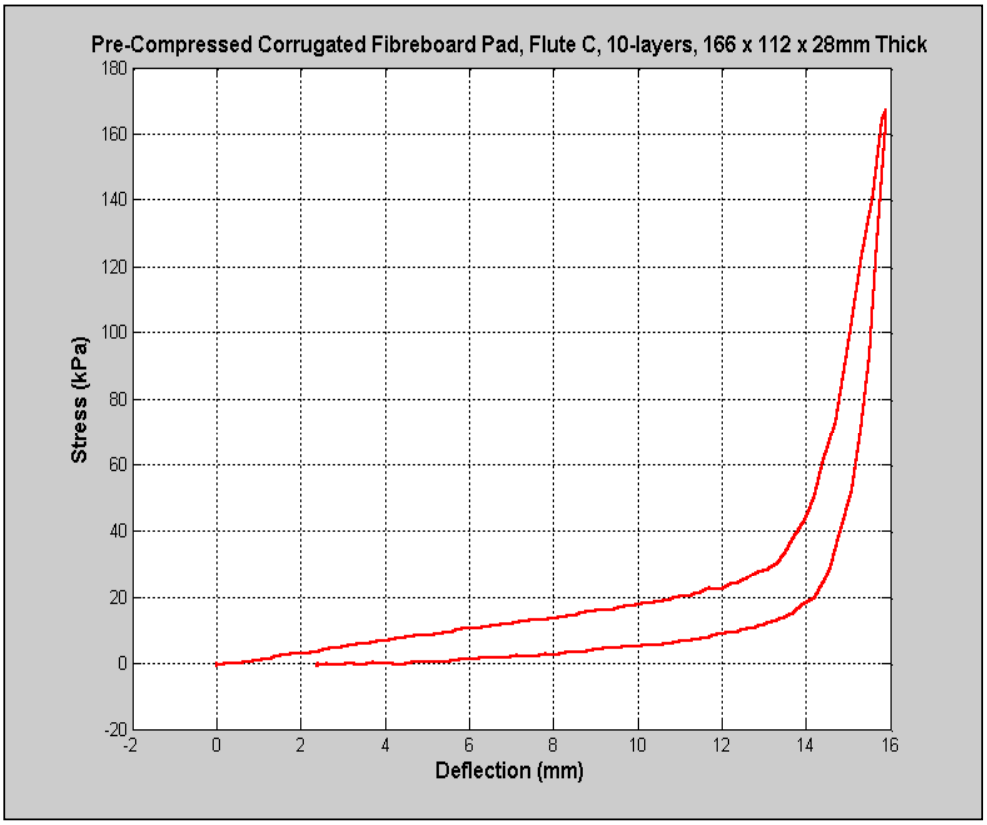

Figure 3.2 Stress – Deflection curve of Virgin and pre-compressed Corrugated Fibreboard

As discussed in chapter 2 Thakur, K. and McDougall, A. (1996) investigated the mechanics of foam and considered the first two phases of the stress-strain relationship. Phase one being the stiffer and linear section at the beginning of the stress-deflection curve, which can be considered to obey Hooke's Law. The second phase being a softer more fluid phase or visco-elastic phase experiencing large strains due to the air trapped within cells being compressed.

They developed an expression to predict the static stress for this duel phase process and suggested that this approach could be used for corrugated fibreboard.

To be applied to multi-layered corrugated fibreboard cushions the layer collapsing mechanism would need to be taken into account.

$$\sigma_s = \alpha_1\left[1-e^{-a\varepsilon}\right]+B\left(\frac{1}{x_0-\varepsilon}-\frac{1}{x_0}\right) \qquad \textbf{(3.1)}$$

By introducing a periodic function and some explanation of the constants it is possible to describe the static behaviour of multi-layered corrugated fibreboard using the equation (3.2). The first stage of the compression process is the elastic stage and is determined by P1 and the mean force is required from experimental data. The second stage the visco-elastic stage is represented by P2 and requires a slope function, and the third stage being the periodic stage requires the alternating force, as the individual layers collapse.

$$P1 = F_m\left(1 - e^{-a\varepsilon}\right) \qquad \text{Phase 1 Elastic}$$

$$P2 = SF\left(\frac{1}{(\varepsilon_0 - \varepsilon)} - \frac{1}{\varepsilon_0}\right) \quad \text{Phase 2 Visco-Elastic}$$

$$P3 = F_a \cos(2N\pi y / b) \quad \text{Periodic Phase}$$

$$F = P1 + P2 + P3$$

Therefore

$$F = F_m\left(1 - e^{-a\varepsilon}\right) + SF\left(\frac{1}{(\varepsilon_0 - \varepsilon)} - \frac{1}{\varepsilon_0}\right) + F_a \cos(2N\pi y / b)$$

where

F = the instantaneous force

F_m = the mean force

F_a = the alternating force

SF = the slope factor

N = the number of cushion layers

y = the displacement record

ε = the strain - the ratio of deflection to unloaded thickness

ε_0 = the maximum strain

b is a multiplier

(3.2)

Figure 3.3 shows a simulated static compression curve indication the collapsing mechanism using equation (3.2). Once the instantaneous force is known the stiffness of pre-compressed fibreboard cushions can be found by the simple well-known equation (3.3) as the material has a linear nature up to the point of the material squashing.

$$\text{Static Stress} = \frac{F}{A} = \frac{k\delta}{A}$$

where

F = the applied force

δ = deflection

k = cushion stiffness

A = the cushion area

(3.3)

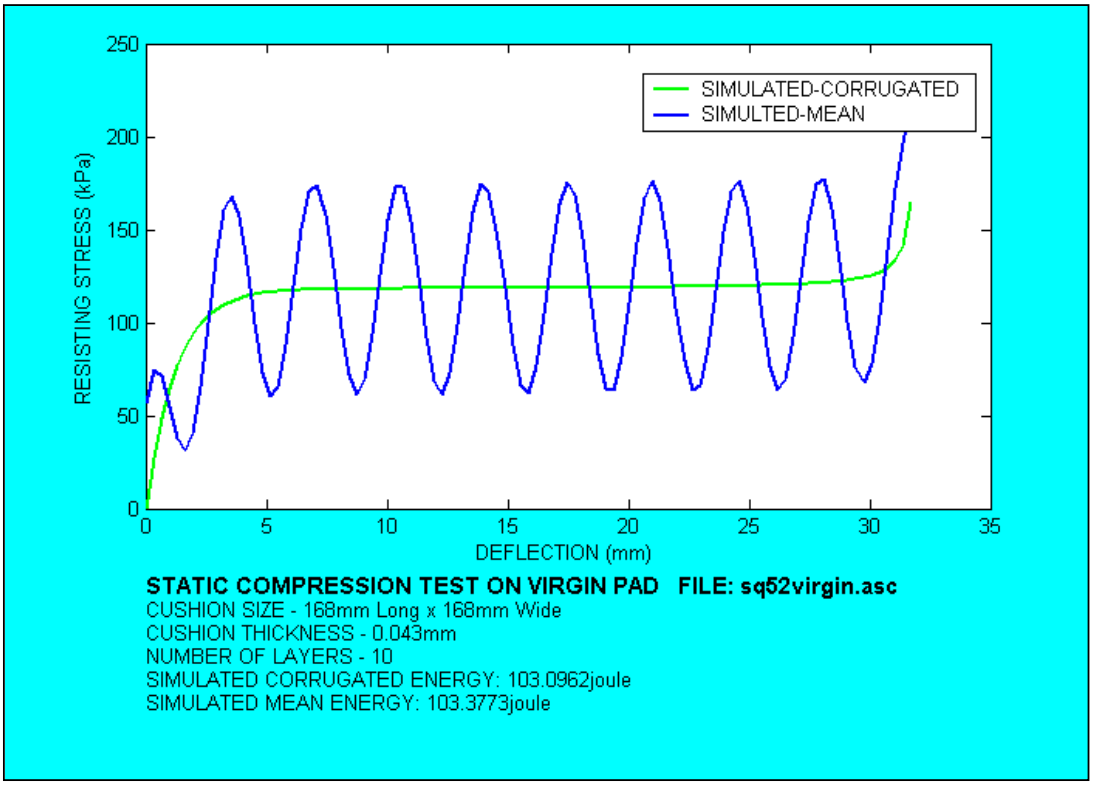

Figure 3.3 Simulated Static Compression Curve

3.2 Post Contact Airflow Model

The dynamic factor proposed by Sek and Kirkpatrick (1997) and the refined "dynamic factor" method proposed by Sek, *et al.* (2000) can be a function of many variables caused by dynamic effects such as the flow of air during compression, structural damping and buckling.

The flow of air plays a major role in the dynamic behaviour of multi-layered corrugated fibreboard cushions and is particularly important for pre-compressed fibreboard, as the structural properties are less significant. As was discussed in chapter 2, the testing procedure for cushion material is to drop a platen or mass upon the test cushion and measure the acceleration or more correctly the deceleration. The platen mass and the cushion under test become a spring mass system after contact and behave according to the following second order differential equation.

$$ma + cv + kx = F \tag{3.4}$$

where

m = platen mass
c = damping constant
F = some forcing function
a = acceleration of the platen mass
v = velocity of the platen mass
x = displacement of the platen mass

For the remainder of this study the platen displacement will be referred to as Δh. During impact if the air is throttled, and it most probably is as impact is over a very short time of a bout 20ms, it will be acting in the role of damping section in equation (3.4). It must be pointed out that calculations have shown that although impact takes

place over a small time interval the airflow is incompressible. To understand this more fully it is necessary to develop a relationship between the platen and the flow of air through the flutes of a corrugated fibreboard cushion.

The aim is to derive an expression for platen acceleration in terms of the design properties of the corrugated fibreboard cushion such as length, width number of layers, etc. Minett, M. and Sek, M. (2002), suggested a model based on the linear momentum of air which clearly shows that flute geometry affects the resultant dynamic properties during impact.

To develop such a model, consider a cross-section of multi-layered corrugated fibreboard cushion subjected to a vertical impact load as shown in Figure 3.4 . This mechanism can be thought of as applied load by the platten of a cushion testing machine which simulates the process of a package being dropped during handling or transportation.

Singh, R. et al (2002) discussed the use of control volume theory to model the transient response of a hydraulic engine mount. They lumped the fluid systems into a series of control volumes that represented the hydraulic system. The air content within a multi-layered fibreboard cushion is also a fluid system that can be considered as a one dimensional control volume of air.

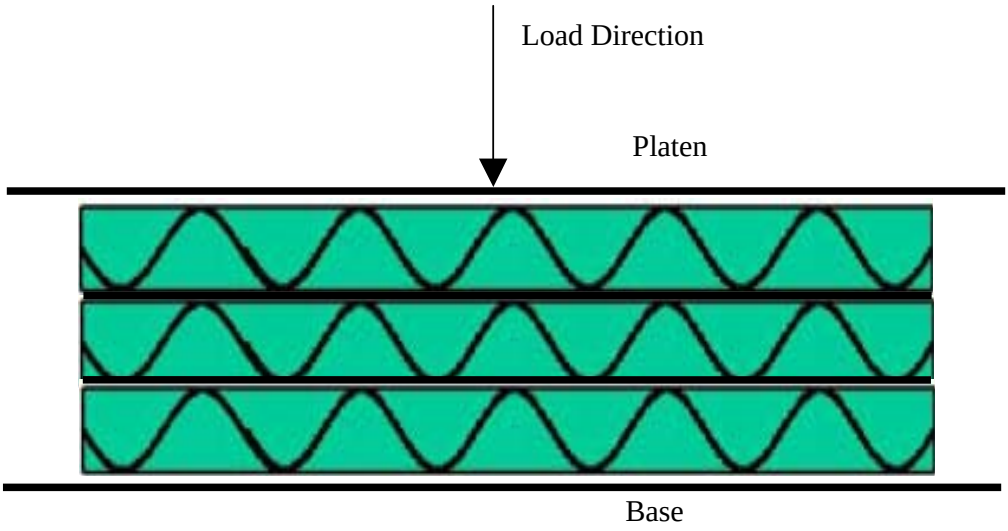

Figure 3.4 Representation of Multi-layered Corrugated fibreboard cushion

An approximation for a one dimensional momentum flux in a control volume, according to White, Frank. M. (1999) *Fluid Mechanics* is used for engineering analysis and is quoted as:

$$\sum F = \frac{d}{dt}\left(\int_{cv} V\rho \, d\boldsymbol{V} \right) + \sum \left(\dot{m}, v_i \right)_{out} - \sum \left(\dot{m}, v_i \right)_{in} \qquad (3.5)$$

Consider the volume of air within the cushion as the control volume. A relationship between the platen velocity and the air velocity through the flutes of the corrugated fibreboard can be developed. The following Figure 3.5 shows the difference in the control volume over a small change in time.

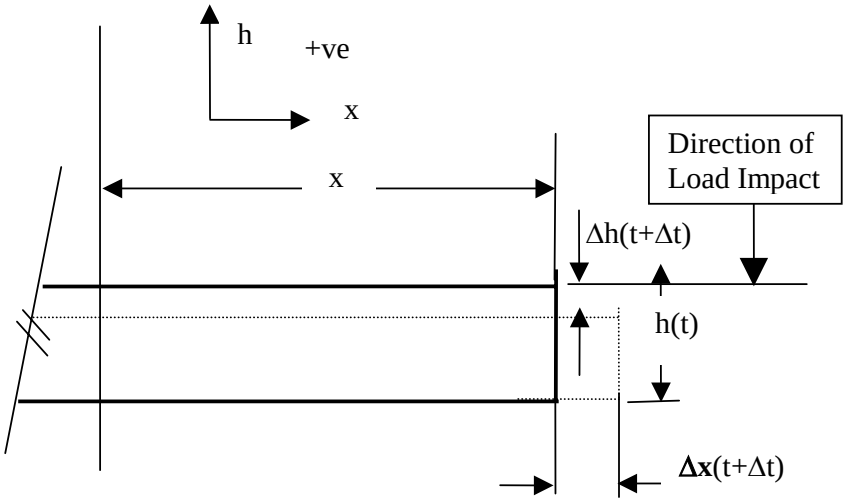

Figure 3.5 Volumetric change of air during impact. The dotted line representing change

x = Control Volume length

h = Control Volume height

t = Time

Δt = Time step

D = Width

At time t the layer height is equal to h_t and at time $t + \Delta t$ the layer height is equal to $h - \Delta h$

The volume of air at time t $\quad vol = h_t D x$

and at time $t + \Delta t$ $\quad vol = (h_t - \Delta h) D x$

From the Figure 3.5 and by arranging the terms it can be seen that the volume difference of the cushion due to compression becomes

$$vd = h_t D x - (h_t - \Delta h) D x = \Delta h D x \tag{3.6}$$

Also from Figure 3.5 it can be seen that the volume of discharged air is equal to

$$vc = (h_t - \Delta h) \Delta x D \tag{3.7}$$

Equating (3.6) to (3.7) with respect to time change and simplifying to determine the velocity of the air at point x.

$$\frac{\Delta x}{\Delta t} = \frac{\Delta h}{\Delta t}\left(\frac{x}{h_t - \Delta h}\right)$$

$$\text{for } t \to 0 \tag{3.8}$$

$$V = \frac{dh}{dt}\frac{x}{h_t}$$

Where V is the air velocity through the cushion, and $\frac{dh}{dt}$ is the rate of change in

cushion height which is also equal to the platen or load velocity. This expression is useful in that allows for the conversion of air velocity through cushion flutes to platen velocity.

To find an expression for acceleration consider conservation of linear momentum and referring to Figure 3.6 the assumption is made that pressure in the x direction is equal to that in the h direction.

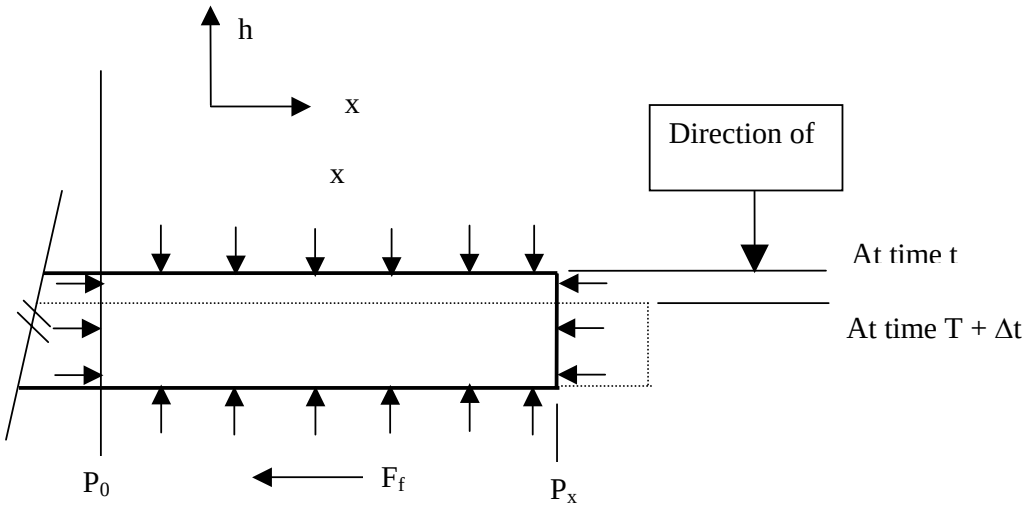

Figure 3.6 Conservation of Momentum

Restating the control volume equation (3.5)

$$\sum F = \frac{d}{dt}\left(\int_{cv} V\rho \, d\boldsymbol{V} \right) + \sum \left(\dot{m}, v_i \right)_{out} - \sum \left(\dot{m}, v_i \right)_{in} \tag{3.9}$$

The net vector force on a control volume equals the rate of change of vector momentum within the control volume plus the vector sum of outlet momentum fluxes minus the vector sum of inlet momentum fluxes.

Firstly looking at the control volume with respect to the x direction

$$\int_{cv} V\rho \, d\boldsymbol{V} = \int_0^x V\rho A \, dx \tag{3.10}$$

Momentum in the control volume at time t and substituting equation (3.8) then

$$\int_{cv} V\rho \, d\boldsymbol{V} = A_t \rho \int_o^x \frac{dh}{dt} \frac{x}{h_t} dx \tag{3.11}$$

by integrating and simplifying then

$$\int_{cv} V\rho \, d\boldsymbol{V} = \frac{1}{h_t} \frac{dh}{dt}\Big|_t \rho A_t \frac{x^2}{2} \tag{3.12}$$

similarly for the momentum in the control volume time $t + \Delta t$ then

$$\int_{cv} V\rho \, d\boldsymbol{V} = \frac{1}{h_t - \Delta h} \frac{dh}{dt}\Big|_{t+\Delta t} \rho A_{t+\Delta t} \frac{x^2}{2} \tag{3.13}$$

Therefore to obtain the momentum difference in the control volume from t to Δt subtract the right hand side of equation (3.12) from the right hand side of (3.13) to yield an expression for the momentum within the control volume.

$$\frac{d}{dt}\int_{cv} V\rho \, d\boldsymbol{V} = \frac{\rho x^2}{2}\left[\left(\frac{A_{t+\Delta t}}{h_t - \Delta h}\left(\frac{dh}{dt}\right)_{t+\Delta t}\right) - \left(\frac{A_t}{h_t}\left(\frac{dh}{dt}\right)_t\right)\right] \tag{3.14}$$

Substituting for area $A_t = Dh$ and $A_{t+\Delta t} = D\left(h_t - \Delta h\right)$ and the rate of difference between velocities is equal to acceleration.

$$\frac{d}{dt}\int_{cv} V\rho \, d\boldsymbol{V} = \frac{\rho D x^2}{2}\left[\left(\frac{dh}{dt}\right)_{t+\Delta t} - \left(\frac{dh}{dt}\right)_t\right]$$

or (3.15)

$$\frac{d}{dt}\int_{cv} V\rho \, d\boldsymbol{V} = \frac{\rho D x^2}{2}\frac{d^2h}{dt^2}$$

Looking at the momentum flux terms from equation (3.5) and assuming that the air flows either direction from the center of the flute then the momentum flux at the center is equal to zero.

$$\dot{m}_{in} V_{in} = 0$$

and (3.16)

$$\dot{m}_{out} V_{out} = \rho A V^2$$

Using the equation (3.8) for air velocity in terms of load velocity and letting $A = Dh$

$$\dot{m}_{out} V_{out} = \frac{\rho D x^2}{h_t} \left(\frac{dh}{dt} \right)^2 \tag{3.17}$$

Now referring to Figure 3.6 the algebraic sum of the forces in the x direction is equal to

$$\sum F_x = -P_x A + P_0 A - F_f$$

where

A = cushion cross-sectional area

P_x = cushion pressure at any point x

P_0 = cushion pressure at cushion centre

F_f = frictional force

(3.18)

Substituting equations (3.15), (3.17) into equation (3.9) an expression for force can be obtained.

$$\sum F_x = \frac{\rho D x^2}{h_t} \left(\frac{dh}{dt} \right)^2 + \frac{\rho D x^2}{2} \left(\frac{d^2 h}{dt^2} \right) \tag{3.19}$$

Replacing $\sum F_x$ as per equation (3.18) and simplifying yields

$$A_t \left(P_0 - P_x \right) - F_f = \rho D x^2 \left[\frac{1}{h_t} \left(\frac{dh}{dt} \right)^2 + \frac{1}{2} \left(\frac{d^2 h}{dt^2} \right) \right] \tag{3.20}$$

Re-arranging for acceleration and using dot notation

$$\ddot{h} = 2\left[\frac{A_t\left(P_0 - P_x\right) - F_f}{\rho D x^2} - \frac{1}{h_t}\left(\dot{h}\right)^2\right]$$

where $\ddot{h}$ = acceleration of the platen or load due to air effects.

$\dot{h}$ = platen or load velocity due to air effects

h_t = height at any point in time

A_t = exit area of cushion cross section at any point in time

F_f = frictional resisting force

P_0 = average air pressure

P_x = air pressure at point x and is equal to atmospheric pressure at the extremity

D = control volume width

x = distance from CVcentre to point under consideration

= the cushion length at the extremity

ρ = air density (3.21)

It can be seen in equation (3.21) that if **x** and **D** are the length and width of the control volume or cushion and if these values increase the value of the acceleration $\ddot{\mathbf{h}}$ will decrease thus suggesting that flutes that are longer give lower acceleration levels, which is as the literature suggests. The equation also suggests that if the end pressure p_x is higher there will also be an expectation of lower acceleration.

As was stated earlier if the flow of air is throttled, which would occur if pressure P_0 tended to be overcome by the friction force and the pressure at point x, then lower accelerations were overcome. Equation (3.21) represents the acceleration due to air throttling taking place during impact.

The system operating can be likened to the second order differential equation

describing a mass damper spring system under the influence of a force can be described as follows:

$$ma + cv + k\,\Delta h = F$$

where

m = mass

c = damping constant

F = the forcing function

a = total acceleration of the platen mass

v = velocity of the platen mass

Δh = displacement of the platen mass

(3.22)

During impact according to Juvinall, R. C. and Marshek, K. M. (2000*)* the equivalent force is that which would occur during static loading multiplied by a Impact Factor which is by definition:

$$IF = \sqrt{\frac{2H}{\delta_{st}}}$$

where

IF = impact factor

H = the drop height

δ_{st} = static deflection due to platen mass

(3.23)

If the position x is at the extremity of the cushion it can be renamed L and if the acceleration due to damping with its mass component is covered by equation (3.21) and the impact factor covered by (3.23) then the acceleration of the platen mass (deceleration pulse) can be determined by:

$$a = \left(\frac{F \times IF}{m}\right) - \left(\frac{k\,\Delta h}{m}\right) - 2\left[\frac{A_t\left(P_0 - P_x\right) - F_f}{\rho DL^2} - \frac{1}{h_t}\left(\dot{h}\right)^2\right] \qquad (3.24)$$

where

a = platen total acceleration

F = forcing function

IF = impact factor

h = cushion displacement

k = cushion static stiffness

m = platen mass

D = cushion width

L = the flute length

Software to test this equation was developed and is shown in appendix A. the software includes a model developed in simulink to represent equation (3.24) and is shown in Figure 3.7. The model is a second order differential equation and simulink is an ideal method for solving such models as it simulates using differential equation solvers.

For simplicity P_0 in equation (3.24) is taken as the platen force divided by the cushion area multiplied by the impact factor. The pressure P_x can be taken as atmospheric pressure for fully opened flutes or a higher value to model end restrictions.

To test this model experimentally cushion tests can be carried out on multi-layered corrugated fibreboard by:

1. Progressively blocking the ends to increase the flute exit pressure P_x thus varying the pressure terms of the model to lower the acceleration.
2. For identical dimensions of rectangular cushions with the orientation of the flutes either along the larger dimension or along the smaller dimension thus varying the denominator of the model to lower the acceleration.

These concepts are checked experimentally and simulated in chapter 4.

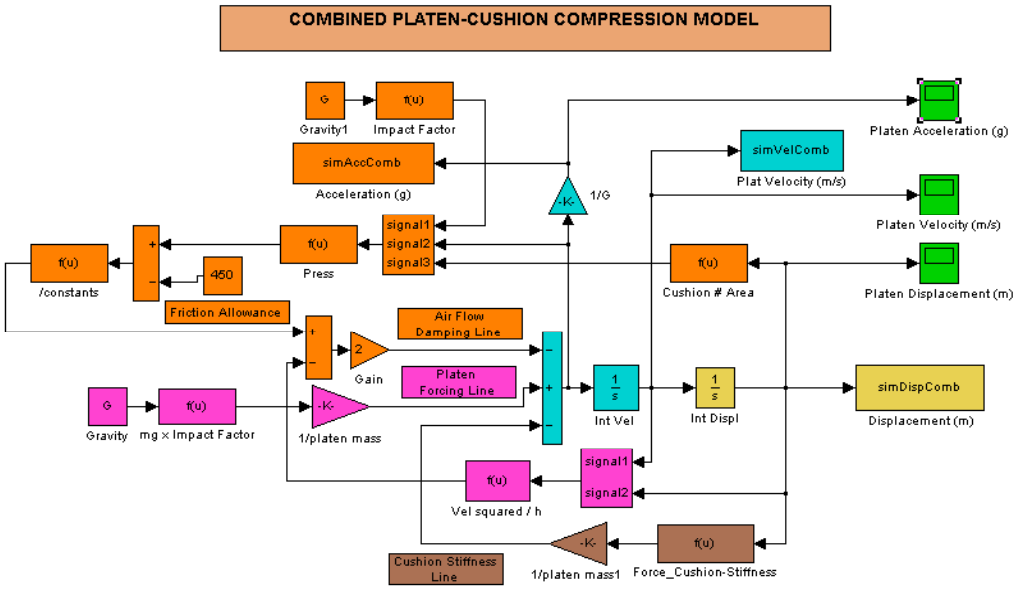

Figure 3.7 Simulink Model for Determining Acceleration of Pre-Compressed Cushions

Chapter 4 Experimental Work and Further Developments

In chapter 2 the literature was discussed on how the dynamic behaviour of corrugated fibreboard used as protective cushions can be predicted and how this behaviour could be explained. A model describing the behaviour during impact was developed in chapter 3 suggests the flow of air, or the restriction to the flow of air, together with the cushion geometry plays a significant role in determining the acceleration of pre-compressed multi-layered corrugated fibreboard cushions. Minett, M. and Sek, M. (2002) noticed during routine testing some unusual humps occurred on the deceleration side of the acceleration pulse which lead to difficulty in determining exactly when the pulse begins. This chapter presents experimental work firstly to show static testing, as it is the method for pre-compressing the corrugated fibreboard. Secondly to determine where the acceleration pulse begins by measuring the contact point and velocity and thirdly to verify the models developed in chapter 3.

4.1 Static Pre-Compression

The pre-compression of corrugated fibreboard was carried out on an Instron Universal testing machine as shown in Figure 4.1. The static tests have a dual purpose firstly to prepare cushions for the pre-compressed state and secondly to provide information about the stiffness of the material and an insight to the collapsing mechanism discussed in chapter 2.
The static testing procedure used was a two-stage process where firstly virgin cushions were compressed at an approximate rate of 1mm/sec to allow the layers to collapse. After a recovery period the cushions were compressed again at the same rate to obtain the stiffness in the pre-compressed state. Even though the loading process is not static, the rate is so low that the loading mechanism can be considered to be static. Load-deflection data was recorded for

both of these processes. The resulting graphs of load vs deflection are shown in Figure 4.3 and Figure 4.4.

Figure 4.1 Instron universal testing machine for pre-compressing.

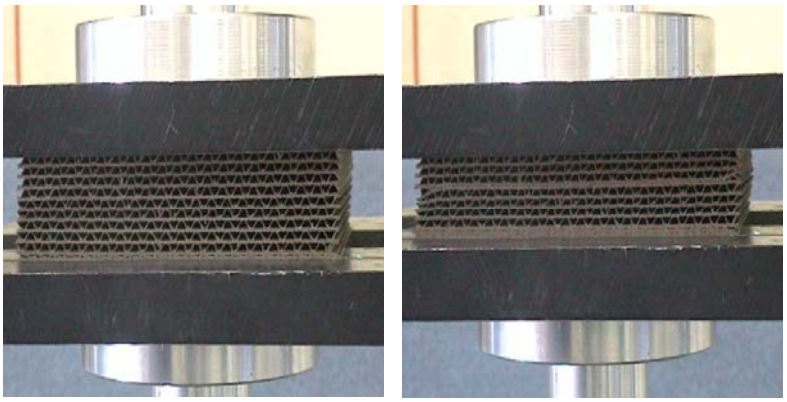

Figure 4.2 Close up of typical static tests and pre-compression

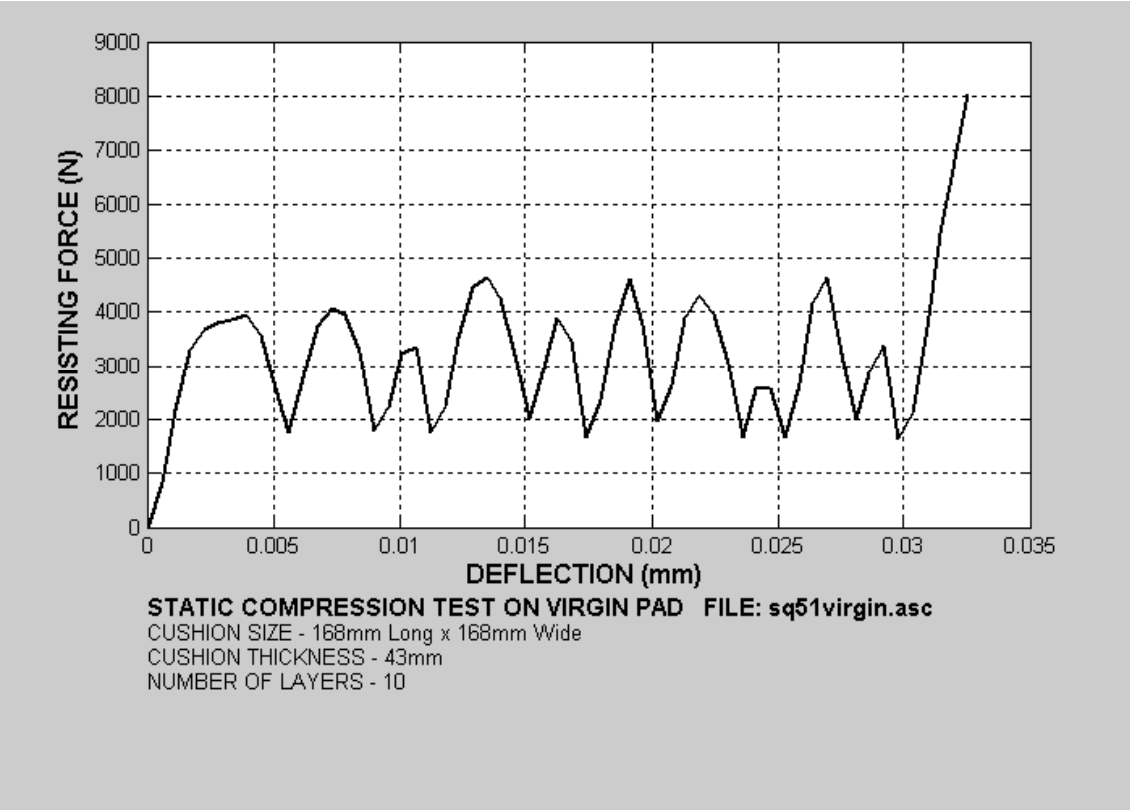

Figure 4.3 Typical Static Compression test for virgin Corrugated Fibreboard Cushion

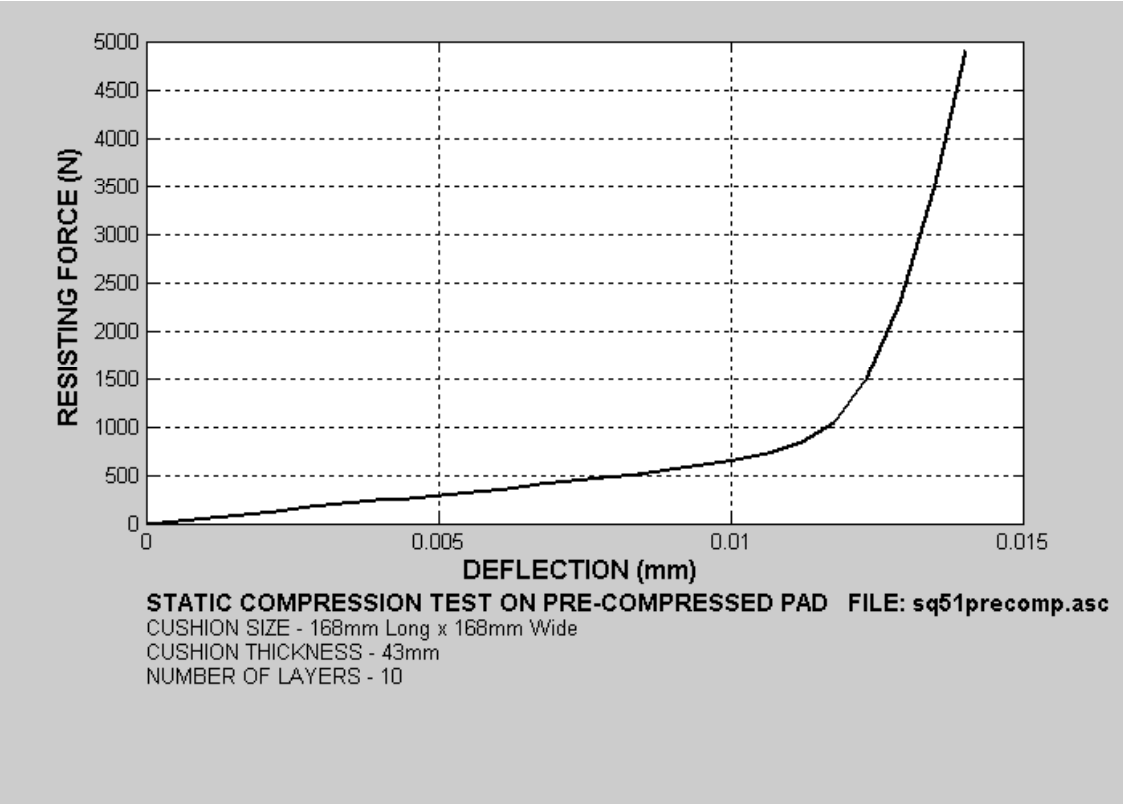

Figure 4.4 Typical Static Compression for Pre-Compressed Corrugated Fibreboard Cushion

The stiffness of the pre-compressed cushion is easily obtained by using the equation of a straight line from the linear part of Figure 4.4.

The equation for static compression developed in chapter 2 is stated here

$$F = A\left(\left(1-sech\left(y\right)\right)+dS\left(\frac{1}{\left(y0-y\right)}-\frac{1}{y0}\right)\right)+C\,Sin\left(2y\right) \qquad (4.1)$$

Using software developed to replicate equation (4.1) the following graph, Figure 4.5 that shows the energy for experimental data and the theoretical data based on equation (4.1) is plotted.

The software can be viewed in appendix A.

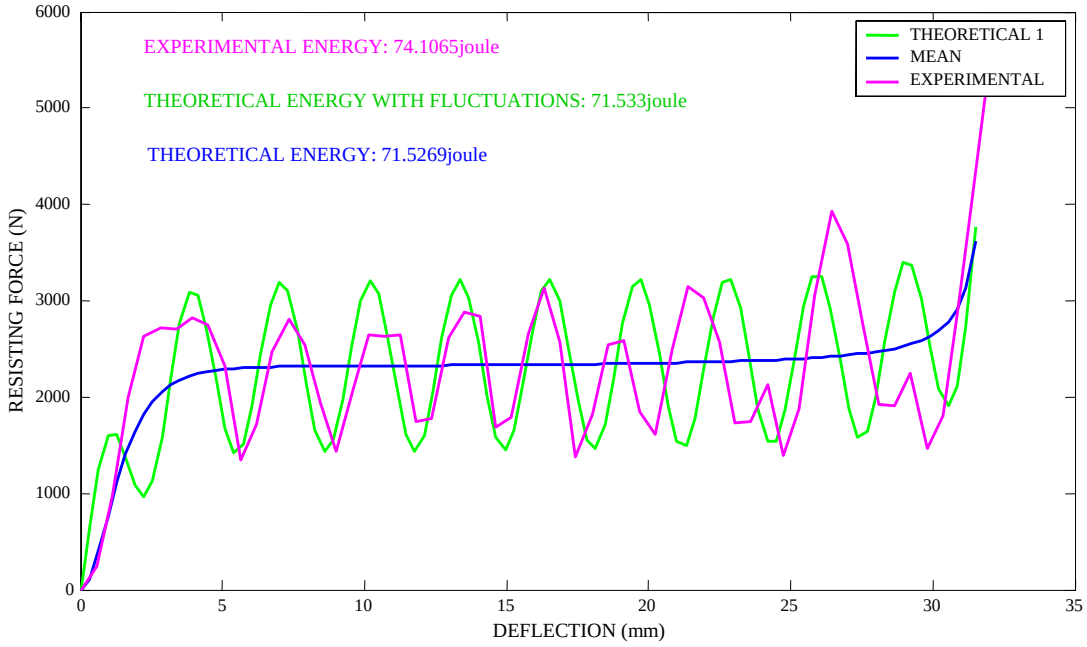

Figure 4.5 Comparison of experimental to theoretical static compression for virgin corrugated fibreboard

4.2 Cushion Testing for Contact Point and Velocity

Generally the platen velocity just prior to impact can be determined by calculation using the well-known expression based on equating the equations for potential and kinetic energy.

$$mgh = \frac{1}{2}mv^2$$

$$v = \sqrt{2gh}$$

where

m = the platen mass (4.2)

v = the velocity on contact

g = gravitational acceleration

h = drop height

Although analytically correct cushion tests were carried out to try to establish the pre-contact velocity and at what stage within acceleration pulses does the platen makes contact with the cushion. These test were carried out on a Lansmont cushion testing machine using 1.2kg and 5.8kg platens. The 1.2kg platen was fitted with a plate 4.58mm wide and the 5.8kg platen fitted with 5.53mm wide plate, the plates were mounted such to allow the slicing of a infrared beam. The infrared beam was adjustable and wired for 5 volts to indicate when the beam is broken. When the platen was statically placed on the top of the cushion, it could be adjusted to off ie the beam turns off at the trailing edge of the plate. When the platen was dropped and the beam interrupted the time was measured thus establishing the velocity prior to impact. By knowing the slicing time together with the plate width an approximation of the platen velocity can be measured. The experimental set up is shown in Figure 4.7 in schematic form.

This data as well as the acceleration data from an accelerometer mounted on the platen was recorded using Data Physics SignalCalc ACE V 4.0 data acquisition system. A typical data capture set-up is shown in Figure 4.6. The upper graph represents the acceleration pulse and the bottom representing the plate slicing through the infrared beam.

The acceleration was measured by a Brüel & Kjær type 4383V of sensitivity 2.851pC/ms^{-2} with an upper frequency limit of 8400 Hz with the signal conditioning performed by a Rion charge amplifier.

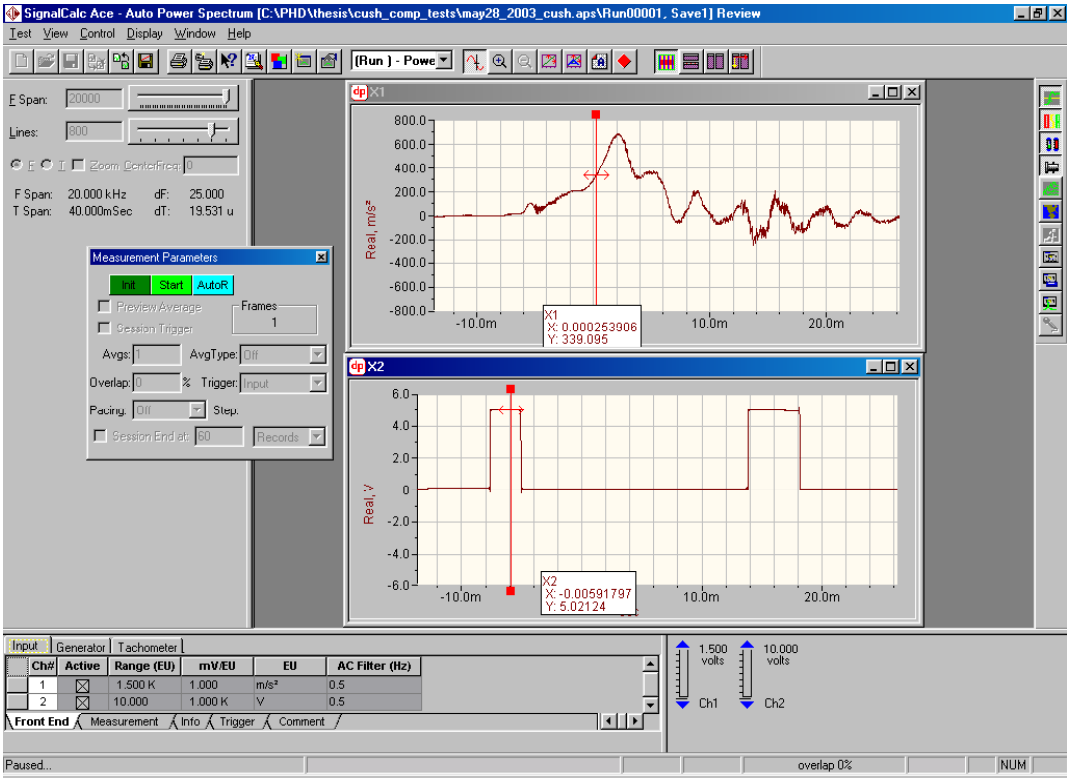

Figure 4.6 Data capture set up using Signal Calc

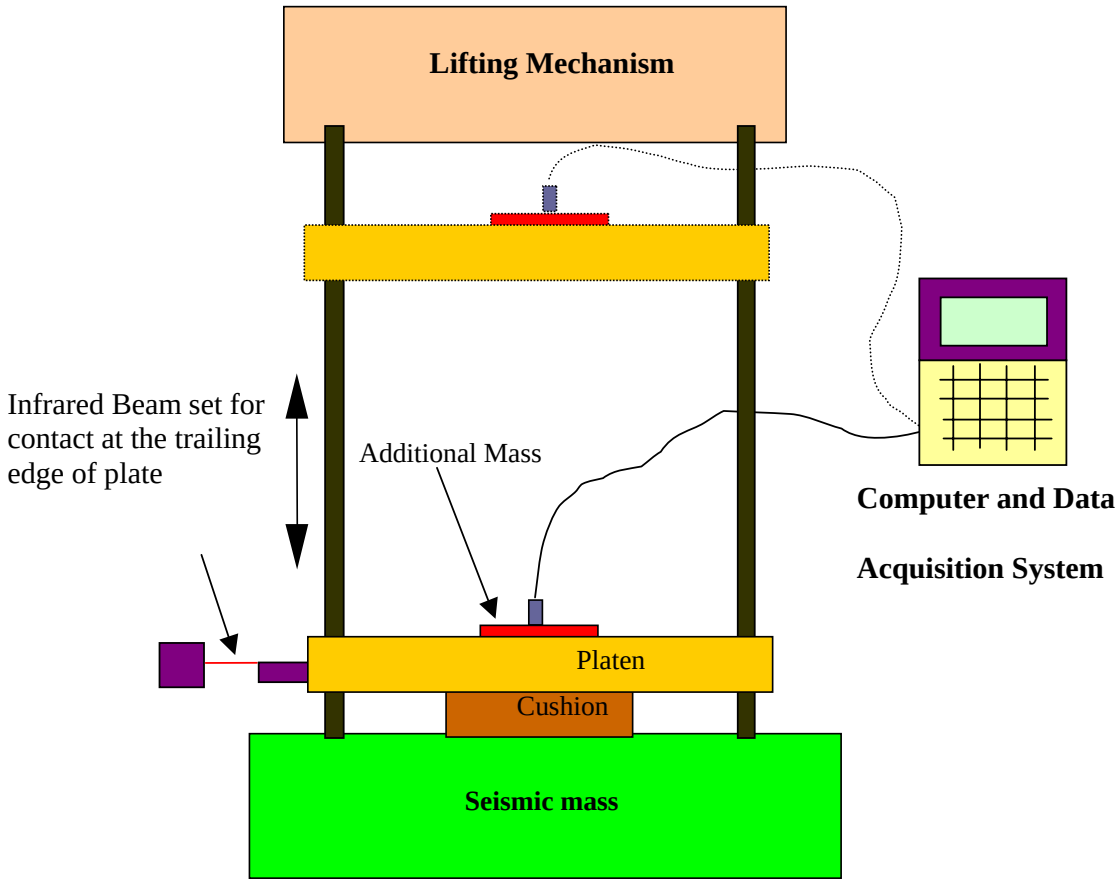

Figure 4.7 Experimental set up for determining contact velocity

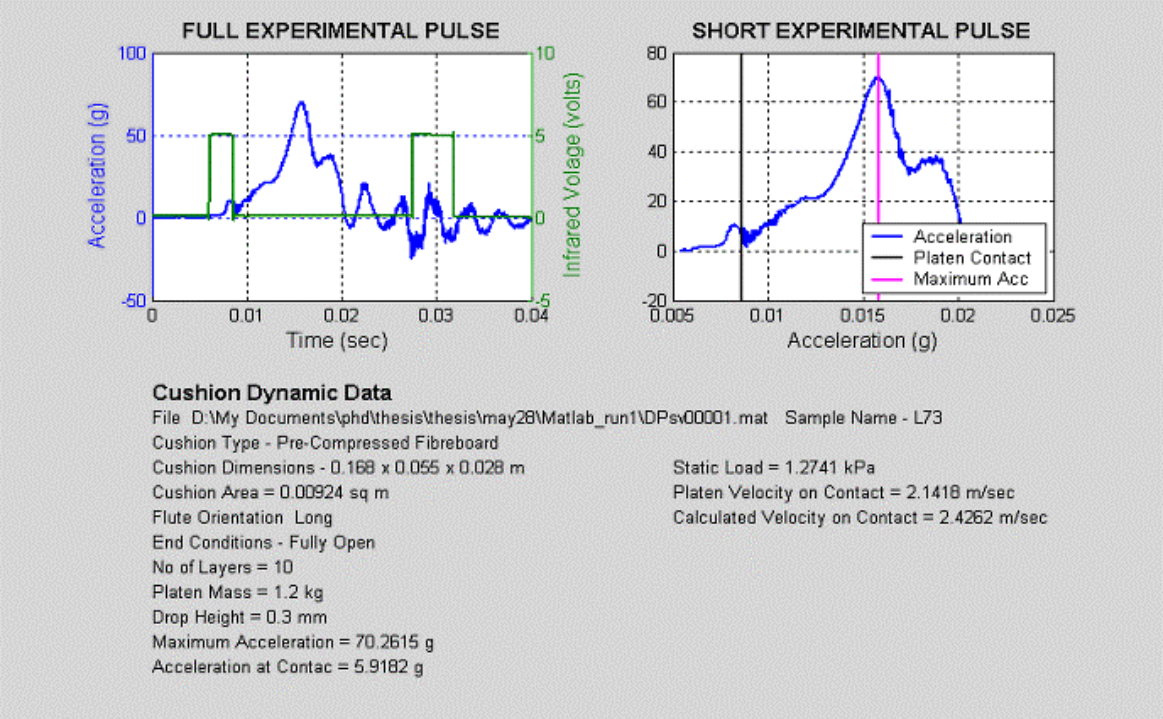

Figure 4.8 Analysis of 168 x 55 x 28 mm Corrugated Fibreboard Cushion Test at 300mm Drop height

Table 4.1 Testing of 166 x 55 Pre-Compressed Corrugated fibreboard Cushions showing Peak Acceleration and Pre-Contact Accelerations and Velocity. Drop height 300 – 250mm.

Preliminary Testing of Corrugated Fibreboard Cushions May28-2003			
Sample Number	L73		
Size (mm)	166 x 55 x 28		
No of Layers	10		
Drop Height (mm)	300		
Platen Mass (kg)	1.2		
Static Load (kPa)	1.274		
Calc Velocity (m/s)	2.426		
File Path	\Matlab_run1\DPsv000		
File	**Maximum Acceleration (g)**	**Contact Acceleration (g)**	**Contact Velocity (m/s)**
1	70.262	5.918	2.142
2	80.644	11.044	2.319
3	80.644	11.034	2.319
4	91.315	4.238	2.750
5	96.379	9.205	3.049
6			
Mean	83.849	8.288	2.516
Standard Deviation	10.221	3.082	0.373

Sample Number	L73		
Size (mm)	166 x 55 x 28		
No of Layers	10		
Drop Height (mm)	250		
Platen Mass (kg)	1.2		
Static Load (kPa)	1.274		
Calc Velocity (m/s)	2.215		
File Path	\Matlab_run2\DPsv000		
File	**Maximum Acceleration (g)**	**Contact Acceleration (g)**	**Contact Velocity (m/s)**
1	63.727	8.933	3.507
2	66.092	7.599	4.676
3	65.957	3.953	1.935
4	65.957	3.953	1.935
5	68.009	5.306	2.227
6	69.718	6.941	1.976
7	77.209	5.501	3.263
Mean	66.577	6.027	2.788
Standard Deviation	2.052	1.878	1.060

Table 4.2 Testing of 166 x 168 Pre-Compressed Corrugated fibreboard Cushions showing Peak Acceleration and Pre-Contact Accelerations and Velocity with Drop height 300mm.

Preliminary Testing of Corrugated Fibreboard Cushions May28-2003			
Sample Number	SQ50		
Size (mm)	166 x 166 x 28		
No of Layers	10		
Drop Height (mm)	300		
Platen Mass (kg)	1.2		
Static Load (kPa)	0.417		
Calc Velocity (m/s)	2.426		
File Path	\Matlab_run69\DPsv000		
File	**Maximum Acceleration (g)**	**Contact Acceleration (g)**	**Contact Velocity (m/s)**
1	59.217	28.022	2.018
2	51.487	21.689	2.281
3	53.290	22.529	2.527
4	53.494	11.787	2.923
5	52.843	26.286	2.358
6	55.507	20.471	3.083
Mean	54.306	21.797	2.532
Standard Deviation	2.733	5.682	0.403

Preliminary Testing of Corrugated Fibreboard Cushions May28-2003			
Sample Number	SQ51		
Size (mm)	166 x 166 x 28		
No of Layers	10		
Drop Height (mm)	300		
Platen Mass (kg)	1.2		
Static Load (kPa)	0.417		
Calc Velocity (m/s)	2.426		
File Path	\Matlab_run50\DPsv000		
File	**Maximum Acceleration (g)**	**Contact Acceleration (g)**	**Contact Velocity (m/s)**
1	54.756	30.936	2.834
2	54.466	18.555	3.017
3	56.841	26.721	2.953
4			
5			
6			
Mean	55.354	25.404	2.935
Standard Deviation	1.296	6.295	0.093

Table 4.3 Testing of 166 x 166 Pre-Compressed Corrugated fibreboard Cushions showing Peak Acceleration and Pre-Contact Accelerations and Velocity with Drop height 300mm and differing Platen masses.

Preliminary Testing of Corrugated Fibreboard Cushions May28-2003			
Sample Number	SQ54		
Size (mm)	166 x 166 x 28		
No of Layers	10		
Drop Height (mm)	300		
Platen Mass (kg)	1.217		
Static Load (kPa)	0.417		
Calc Velocity (m/s)	2.426		
File Path	\Matlab_run43\DPsv000		
File	**Maximum Acceleration (g)**	**Contact Acceleration (g)**	**Contact Velocity (m/s)**
1	57.715	20.106	3.331
2	56.309	26.883	2.551
3	55.271	20.402	3.181
4	54.408	19.089	2.506
5	64.344	25.261	2.045
6			
Mean	57.609	22.348	2.723
Standard Deviation	3.962	3.482	0.528

Preliminary Testing of Corrugated Fibreboard Cushions June 13-2003			
Sample Number	SQ54		
Size (mm)	166 x 166 x 28		
No of Layers	10		
Drop Height (mm)	320		
Platen Mass (kg)	5.8		
Static Load (kPa)	0.417		
Calc Velocity (m/s)	2.506		
File Path	\Matlab_run28\DPsv000		
File	**Maximum Acceleration (g)**	**Contact Acceleration (g)**	**Contact Velocity (m/s)**
1	114.380	5.144	2.919
2	124.838	3.400	3.292
3	132.349	3.694	3.539
4	135.442	3.035	3.879
5	136.994	4.535	2.696
6			
Mean	128.801	3.962	3.265
Standard Deviation	9.321	0.862	0.473

There was some difficulty during these tests to obtain consistency in the measurement of the contact velocity and acceleration at the contact point. However it can be clearly seen from Figure 4.8 and from Table 4.1 to Table 4.3, that there is some registration of acceleration prior to the platen making contact with the test cushion despite inaccuracies of velocity measurement. This confirms that there may be difficulty in deciding exactly when the acceleration pulse begins. The curve in Figure 4.8 also shows a fluctuation around the area of platen contact. It is thought that this observation is a result of air being trapped just above the cushion before impact.

It can be seen by comparing the results of Table 4.1and Table 4.2 as the size of the cushion is increased (from 55mm wide to 168mm wide), the pre-contact acceleration increases from approximately 8g to somewhere about 25g, which suggests a larger contact are would allow more air to be trapped. The results from Table 4.3 where the load was increased from a light (1.2kg) to heavy platen (5.8kg) the pre-contact acceleration decreased suggesting the impact force is so great the pre-acceleration has less significance. It was also noticed that the testing procedure used for this testing could not accurately determine the contact velocity.

The results have shown that as the platen approaches the cushion there exists some pre-contact acceleration. A consequence is that more than peak acceleration should be considered during cushion testing.

Based on these results the hypotheses posed in chapter two should have the additional question:

> Is there build up of air pressure just prior to impact and how does it affect the acceleration pulse and the deformation velocity?

This will be further discussed in chapter 5.

4.3 Testing for Acceleration with Differing End Conditions

As suggested in chapter 3 developed models should be checked experimentally by progressively blocking the ends to increase the flute exit pressure P_x thus varying the pressure terms of the model to lower the acceleration. To assist in the verification of the post contact model developed in chapter 3 equations (3.20 and (3.23) are restated here as equations (4.3) and (4.4). Cushion tests were carried out on square cushions of multi layered corrugated fibreboard with the view of changing the pressure conditions.

$$\ddot{h} = 2\left[\frac{A_t\left(P_0 - P_x\right) - F_f}{\rho D x^2} - \frac{1}{h_t}\left(\dot{h}\right)^2\right]$$

where $\ddot{h}$ = acceleration of the platen or load due to air effects.

$\dot{h}$ = platen or load velocity

h_t = height at any point in time

A_t = exit area of cushion cross section at any point in time

F_f = frictional resisting force

P_0 = average air pressure

P_x = air pressure at point x and is

equal to atmospheric pressure at the extremity

D = control volume width

x = distance from CVcentre to point under consideration

= the cushion length at the extremity

ρ = air density (4.3)

$$a = \left(\frac{F \times IF - kx_d}{m} \right) - 2\left[\frac{A_t \left(P_0 - P_x \right) - F_f}{\rho DL^2} - \frac{1}{h_t} \left(\dot{h} \right)^2 \right]$$

where

a = platen total acceleration

F = forcing function

IF = impact factor (4.4)

x_d = cushion displacement

k = cushion satic stiffness

m = platen mass

L = the cushion length

The end conditions were varied by progressively closing the ends by taping then performing five consecutive cushion tests at each situation. This has the effect of throttling the flow of air in some flutes, apart from some leakage. In theory the pressure term $\left(P_0 - P_x \right)$ in equation (4.4) tends to be equalized resulting in direct pressure resistance.

The cushion tests were carried out on a Lansmont cushion tester using the 5.8kg platen. The data was recorded using Data Physics SignalCalc ACE V 4.0 data acquisition system. These test were carried out at the same time as those carried out in section 4.2.

The data captured was converted to Matlab® mat files. Software was written to read and analyse the data gathered in these files. The software can be referred to in Appendix A. The following graphs show the resulting acceleration pulses for the end conditions fully open, 70% open , 50% open, 25% open and fully closed. Five drops were performed on each cushion

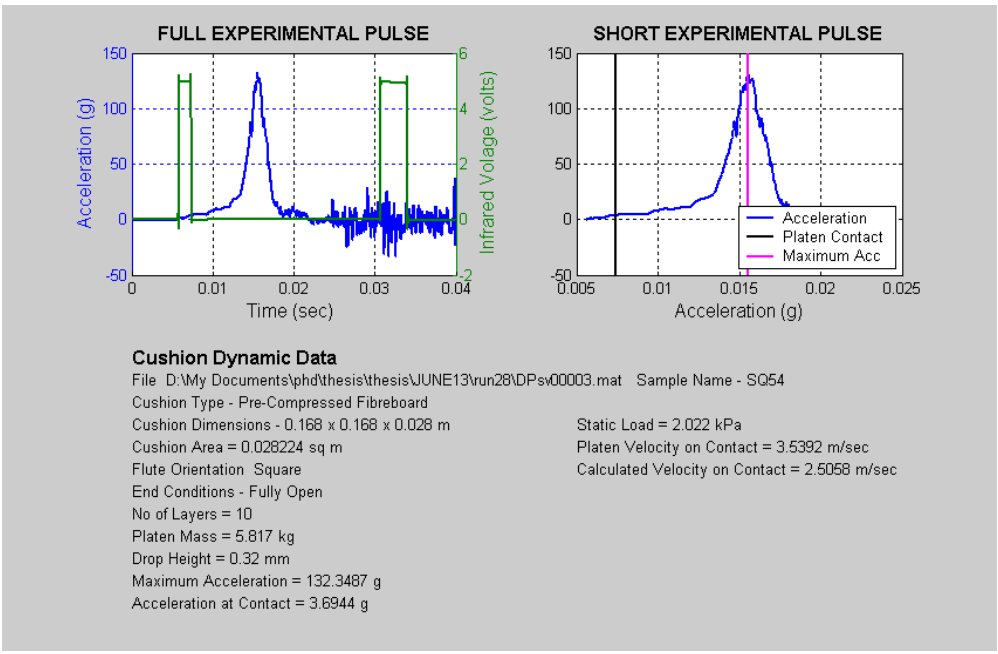
FULL EXPERIMENTAL PULSE
SHORT EXPERIMENTAL PULSE
Acceleration (g)
Infrared Volage (volts)
Time (sec)
Acceleration (g)
Acceleration
Platen Contact
Maximum Acc
Cushion Dynamic Data
File D:\My Documents\phd\thesis\thesis\JUNE13\run28\DPsv00003.mat Sample Name - SQ54
Cushion Type - Pre-Compressed Fibreboard
Cushion Dimensions - 0.168 x 0.168 x 0.028 m
Cushion Area = 0.028224 sq m
Flute Orientation Square
End Conditions - Fully Open
No of Layers = 10
Platen Mass = 5.817 kg
Drop Height = 0.32 mm
Maximum Acceleration = 132.3487 g
Acceleration at Contact = 3.6944 g
Static Load = 2.022 kPa
Platen Velocity on Contact = 3.5392 m/sec
Calculated Velocity on Contact = 2.5058 m/sec

(a)

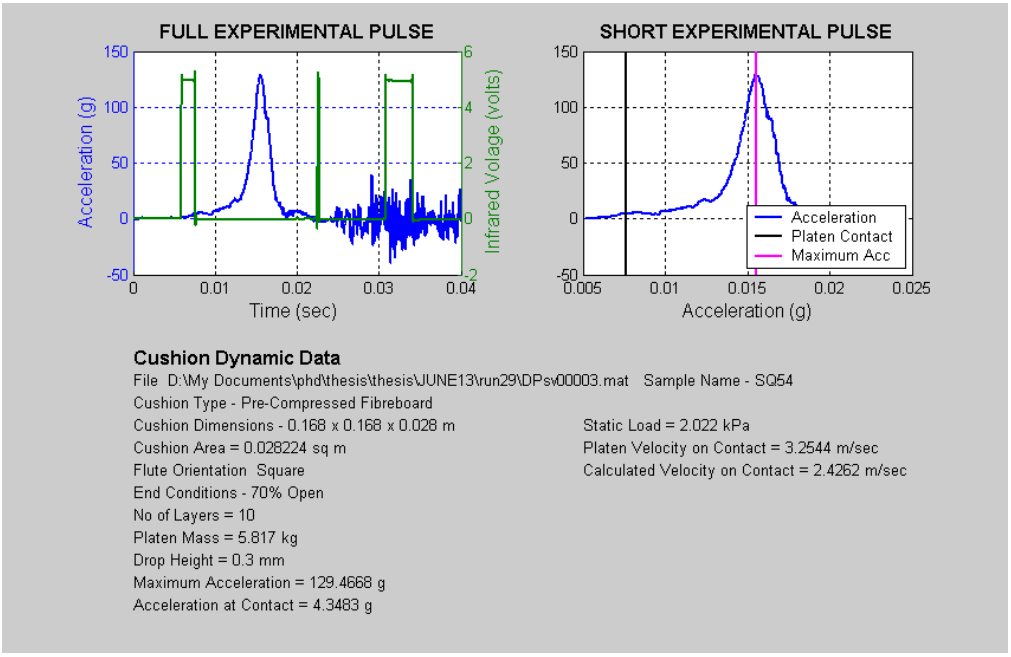
FULL EXPERIMENTAL PULSE
SHORT EXPERIMENTAL PULSE
Acceleration (g)
Infrared Volage (volts)
Time (sec)
Acceleration (g)
Acceleration
Platen Contact
Maximum Acc
Cushion Dynamic Data
File D:\My Documents\phd\thesis\thesis\JUNE13\run29\DPsv00003.mat Sample Name - SQ54
Cushion Type - Pre-Compressed Fibreboard
Cushion Dimensions - 0.168 x 0.168 x 0.028 m
Cushion Area = 0.028224 sq m
Flute Orientation Square
End Conditions - 70% Open
No of Layers = 10
Platen Mass = 5.817 kg
Drop Height = 0.3 mm
Maximum Acceleration = 129.4668 g
Acceleration at Contact = 4.3483 g
Static Load = 2.022 kPa
Platen Velocity on Contact = 3.2544 m/sec
Calculated Velocity on Contact = 2.4262 m/sec

(b)

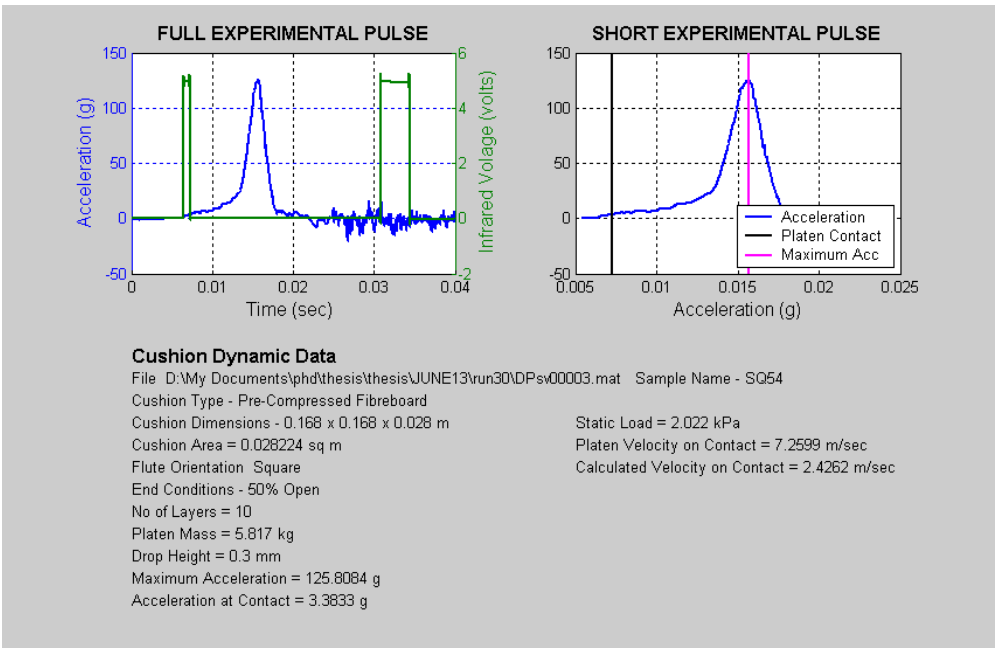
FULL EXPERIMENTAL PULSE
SHORT EXPERIMENTAL PULSE
Acceleration (g)
Infrared Volage (volts)
Time (sec)
Acceleration (g)
Acceleration
Platen Contact
Maximum Acc
Cushion Dynamic Data
File D:\My Documents\phd\thesis\thesis\JUNE13\run30\DPsv00003.mat Sample Name - SQ54
Cushion Type - Pre-Compressed Fibreboard
Cushion Dimensions - 0.168 x 0.168 x 0.028 m
Cushion Area = 0.028224 sq m
Flute Orientation Square
End Conditions - 50% Open
No of Layers = 10
Platen Mass = 5.817 kg
Drop Height = 0.3 mm
Maximum Acceleration = 125.8084 g
Acceleration at Contact = 3.3833 g
Static Load = 2.022 kPa
Platen Velocity on Contact = 7.2599 m/sec
Calculated Velocity on Contact = 2.4262 m/sec

(c)

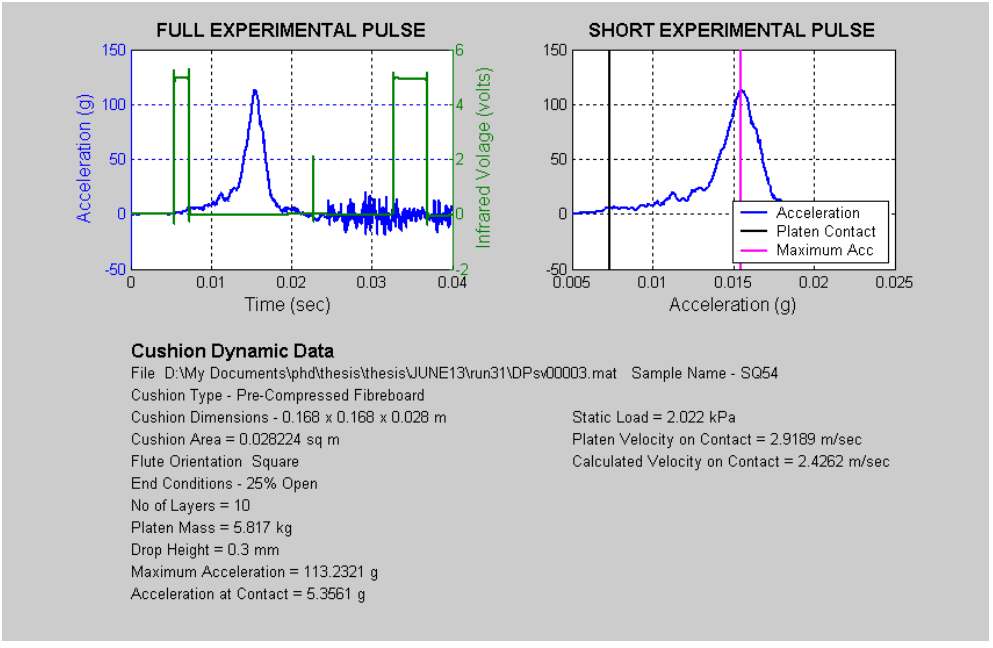
FULL EXPERIMENTAL PULSE
SHORT EXPERIMENTAL PULSE
Acceleration (g)
Infrared Volage (volts)
Time (sec)
Acceleration (g)
Acceleration
Platen Contact
Maximum Acc
Cushion Dynamic Data
File D:\My Documents\phd\thesis\thesis\JUNE13\run31\DPsv00003.mat Sample Name - SQ54
Cushion Type - Pre-Compressed Fibreboard
Cushion Dimensions - 0.168 x 0.168 x 0.028 m
Cushion Area = 0.028224 sq m
Flute Orientation Square
End Conditions - 25% Open
No of Layers = 10
Platen Mass = 5.817 kg
Drop Height = 0.3 mm
Maximum Acceleration = 113.2321 g
Acceleration at Contact = 5.3561 g
Static Load = 2.022 kPa
Platen Velocity on Contact = 2.9189 m/sec
Calculated Velocity on Contact = 2.4262 m/sec

(d)

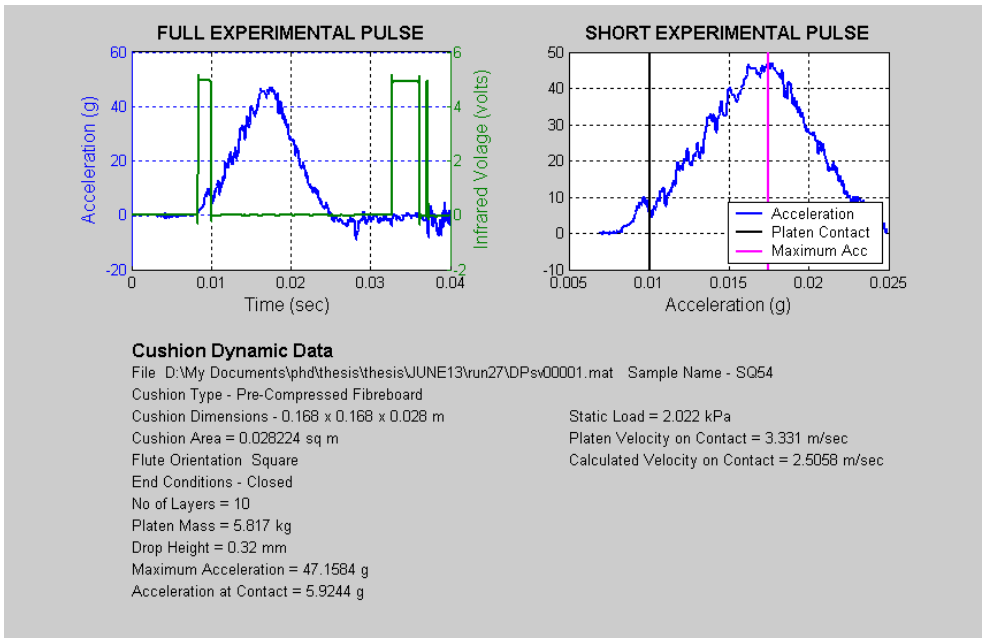

(e)

Figure 4.9 (a) (b) (c) (d) and (e) Show results of software analysis of varying end condition tests.

Table 4.4 Typical summary of results of varying end condition tests

Testing of Corrugated Fibreboard Cushions June13-2003

Sample Number	SQ54
Size (mm)	166 x 166 x 28
No of Layers	10
Drop Height (mm)	300
Platen Mass (kg)	5.817
Static Load (kPa)	2.022
Calc Velocity (m/s)	2.426
End Condition	Fully Open
File Path	\Matlab_run28\DPsv000

File	Maximum Acceleration (g)	Contact Acceleration (g)
1	114.380	5.147
2	124.837	3.999
3	132.349	3.694
4	135.442	3.034
5	136.994	4.535
6		
Mean	128.800	4.082
Standard Deviation	9.321	0.805

Sample Number	SQ54
Size (mm)	166 x 166 x 28
No of Layers	10
Drop Height (mm)	300
Platen Mass (kg)	5.817
Static Load (kPa)	2.022
Calc Velocity (m/s)	2.506
End Condition	70% Open
File Path	\Matlab_run29\DPsv000

File	Maximum Acceleration (g)	Contact Acceleration (g)
1	111.197	5.109
2	127.616	2.357
3	129.470	4.348
4	133.070	3.560
5	135.034	3.423
6		
Mean	127.277	3.759
Standard Deviation	9.450	1.035

Sample Number	SQ54
Size (mm)	166 x 166 x 28
No of Layers	10
Drop Height (mm)	300
Platen Mass (kg)	5.817
Static Load (kPa)	2.022
Calc Velocity (m/s)	2.506
End Condition	50% Open
File Path	\Matlab_run30\DPsv000

File	Maximum Acceleration (g)	Contact Acceleration (g)
1	103.116	5.400
2	126.960	2.718
3	125.810	3.383
4	130.945	3.562
5	127.036	3.458
6		
Mean	122.773	3.704
Standard Deviation	11.159	1.004

Table 4.5 Typical summary of results of varying end condition tests (continued)

Sample Number	SQ54	
Size (mm)	166 x 166 x 28	
No of Layers	10	
Drop Height (mm)	300	
Platen Mass (kg)	5.817	
Static Load (kPa)	2.022	
Calc Velocity (m/s)	2.506	
End Condition	25% Open	
File Path	\Matlab_run31\DPsv000	
File	**Maximum Acceleration (g)**	**Contact Acceleration (g)**
1	84.715	6.837
2	116.348	4.972
3	113.238	5.356
4	115.452	4.359
5	120.027	5.335
6		
Mean	109.956	5.372
Standard Deviation	14.321	0.913

Sample Number	SQ54	
Size (mm)	166 x 166 x 28	
No of Layers	10	
Drop Height (mm)	300	
Platen Mass (kg)	5.817	
Static Load (kPa)	2.022	
Calc Velocity (m/s)	2.506	
End Condition	Fully Closed	
File Path	\Matlab_run27\DPsv000	
File	**Maximum Acceleration (g)**	**Contact Acceleration (g)**
1	47.158	5.920
2	49.833	6.181
3	50.944	6.282
4	53.196	6.193
5	51.571	6.078
6		
Mean	50.540	6.131
Standard Deviation	2.248	0.138

SQ54	300mm Drop Height	
Percentage Open	Average Peak Acceleration	Average Contact Acceleration
100	128.800	4.082
70	127.277	3.759
50	122.773	3.704
25	109.956	5.372
0	50.540	6.131

The average peak accelerations for the various end conditions for three cushions of identical dimensions were plotted in Figure 4.10 and the contact acceleration in Figure 4.11.

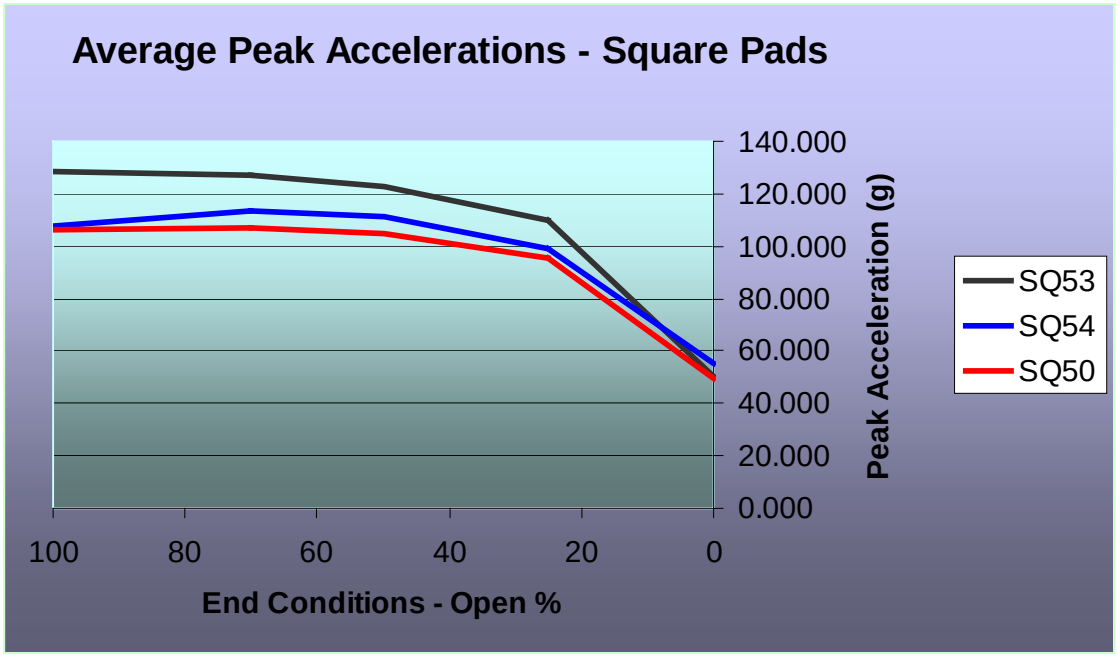

Figure 4.10 Plot of average peak accelerations versus end condition.

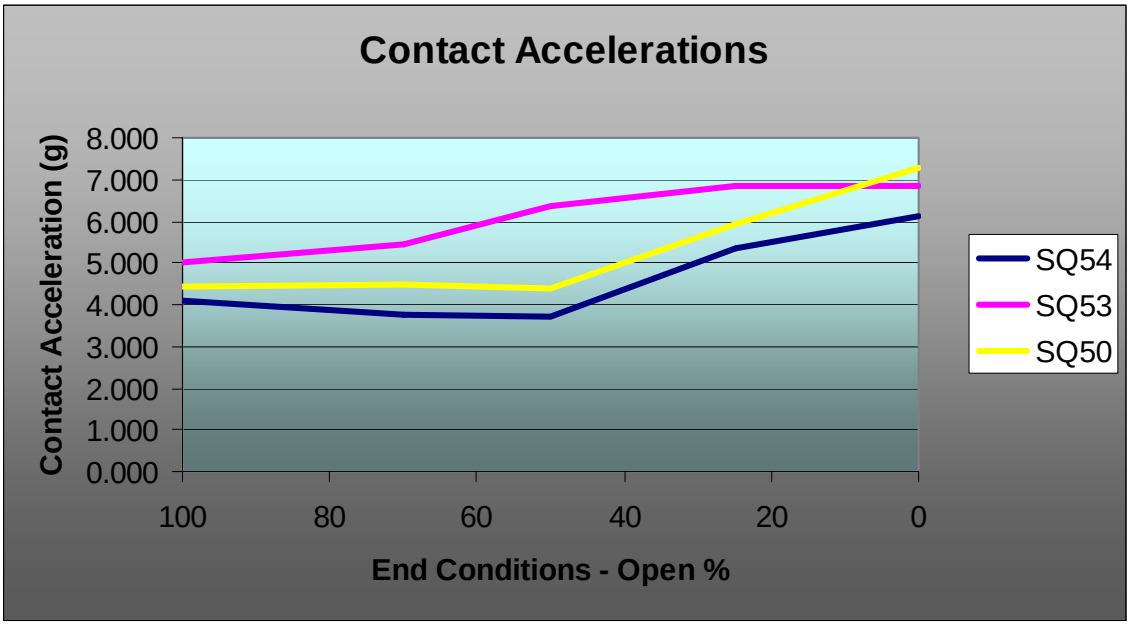

Figure 4.11 Plot of contact accelerations versus the end condition

4.4 Simulation for Acceleration with Differing End Conditions

To compare the airflow model developed in chapter 3 and repeated in this chapter as equations (4.3) and (4.4) with the experimental results of peak acceleration levels shown in Figure 4.10 to Figure 4.11 a simulink model and accompanying software was written with the model is shown in Figure 4.12.

To simulate the experimental work where the ends or flutes were progressively blocked to alter the end conditions, the force term $A_t\left(P_0 - P_x\right) - F_f$ in equation (4.4) is required to be split between representing airflow conditions and pure resisting force. If is allowed to equal F_t then:

$$a = \left(\frac{F \times IF - kx_d}{m}\right) - 2\left[\frac{F_t}{\rho DL^2} - \frac{1}{h_t}\left(\dot{h}\right)^2\right]$$

where (4.5)

$F_t = A_t\left(P_0 - P_x\right)$ is the flute force if fully open

If ends are partly blocked the term F_t can be split as:

$$F_t = F_o + F_c$$

$$F_o = A_t\left(P_0 - P_x\right)K_o$$

and

$$F_c = \frac{F_p}{CA}K_c$$

where

F_t = the pressure force (4.6)

F_o = flute force due to open flutes from the previous model

F_c = resistive for due to closed flutes

CA = cushion area

F_P = platen force

K_o and K_c are experimental and percentage factors

This split pressure term is incorporated in the simulink model based on equation (4.6) and shown in Figure 4.12. The platen force F_p was found to approximately equal to 0.07 * Platen Mass / cushion Area . This is reflected in the Simulink model.

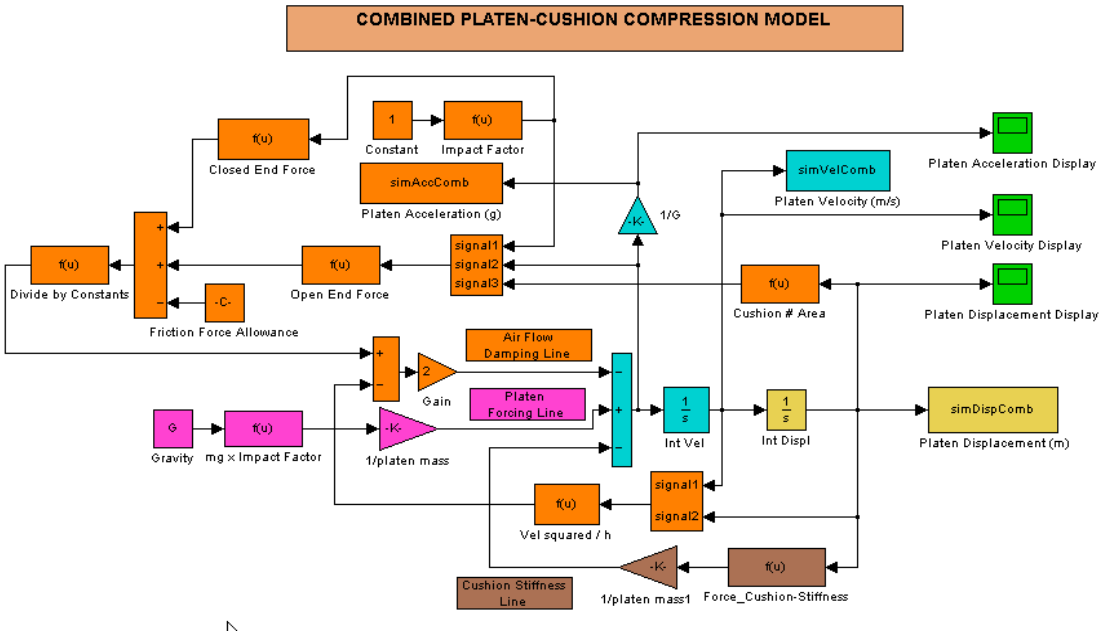

Figure 4.12 Similink Model of Post Contact Dynamic Behaviour of Pre-Compressed Fibreboard

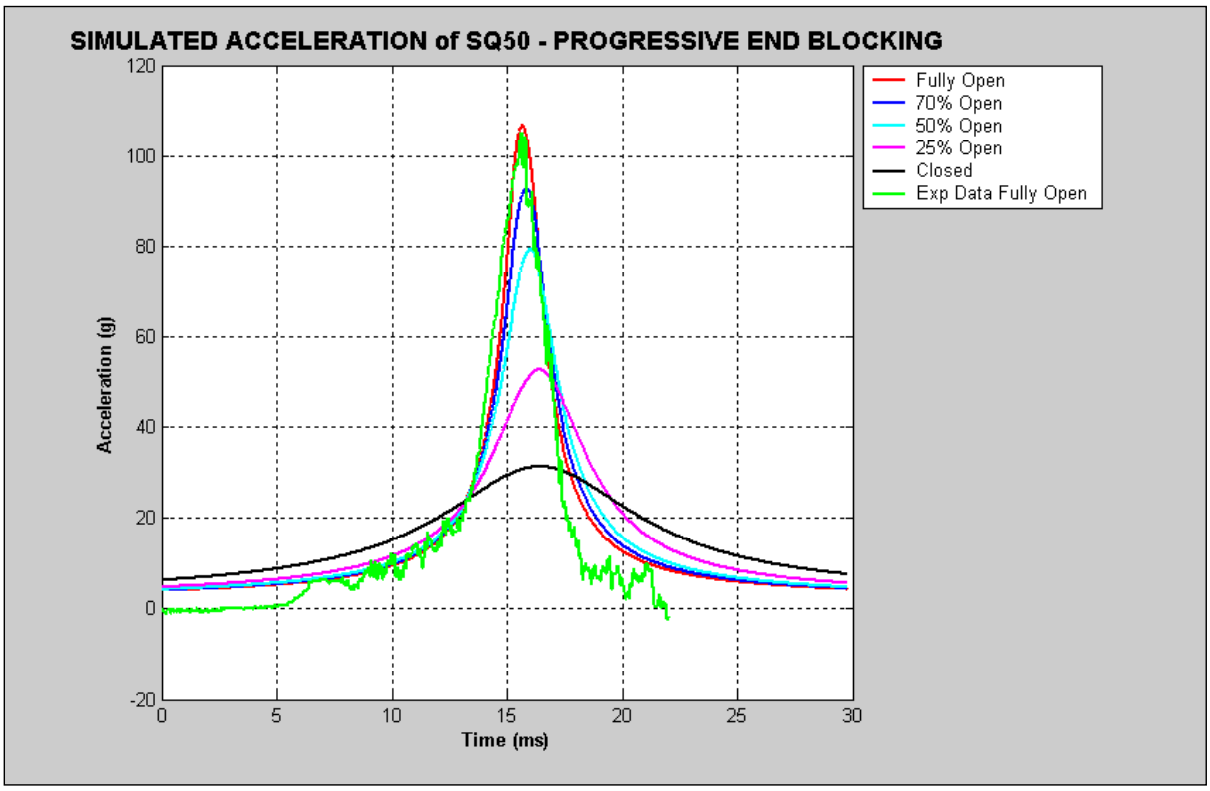

Figure 4.13 Acceleration Simulations for Sample SQ50 with progressive end closing together with Experimental Data

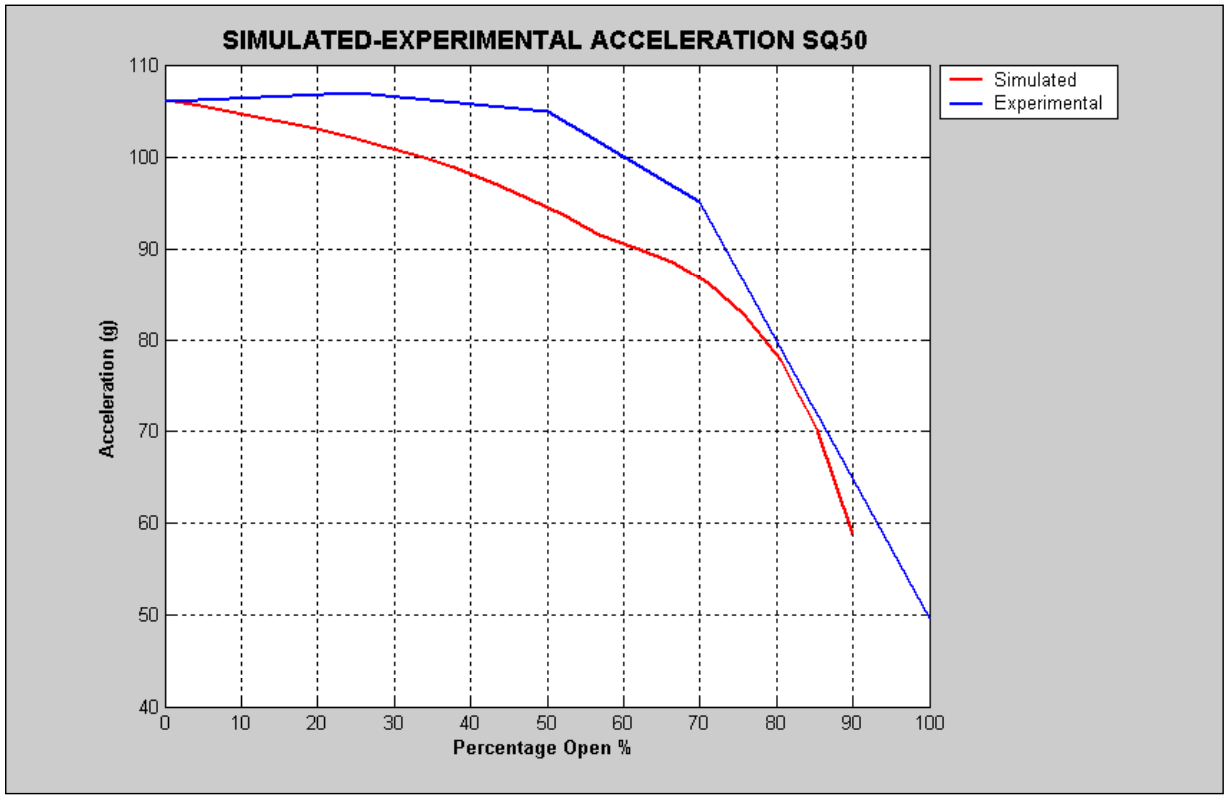

Figure 4.14 Simulations of sample SQ50 – Peak Acceleration vs End Openings

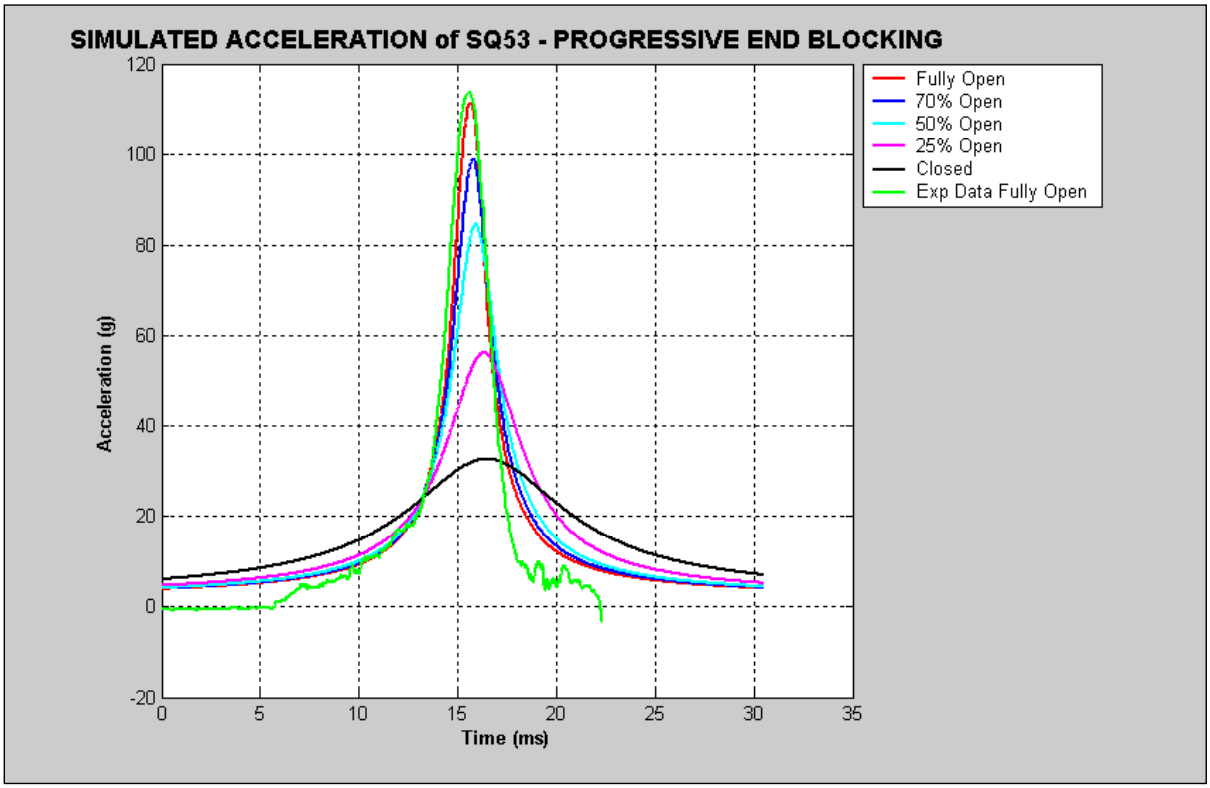

Figure 4.15 Acceleration Simulations for Sample SQ53 with progressive end closing together with Experimental Data

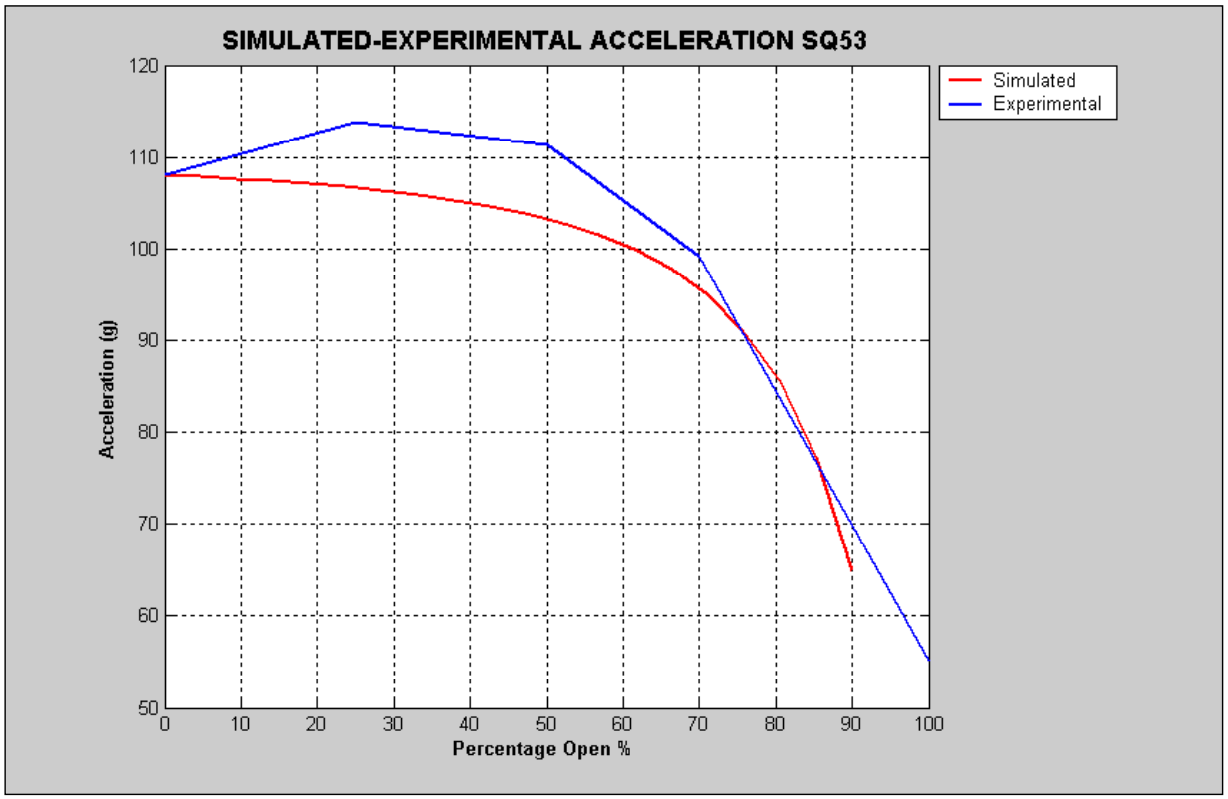

Figure 4.16 Simulations of sample SQ53 – Peak Acceleration vs End Openings

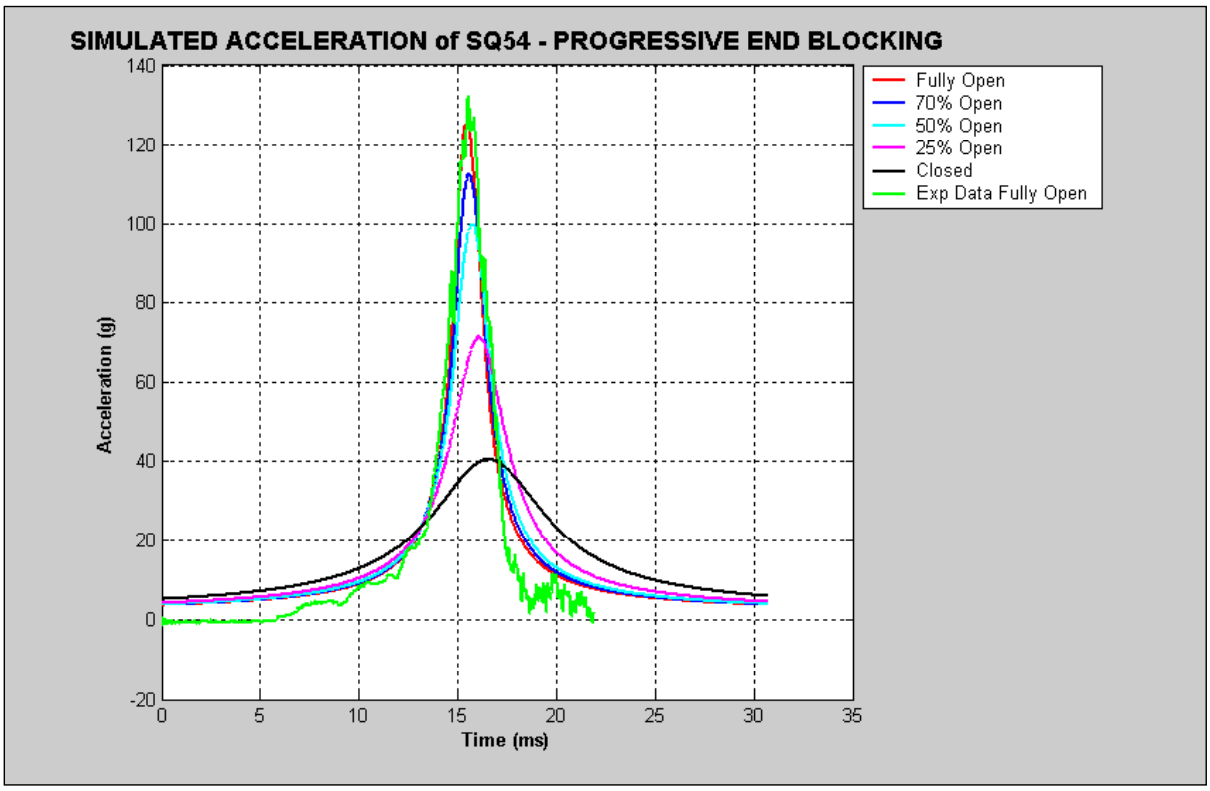

Figure 4.17 Acceleration Simulations for Sample SQ54 with progressive end closing together with Experimental Data

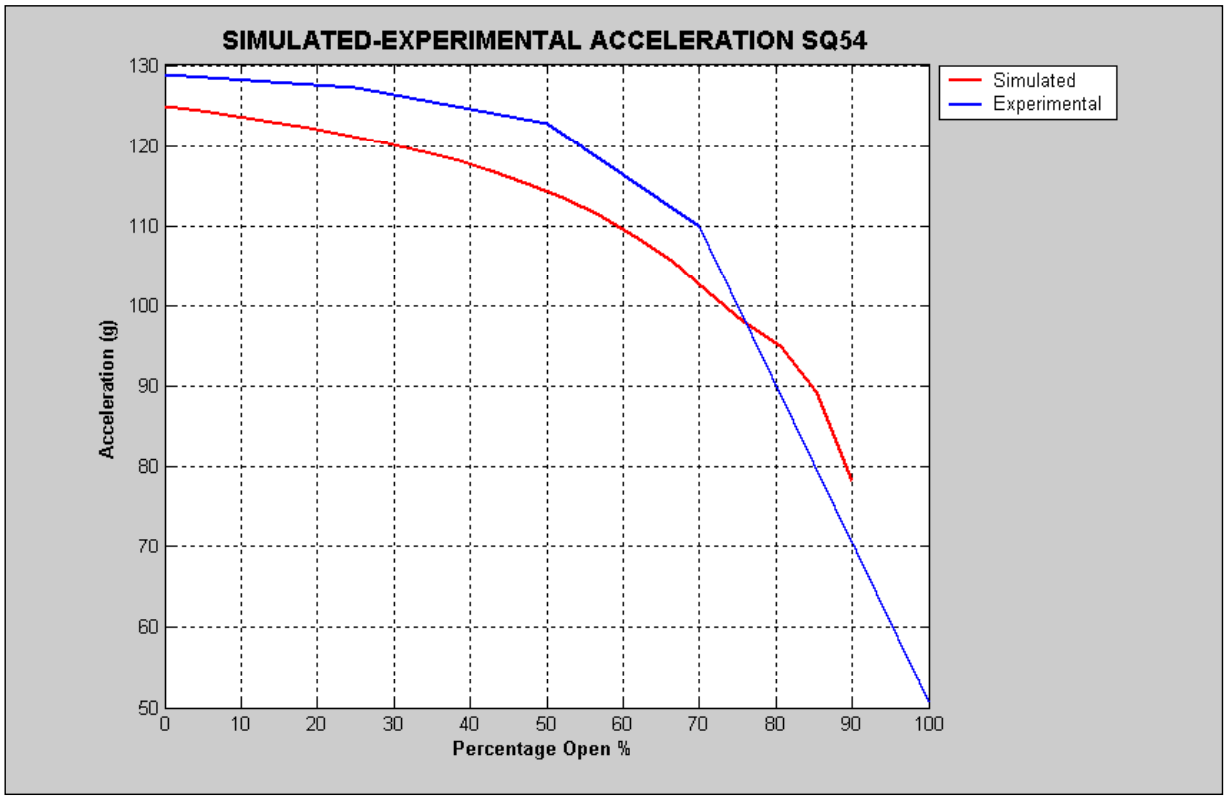

Figure 4.18 Simulations of sample SQ54 – Peak Acceleration vs End Openings

The graphs shown in Figure 4.13 to Figure 4.18 show a comparison of the simulated to the experimental results. In a qualitative way the simulated results tend to coincide with experimental results and verify equations developed in chapter 3.

4.5 Testing for Differing Flute Lengths

As suggested in chapter 3 for identical dimensions of rectangular cushions with the orientation of the flutes either along the larger dimension or along the smaller dimension thus varying the denominator of the model to lower or raise the acceleration. Cushion tests were carried out on rectangular cushions using a Lansmont cushion tester using the 5.8kg platen similar to to those carried out in section 4.3. The data was also recorded using Data Physics SignalCalc ACE V 4.0 data acquisition system and were carried out at the same time as those carried out in section 4.3.

The tests were carried out on pre-compressed corrugated fibreboard cushions of 10 layers using configurations of 112mm long flutes referred to short flutes and 166mm long flutes referred as long flutes. This was to test the theory proposed by Naganathan P., Marcondes J., (1995) and the hypotheses from chapter 2 that with ends completely open to atmosphere longer flutes create more air-flow restriction thus increasing damping and subsequently lower the peak acceleration. The results of these tests are now presented firstly as typical cushion test results followed by a table of results.

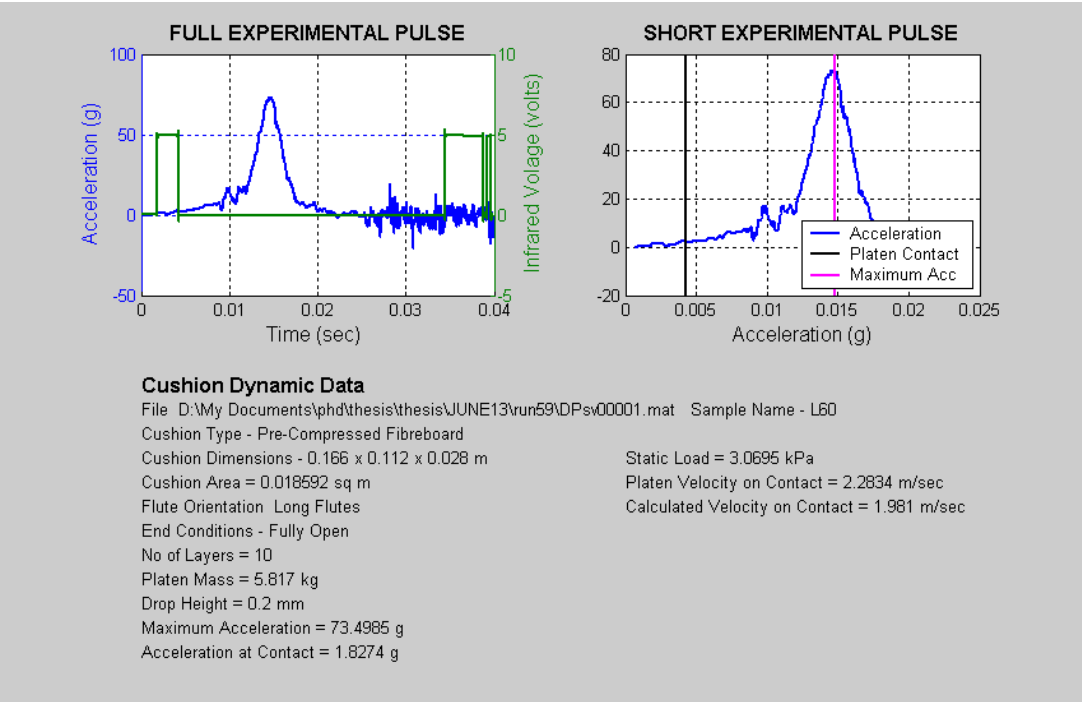

Figure 4.19 Analysis of 168 x 112 mm corrugated fibreboard cushion with long flutes

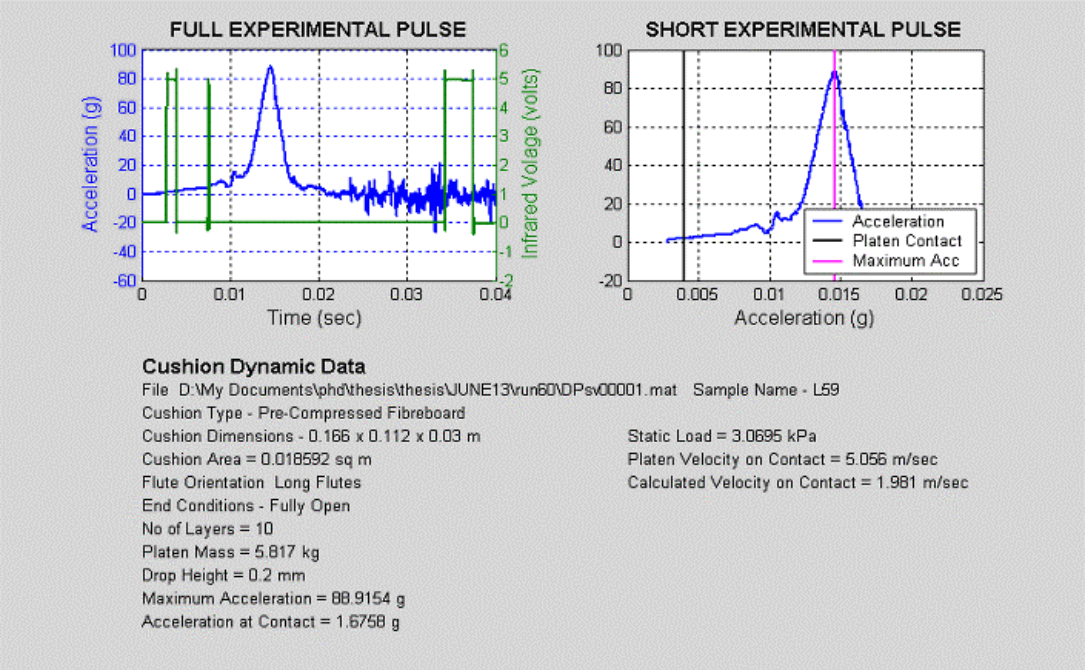

Figure 4.20 analysis of 168 x 112 mm corrugated fibreboard cushion with long flutes

Table 4.6 Typical Results of Long flutes

Testing of Corrugated Fibreboard Cushions June 13-2003

Sample Number	L60	
Size (mm)	166 x 112 x 30	
No of Layers	10	
Flute Configuration	Long 166mm	
Drop Height (mm)	200	
Platen Mass (kg)	5.817	
Static Load (kPa)	3.07	
End Condition	Fully Open	
File Path	\June13\run59\DPsv0000	
File	**Maximum Acceleration (g)**	**Contact Acceleration (g)**
1	73.500	1.830
2	94.100	0.000
3	102.000	0.000
4	102.000	0.000
5	100.000	0.400
Mean	94.320	0.446
Standard Deviation	12.080	0.793

Sample Number	L59	
Size (mm)	166 x 112 x 28	
No of Layers	10	
Flute Configuration	Long 166 mm	
Drop Height (mm)	200	
Platen Mass (kg)	5.817	
Static Load (kPa)	3.07	
End Condition	Fully Open	
File Path	\June13\run60\DPsv0000	
File	**Maximum Acceleration (g)**	**Contact Acceleration (g)**
1	88.900	1.700
2	92.200	1.144
3	98.270	0.500
4	99.600	1.140
5	99.360	0.340
Mean	95.666	0.965
Standard Deviation	4.840	0.550

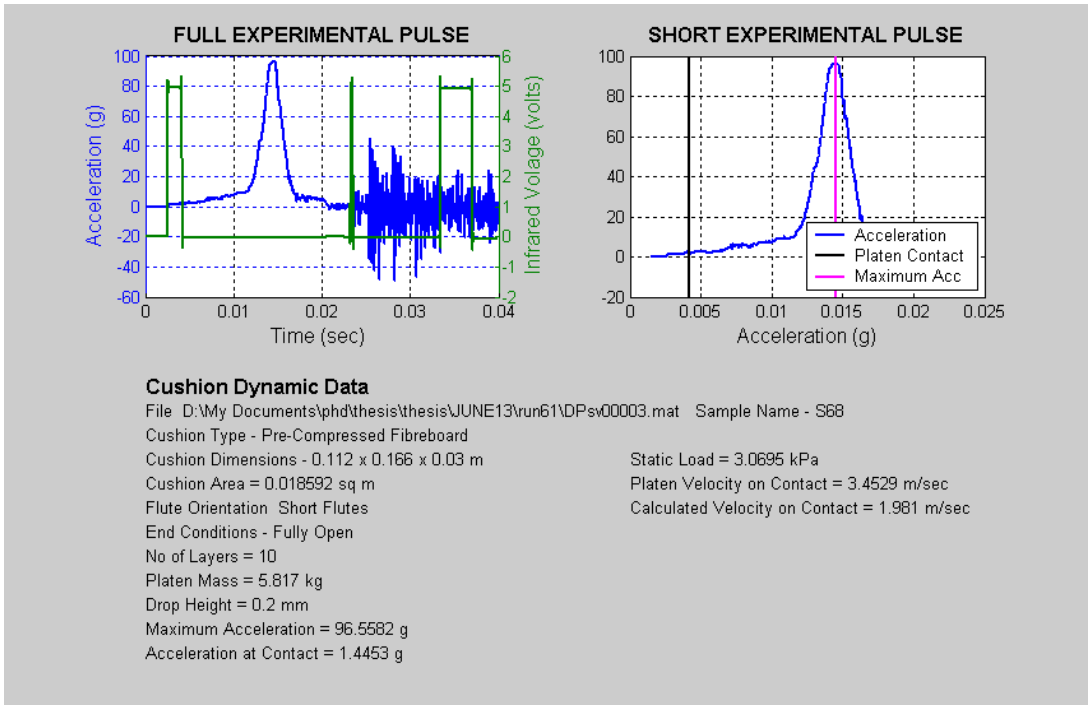

Figure 4.21Analysis of 168 x 112 mm corrugated fibreboard cushion with Short Flutes

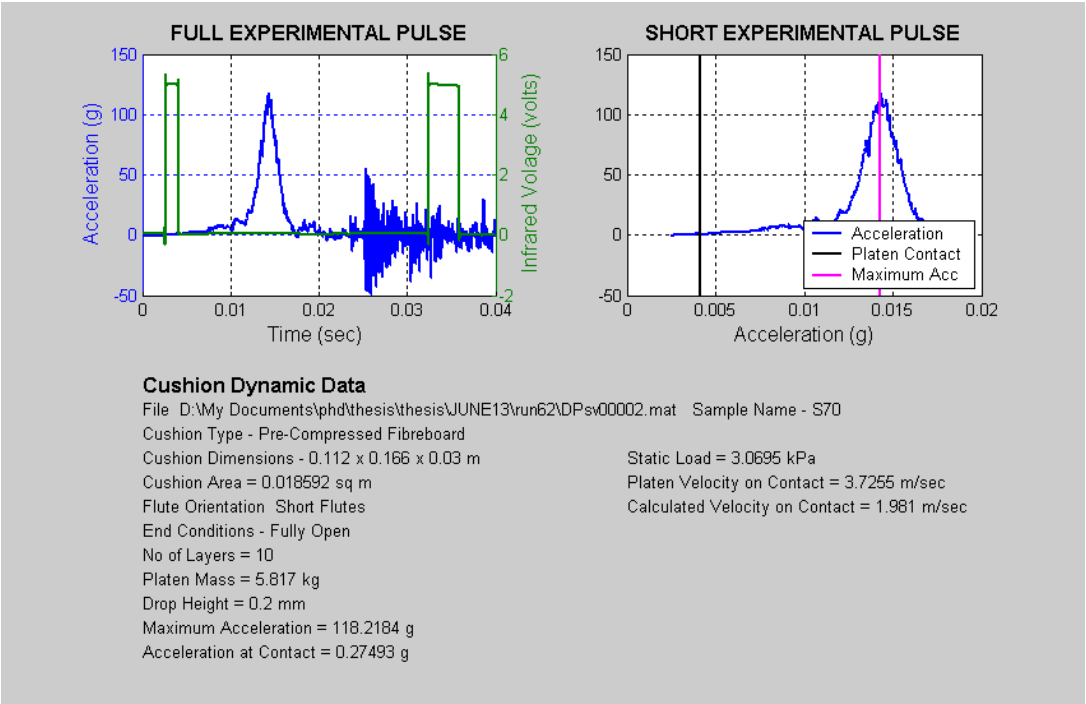

Figure 4.22 Analysis of 168 x 112 mm corrugated fibreboard cushion with Short Flutes

Table 4.7 Typical Results of Long flutes

Testing of Corrugated Fibreboard Cushions June 13-2003		
Sample Number	S68	
Size (mm)	166 x 112 x 28	
No of Layers	10	
Flute Configuration	Short 112 mm	
Drop Height (mm)	200	
Platen Mass (kg)	5.817	
Static Load (kPa)	3.07	
End Condition	Fully Open	
File Path	\June13\run61\DPsv0000	
File	**Maximum Acceleration (g)**	**Contact Acceleration (g)**
1	99.450	2.070
2	95.120	1.440
3	102.430	1.520
4	106.550	1.520
5	105.260	1.450
Mean	101.762	1.600
Standard Deviation	4.612	0.265

Sample Number	S70	
Size (mm)	166 x 112 x 28	
No of Layers	10	
Flute Configuration	Short 112 mm	
Drop Height (mm)	200	
Platen Mass (kg)	5.817	
Static Load (kPa)	3.07	
End Condition	Fully Open	
File Path	\June13\run62\DPsv0000	
File	**Maximum Acceleration (g)**	**Contact Acceleration (g)**
1	104.170	5.590
2	118.220	0.275
3	135.700	0.000
4	145.900	0.000
5	142.500	0.200
Mean	129.298	1.213
Standard Deviation	17.643	2.450

4.6 Simulation for Differing Flute Lengths

To compare the airflow model developed in chapter 3 and repeated in this chapter as equations (4.7) with the experimental results of peak acceleration levels shown in Figure 4.19 to Figure 4.22 a simulink model and accompanying software was written with the model is shown in Figure 4.23.

To simulate the experimental work on cushions with differing flute lengths it is a simple matter of changing the values of D and L in equation (4.7).

$$a = \left(\frac{F \times IF - kx_d}{m} \right) - 2\left[\frac{A_t \left(P_0 - P_x \right) - F_f}{\rho D L^2} - \frac{1}{h_t} \left(\dot{h} \right)^2 \right] \qquad (4.7)$$

where

D and L are the dimensional terms

The graphs in Figure 4.19 to Figure 4.22 show that the simulations coincide with the experimental results.

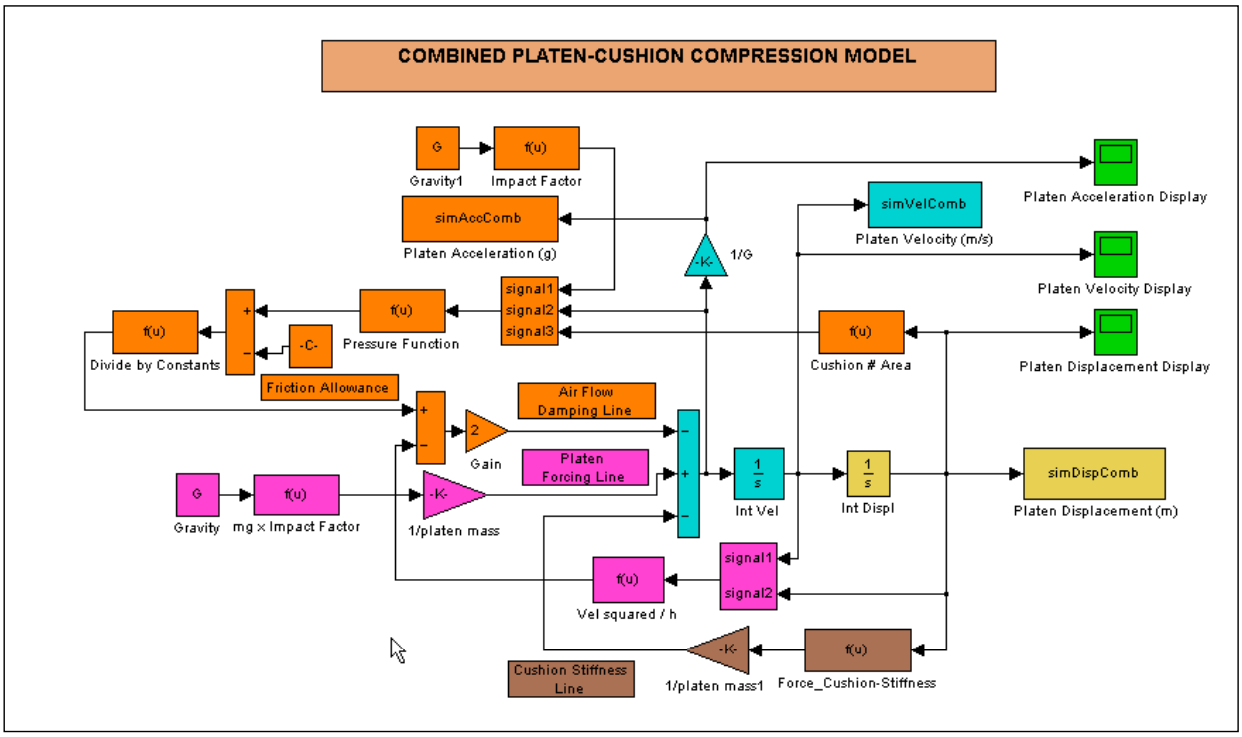

Figure 4.23 Simulink Model to Simulate Cushions of Differing Flute Lengths

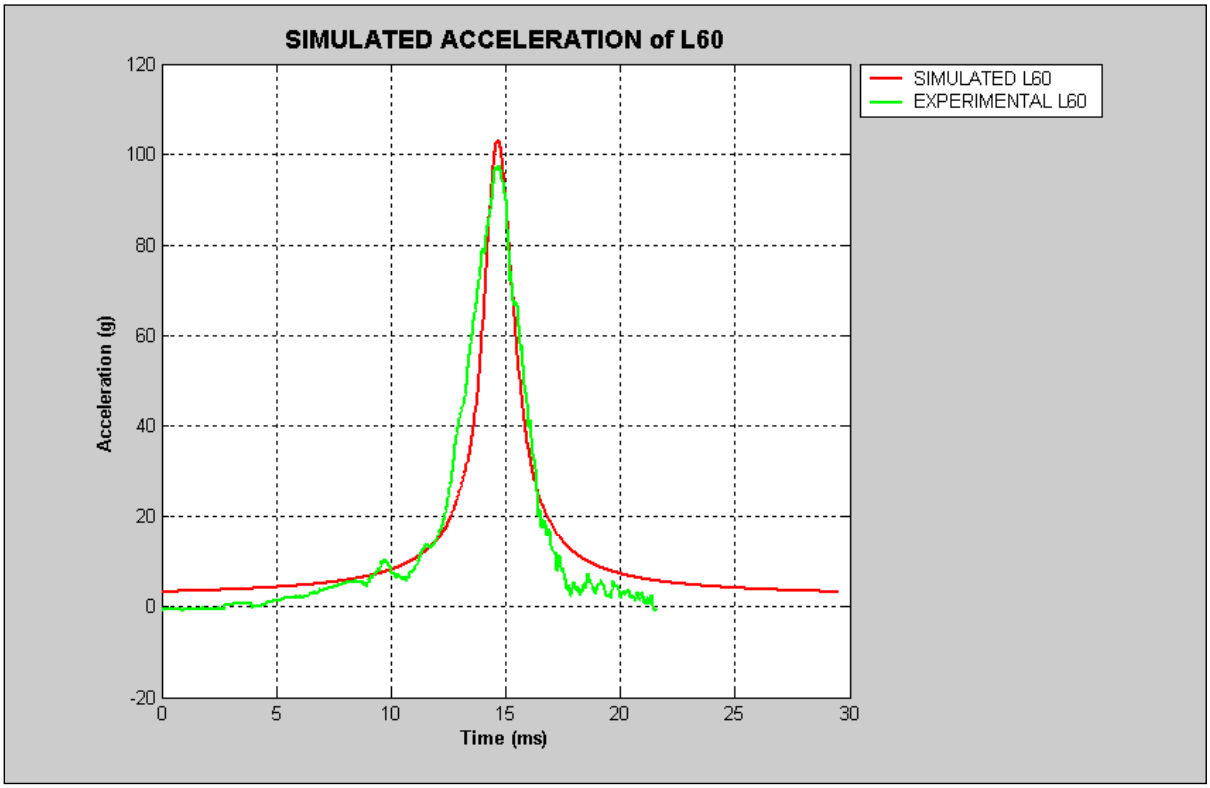

Figure 4.24 Simulated – Experimental Acceleration using long Flutes L60

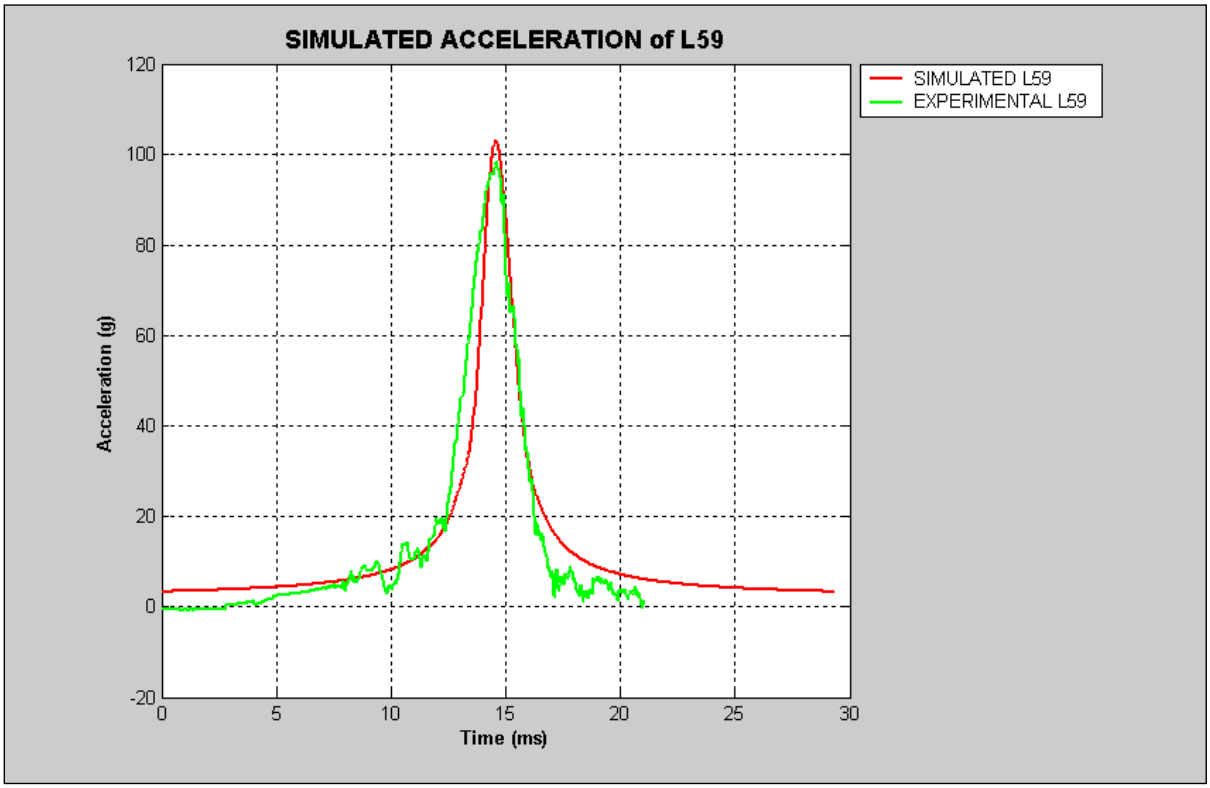

Figure 4.25 Simulated – Experimental Acceleration using long Flutes L59

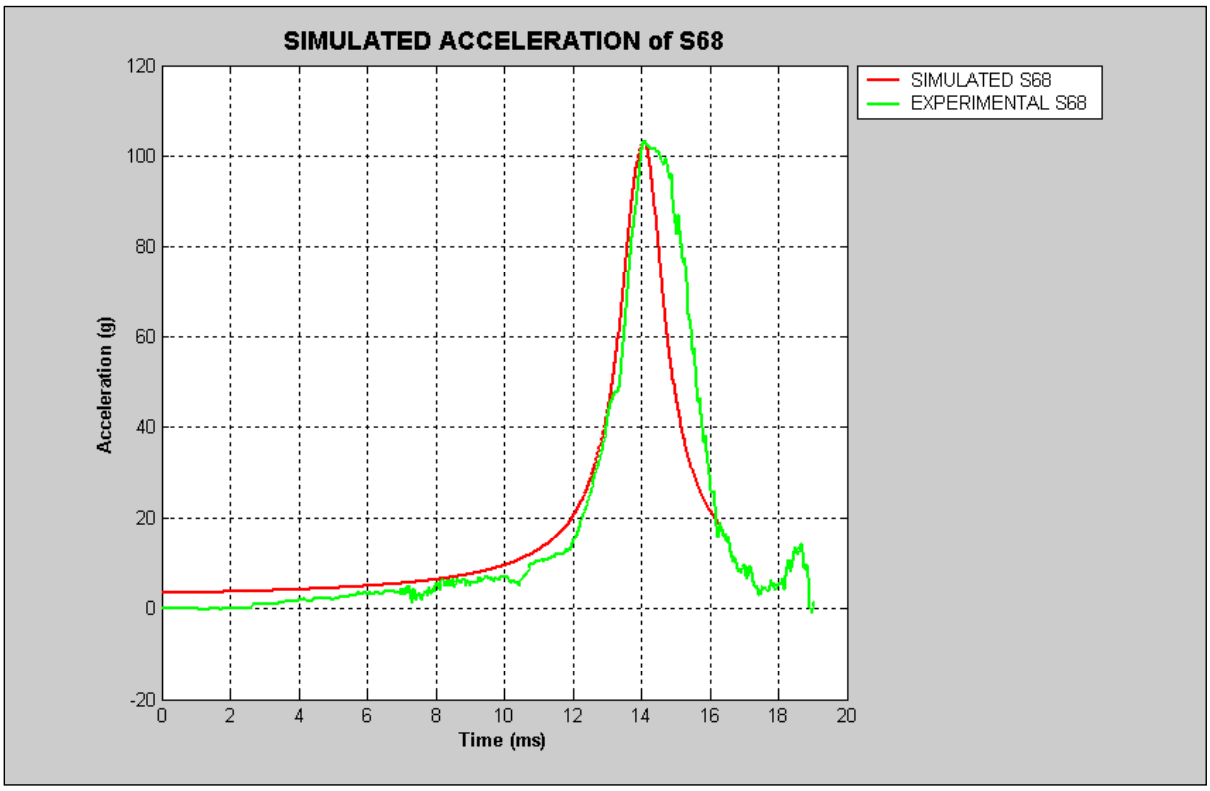

Figure 4.26 Simulated Acceleration using Short Flutes S68

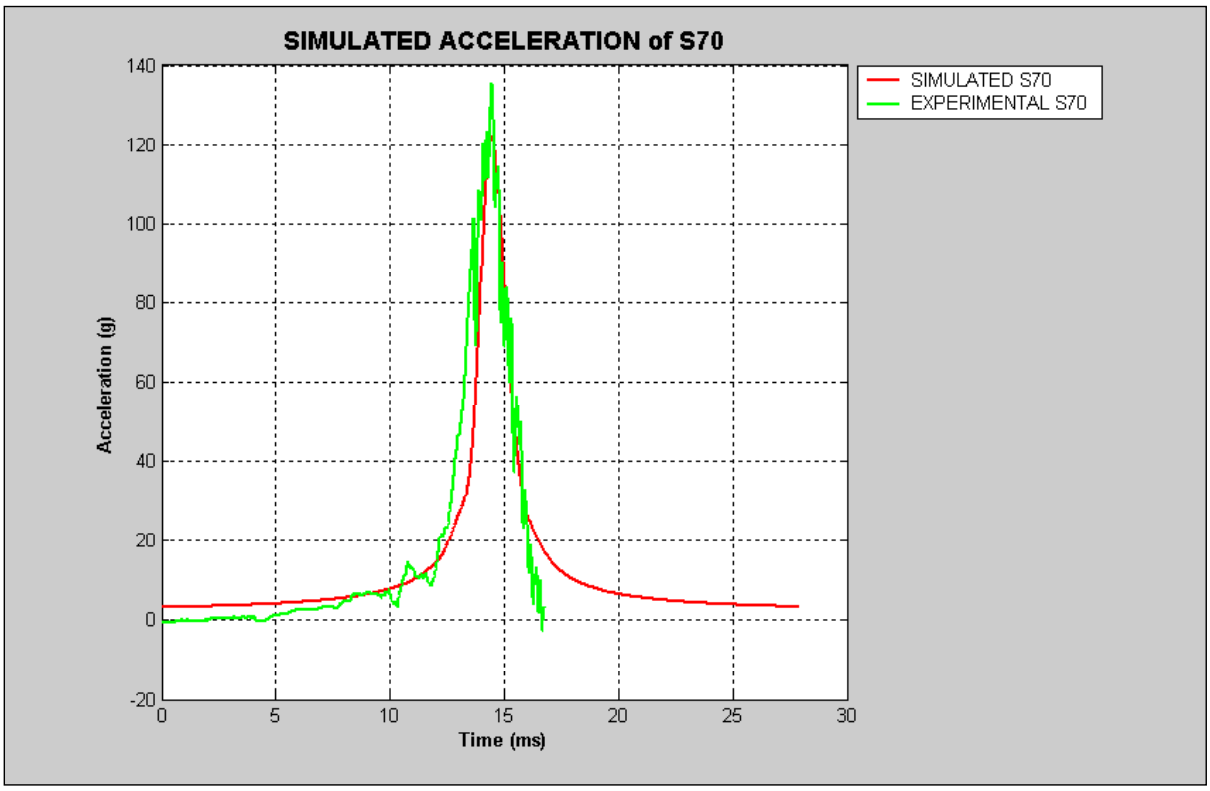

Figure 4.27 Simulated Acceleration using Short Flutes S70

Chapter 5 Development of Platen Pre-Contact Model

This chapter describes the development of mathematical models to describe the flow of air prior to impact when testing multi-layered corrugated fibreboard cushions. Consideration of how the air behaves, the just prior to impact is required for understanding of how acceleration forces manifest themselves during a cushion test.

Reiterating a statement from chapter 4, section 4.2 that an additional hypothesis is posed:

Is there build up of air pressure just prior to impact and how it affects the acceleration pulse and the deformation velocity?

It also means more than peak acceleration should be considered during cushion testing.

The following section is an attempt to derive an expression for the effect of air collection prior to impact of a platen upon a test cushion. This has the effect of registering acceleration even though the platen has made no contact and will explain the difficulties in determining the exact contact point in routine testing.

5.1 Air Behaviour Model Prior to Impact

Due to the speed of a platen approaching a test specimen there will be a build up of pressure because of the inertial effects of the air. To illustrate, consider that blue section of height, h, shown in Figure 5.1 represents the air being trapped between the platen and the cushion. Assuming non-compressible flow a relationship between platen velocity and air velocity can be found by considering the small film or air plate just before impact.

Figure 5.2 shows the difference in the air plate over a small change in time as the platen approaches the cushion.

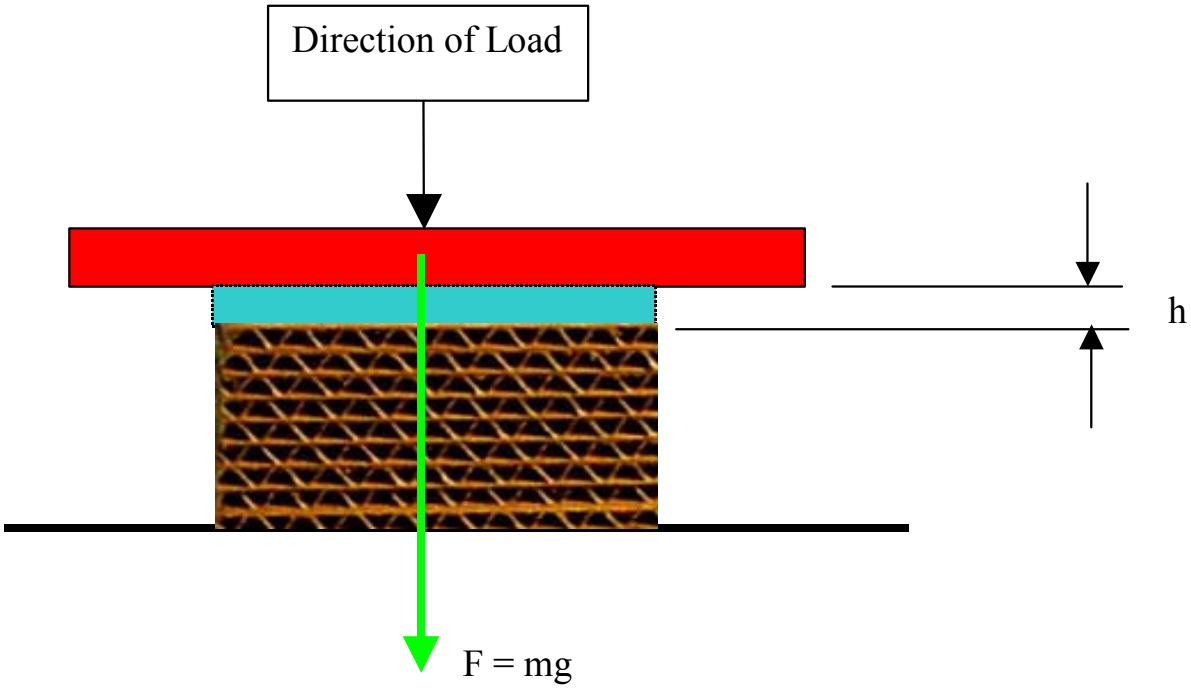

Figure 5.1 Platen approaching the test specimen

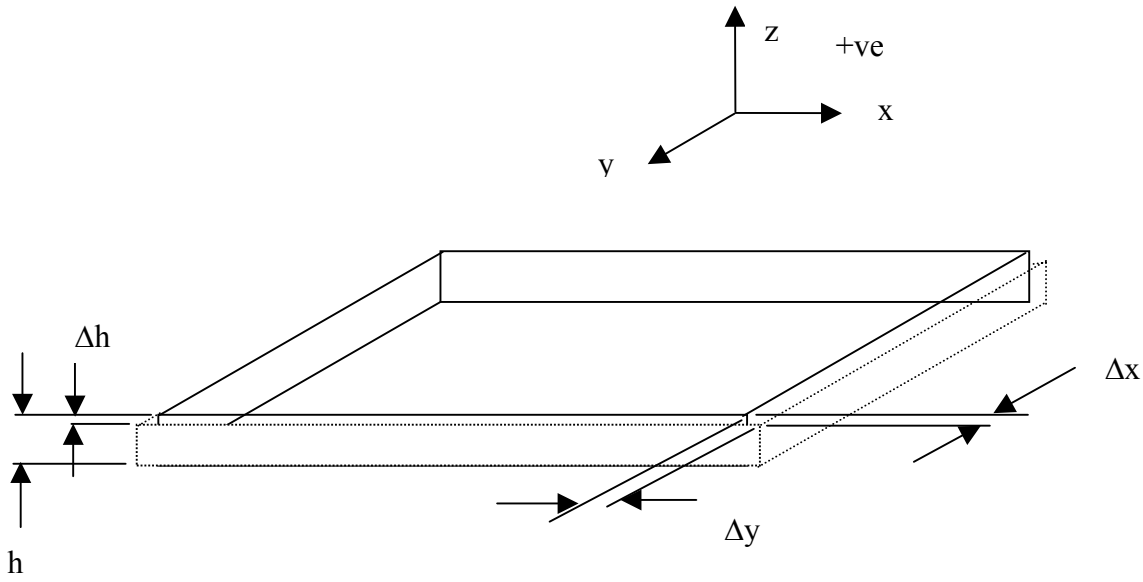

Figure 5.2 Difference in air plate as platen approaches the cushion

White, Frank. M. (1999) suggests that Control Volume or large-scale analysis is a good mathematical tool for fluid-flow applications. This method was successfully employed in chapter 3 for development of the model for post contact dynamics. This method will be used again here, by considering the air plate as as a control volume.

Because of symmetry a quarter of the control volume shown in Figure 5.3 can be considered. To develop a relationship between the platen velocity and the flow velocity of air the principle of conservation of mass must be considered.

$$m_{sys} = \text{constant}$$
$$\frac{dm}{dt} = 0 \qquad (5.1)$$

An assumption will be made that the pressure in the z-direction will be equal to the x and y directions, ie.

$$P_{xz} = P_x$$
$$\text{and} \qquad (5.2)$$
$$P_{yz} = P_y$$

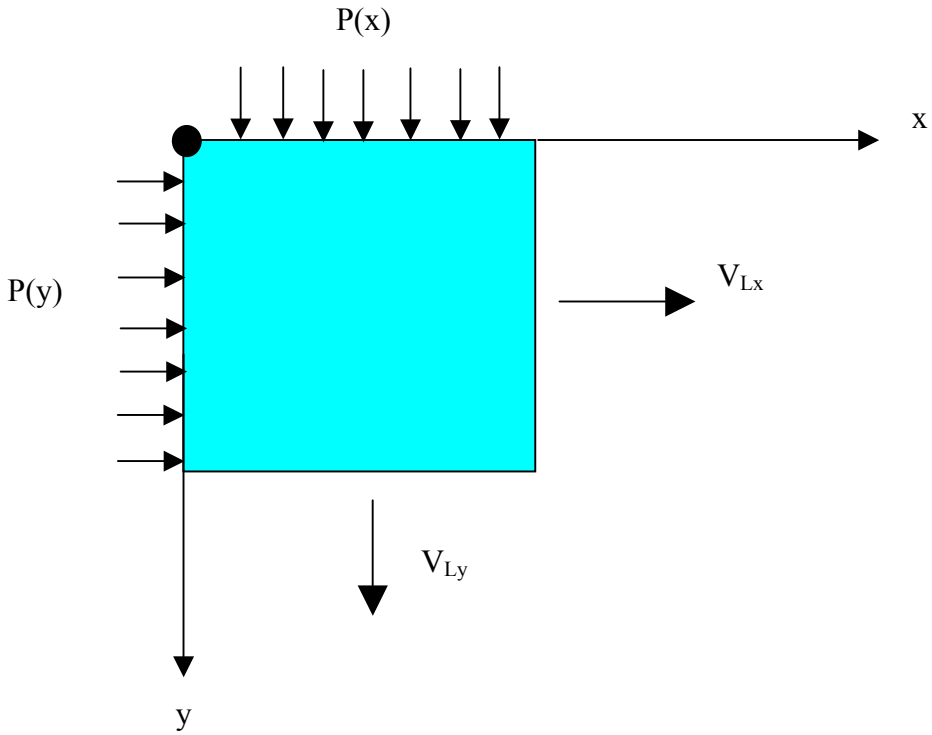

Figure 5.3 Quarter plate representing the control volume

The Figure 5.4 shows the volumetric change of the air prior to impact in the x direction. From which it can be said that

$$\Delta x = \mathbf{V}_x \, \Delta t \tag{5.3}$$

where

Δx = A small change in the x direction for a small change in time.

$\mathbf{V}_x$ = Air Velocity in the x direction Δt = Small change in time

Likewise Figure 5.5 shows the volumetric change of the air prior to impact in the y direction it also can be said that

$$\Delta y = \mathbf{V}_y \, \Delta t \tag{5.4}$$

where

Δy A small change in the y direction for a small change in time.

$\mathbf{V}_y$ = Air Velocity in the y direction

Δt = Small change in time

It is required to consider conservation of mass in both the x and y directions.

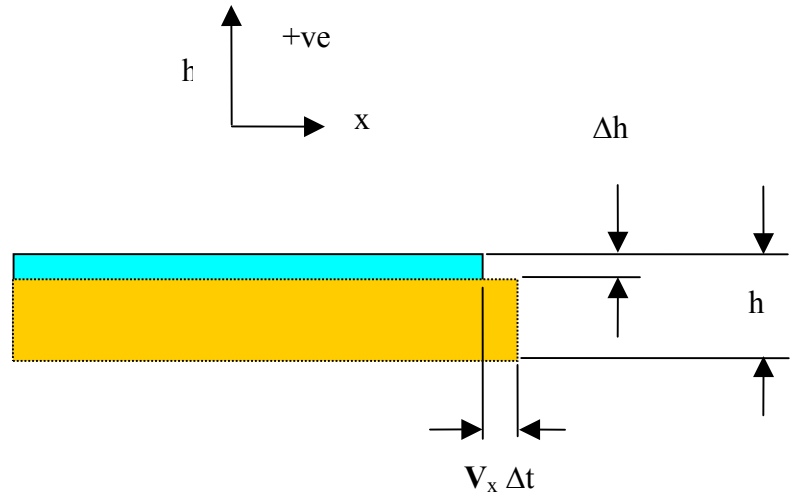

Figure 5.4 Control volume of air in the x-direction

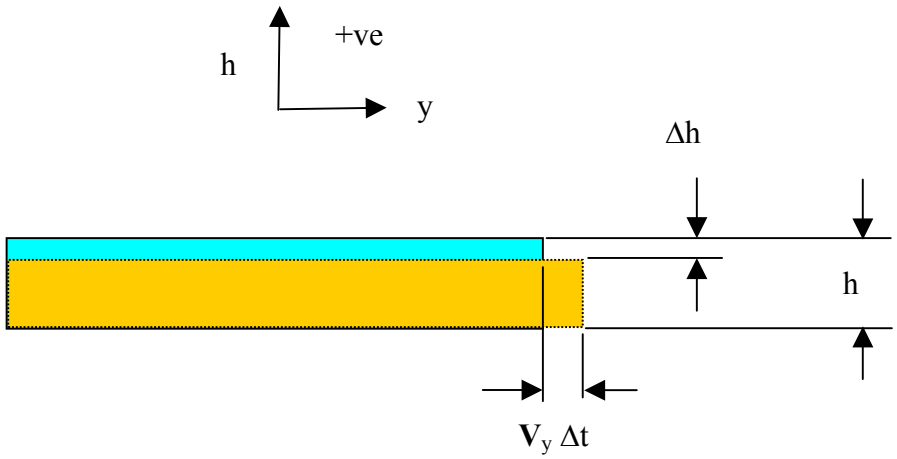

Figure 5.5 Control volume of air in the y-direction.

By conservation of mass, and if the equations of mass are equated in terms of volume difference when considering the velocities at the extremities of the control volume it can be said that

$$\rho h L_y L_x = \rho\left(h - \Delta h\right)\times\left(L_x + \mathbf{V}_{Lx}\Delta t\right)\times\left(L_y + \mathbf{V}_{Ly}\Delta t\right) \tag{5.5}$$

where

$\rho =$ the air density

L_x and $L_y =$ the lengths in the x and y directions.

$\mathbf{V}_{Lx}$ and $\mathbf{V}_{Ly} =$ the velocities of air at the x and y extremities of the control volume

Expanding equation (5.5)

$$\begin{aligned}\rho h L_y L_x = \rho\Big[& h L_x L_y + h L_y \mathbf{V}_{Lx}\Delta t - L_y L_x \Delta h \\ & - L_y \mathbf{V}_{Lx}\Delta h\Delta t + h L_x \mathbf{V}_{Ly}\Delta t + h\mathbf{V}_{Lx}\mathbf{V}_{Ly}\left(\Delta t\right)^2 \\ & - L_x \mathbf{V}_{Ly}\Delta h\Delta t - \Delta h\mathbf{V}_{Lx}\mathbf{V}_{Ly}\left(\Delta t\right)^2\Big]\end{aligned} \tag{5.6}$$

The first term in the square bracket equates to the left hand side of the equation and can be eliminated. Δt^2 and $\Delta t\Delta h$ are small and can also be eliminated leaving

$$\rho\left[h L_y \mathbf{V}_{Lx}\Delta t - L_x L_y \Delta h + h L_x \mathbf{V}_{Ly}\Delta t\right] = 0 \tag{5.7}$$

By factorisation the density ρ is equal to zero. This is of course not so in reality. However an expression for the platen velocity in terms of velocities of air in the x and y directions can be developed with ρ being eliminated.

$$L_x L_y \frac{\Delta h}{\Delta t} = L_y \mathbf{V}_{Lx} h + L_x \mathbf{V}_{Ly} h$$

As time $t \to 0$

$$\frac{dh}{dt} = \mathbf{V}_{Lx} \frac{h}{L_x} + \mathbf{V}_{Ly} \frac{h}{L_y} \qquad (5.8)$$

V_{Lx} = air velocity in x direction

V_{Ly} = air velocity in y direction

h = distance between the platen and the specimen

L_x = the specimen size in the x direction

L_y = the specimen size in the y direction

If the test specimen was square equation (5.8) becomes

$$\frac{dh}{dt} = \frac{2Vh}{L} \qquad (5.9)$$

where

V = air velocity in x and y directions

h = distance between the platen and the specimen

L = the specimen size

An approximation to one dimensional momentum flux used for engineering analysis is:

$$\sum F = \frac{d}{dt}\left(\int_{cv} V\rho \, dV \right) + \sum \left(\dot{m}\mathbf{V}_i \right)_{out} - \sum \left(\dot{m}\mathbf{V}_i \right)_{in} \qquad (5.10)$$

Taken from White, Frank. M. (1999).

The net vector force on a control volume equals the rate of change of vector momentum within the control volume plus the vector sum of outlet momentum fluxes minus the vector sum of inlet momentum fluxes.

Looking at the momentum flux terms, the last two terms of equation (5.10) and assuming that the air flows either direction from the centre of the control volume then the momentum flux at the centre is equal to zero therefore.

$$\dot{m}_{in}\mathbf{V}_{in} = 0 \tag{5.11}$$

Therefore the net vector sum of the forces acting on the air is:

$$\sum F = \frac{d}{dt}\left(\int_{cv} \mathbf{V}\rho \, dV\right) + \sum\left(\dot{m}, \mathbf{v}_i\right)_{out} \tag{5.12}$$

Firstly considering the integral term in the x direction.

$$\int_{cv} \mathbf{V}_x \rho \, dV = \int_{cv} \frac{x}{L_x}\mathbf{V}_{Lx} \, \rho \, dx \, h \, L_y$$

where $\mathbf{V}_x = \frac{x}{L_x}\mathbf{V}_{Lx}$

x = some position in the x-direction

$\mathbf{V}_x$ = the velocity of air at x

$\mathbf{V}_{Lx}$ = the velocity at the extremity in the x-direction

dV = small change in volume = $dx \, h \, L_y$ (5.13)

Integrating between the limits of 0 to L_x to get

$$\int_{cv} \mathbf{V}_x \rho \, dV = \frac{\rho \, h \, L_y}{L_x}\mathbf{V}_{Lx}\int_0^{Lx} x \, dx = \frac{\rho \, h \, L_y}{2L_x}\mathbf{V}_{Lx}x^2\Big|_0^{Lx}$$

therefore (5.14)

$$\int_{cv} \mathbf{V}_x \rho \, dV = \frac{\rho}{2} h L_x L_y V_{Lx}$$

Differentiating (5.14) as required by equation (5.12)

$$\frac{d}{dt}\left(\int_{cv}\mathbf{V}_x\rho\,dV\right)=\frac{d}{dt}\left(\frac{\rho}{2}hL_xL_y\mathbf{V}_{Lx}\right)=\frac{\rho}{2}L_xL_y\left(\mathbf{V}_{Lx}\frac{dh}{dt}+h\frac{d\mathbf{V}_{Lx}}{dt}\right) \tag{5.15}$$

Adding the second term of equation (5.12)

$$\frac{d}{dt}\left(\int_{cv}\mathbf{V}_x\rho\,dV\right)=\frac{\rho}{2}L_xL_y\left(\mathbf{V}_{Lx}\frac{dh}{dt}+h\frac{d\mathbf{V}_{Lx}}{dt}\right)+\dot{m}_x\mathbf{V_{Lx}} \tag{5.16}$$

The mass flow rate is velocity by change in area by the density giving

$$\begin{aligned}&\dot{m}_x=\rho\int_0^{L_y}\mathbf{V_{Lx}}dA=\rho\int_0^{L_y}\mathbf{V_{Lx}}hdy=\rho h\int_0^{L_y}\mathbf{V_{Lx}}dy\\&\text{and for the x direction}\\&\dot{m}_y=\rho\int_0^{Lx}\mathbf{V_{Ly}}dA=\rho\int_0^{L_x}\mathbf{V_{Ly}}hdy=\rho h\int_0^{L_x}\mathbf{V_{Ly}}dx\end{aligned} \tag{5.17}$$

Therefore considering Figure 5.3 and equation (5.16) in the form of equation (5.12) for the x-direction, the force becomes

$$F_x=h\int_0^{L_y}P(y)dy=\frac{\rho}{2}L_xL_y\left(\mathbf{V}_{Lx}\frac{dh}{dt}+h\frac{d\mathbf{V}_{Lx}}{dt}\right)+\rho h\int_0^{L_y}\mathbf{V_{Lx}}dy\mathbf{V_{Lx}} \tag{5.18}$$

In terms of pressure, equation (5.18) reduces to

$$h\int_0^{L_y}P(y)dy=\frac{\rho}{2}L_xL_y\left(\mathbf{V}_{Lx}\frac{dh}{dt}+h\frac{d\mathbf{V}_{Lx}}{dt}\right)+\rho hL_y\mathbf{V_{Lx}^2} \tag{5.19}$$

A similar equation can be developed for the y-direction.

$$h\int_0^{L_x} P(x)\,dx = \frac{\rho}{2} L_x L_y \left(\mathbf{V}_{Ly} \frac{dh}{dt} + h \frac{d\mathbf{V}_{Ly}}{dt} \right) + \rho h L_x \mathbf{V}_{Ly}^2 \qquad (5.20)$$

Most cushion testing is carried out on square samples thus the simplified version of the relationship between the platen velocity and the air flow velocity can be developed.

Taking equation (5.9) and rearranging

$$\frac{dh}{dt} = \frac{2Vh}{L}$$

Thus

$$V = \frac{L}{2h}\frac{dh}{dt} \qquad (5.21)$$

and can be substituted into equation (5.20) for **V** to yield an expression for pressure.

$$h\int_0^{L} Press\,dx = \frac{\rho}{2} L^2 \left[\frac{L}{2h}\left(\frac{dh}{dt}\right)^2 + h \frac{d\left(\frac{dh}{dt}\frac{L}{2h}\right)}{dt} \right] + \frac{\rho L^3}{4h}\left(\frac{dh}{dt}\right)^2 \qquad (5.22)$$

Considering the right hand side of equation (5.22) the terms can be considered separately for simplicity.

$$\text{Term } 1 = \frac{\rho L^3}{4h}\left(\frac{dh}{dt}\right)^2$$

$$\text{Term } 2 = \frac{\rho L^2}{2}\left(\frac{d\left(\frac{dh}{dt}\frac{L}{2h}\right)}{dt}\right) = \frac{\rho L^2}{2}\left(\frac{1}{h}\frac{d^2h}{dt^2} - \frac{1}{h^2}\frac{dh}{dt}\right)$$

$$\text{Term } 3 = \frac{\rho L^3}{4h}\left(\frac{dh}{dt}\right)^2$$

Re-Grouping the terms back into equation (5.22) yields

$$h\int_0^L \text{Press}\, dx = \frac{\rho L^3}{4h}\left(\frac{dh}{dt}\right)^2 + \frac{\rho h L^3}{4}\left(\frac{d^2h}{dt^2}\right) + \frac{\rho L^3}{4h}\left(\frac{dh}{dt}\right)^2 \qquad (5.23)$$

As the integral of pressure with respect to distance then the LHS of the equation becomes $h\frac{m\ddot{h}}{L}$ and an expression for platen acceleration for a square cushion can be developed.

$$\ddot{h}_{i+1} = k\frac{\rho L^4}{2hm}\left[\frac{1}{h}\left(\dot{h}_i\right)^2 + \frac{1}{2}\left(\ddot{h}_i\right)\right] \times IF$$

where

i=1, 2, 3.....n

n = differential equation interation number

m = platen mass

L = cushion length

ρ = air density

h = platen-cushion air space

$\dot{h}$ = platen velocity

$\ddot{h}$ = platen acceleration

k = dimensionless experimental factor

IF = impact factor

(5.24)

The impact factor is taken from the theory from chapter 3.

$$IF = \sqrt{\frac{2H}{\delta_{st}}}$$

where

IF = impact factor (5.25)

H = the drop height

δ_{st} = static deflection due to platen mass

A Simulink model based on equation (5.24) has been developed and used in conjunction with software that simulates the pre-contact acceleration for testing of multi-layered fibreboard cushions. As per the discussion for the post contact model in chapter 3, Simulink is an ideal solution-tool for the differential equation presented here. The accompanying software was developed to read in constant values and experimental data and to control the use of the Simulink model. Figure 5.7 shows the results of simulated acceleration, velocity and displacement after running this model for platen pre-contract.

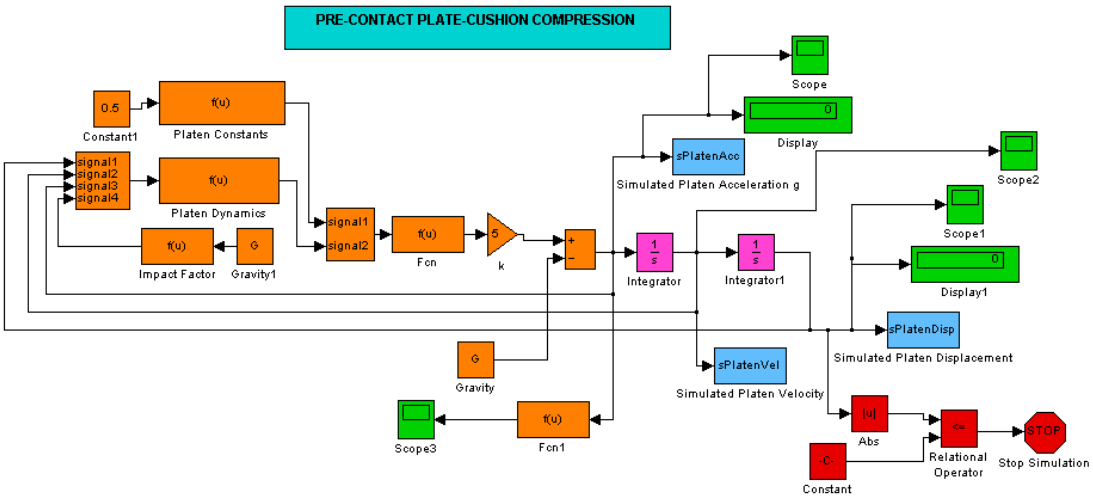

Figure 5.6 Simulink Model for Determination of Pre-Contact Platen Acceleration

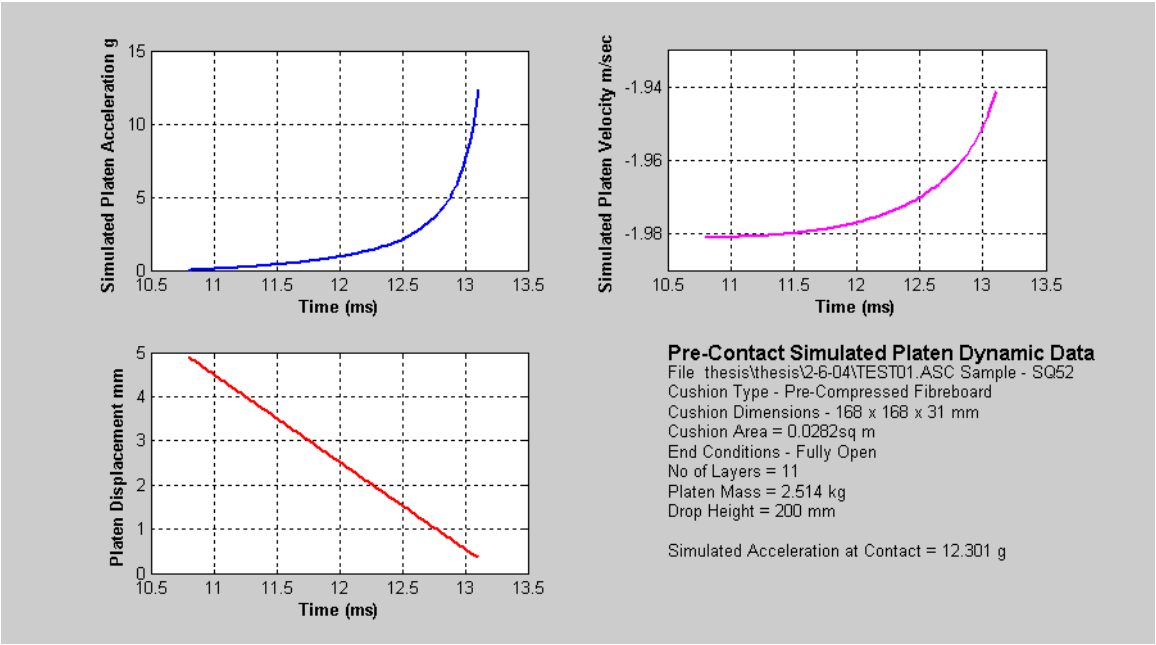

Figure 5.7 Results of Simulation of Pre-Contact Platen Acceleration

Chapter 6 Experimental Procedure for Simulation of Pre-contact Acceleration

In chapter 4 the experimental work attempted to determine where the acceleration pulse begins by measuring the contact point and contact velocity and some inconsistencies were experienced. In this chapter further experimental work is presented in an attempt to understand the concept of pre-contact acceleration and to verify the model developed in chapter 5. Like chapter 4, the experimental results for this study are presented in this chapter in graphical and tabular form, to allow detailed comparison with the discussions and theories.

6.1 Experimental Equipment

There is a need to accurately determine the contact acceleration and velocity. Laser displacement measuring devices were fitted to a custom-built cushion tester. The construction of this tester was not a part of this study. A schematic of this experimental set-up is depicted Figure 6.2 and a photograph shown in Figure 6.3. The data was recorded using an in-house data acquisition developed by others on HP Vee software. A typical data capture set-up is shown in Figure 6.6.

To obtain the exact position of when the platen makes contact with the cushion a metal foil strip was glued to the top of the cushion. A 5volt circuit was set up so as when the platen makes contact the voltage is registered on the data acquisition system. The displacement of the platen and the cushion is measured separately using the laser sensors. An extra stiff and slightly larger layer of corrugated fibreboard was glued to the top for the laser to measure the cushion displacement, a photograph together with the metal foil is shown in Figure 6.1.

The acceleration is measured by the traditional method using an accelerometer. An infrared beam was used to trigger the acquisition system shown in a photograph Figure 6.4.

The accelerometer used was a Piezoelectric Delta Shear charge accelerometer, Brüel & Kjær Type 4383V of sensitivity 2.851pC/ms^{-2} with an upper frequency limit of 8400Hz and is used to measure acceleration change. The accelerometer was mounted in the center of the platen and is connected to the charge amplifier. A sophisticated four channel Type 2692C, Brüel & Kjær charge amplifier is used to condition the signal and is connected to the Data translation DT 3001 8DI.2DAC +/- 10V acquisition card inside a Dell computer . The laser conditioners used were Optisches Weg B System M5.

To have a better understanding of the mechanism of impact and to help to substantiate the theory of chapter 5 these experiments were filmed using a Redlake MotionScope high speed camera at 1000 frames/sec.

Figure 6.1 A typical test sample showing foil strip and larger top layer

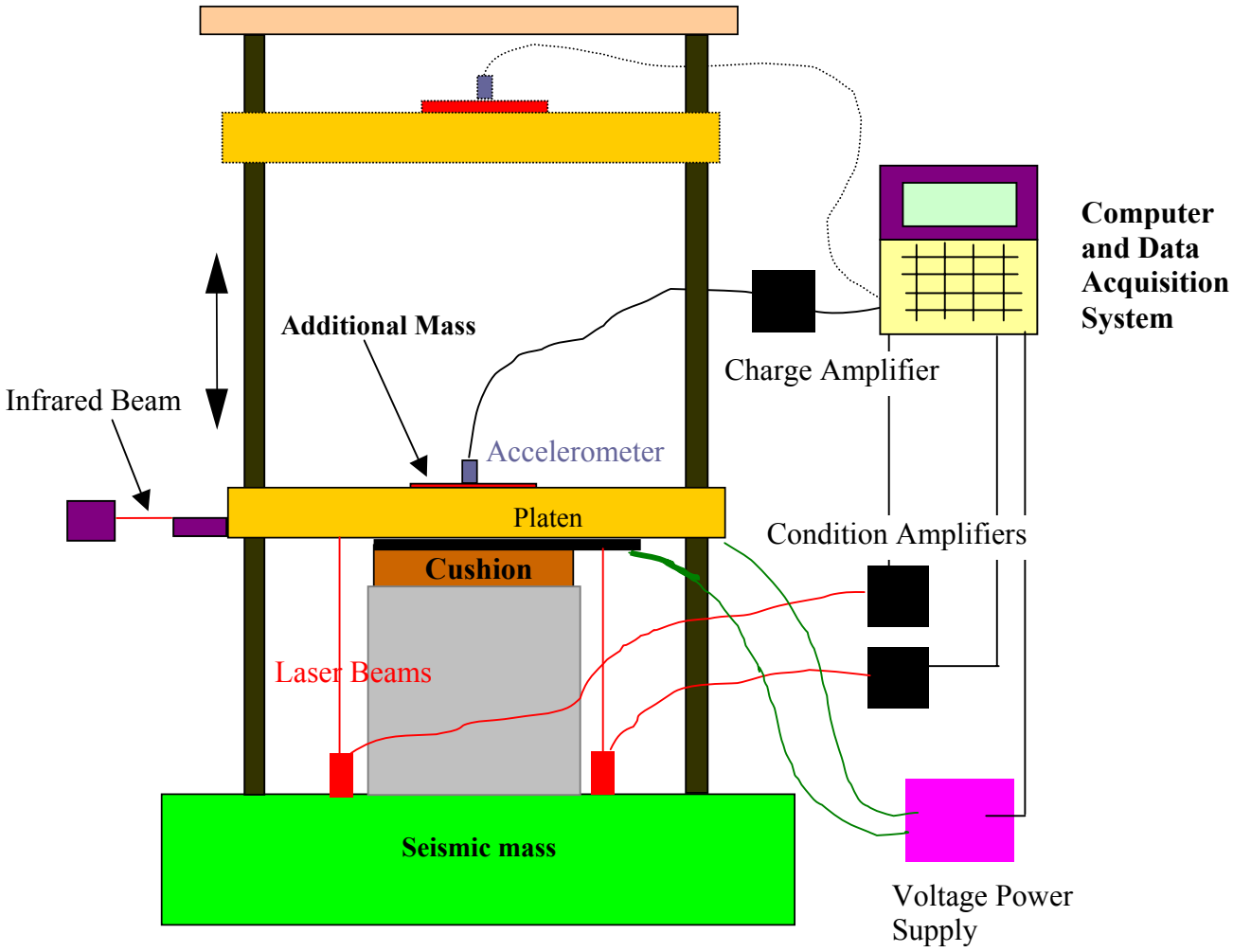

Figure 6.2 Experimental set-up Schematic

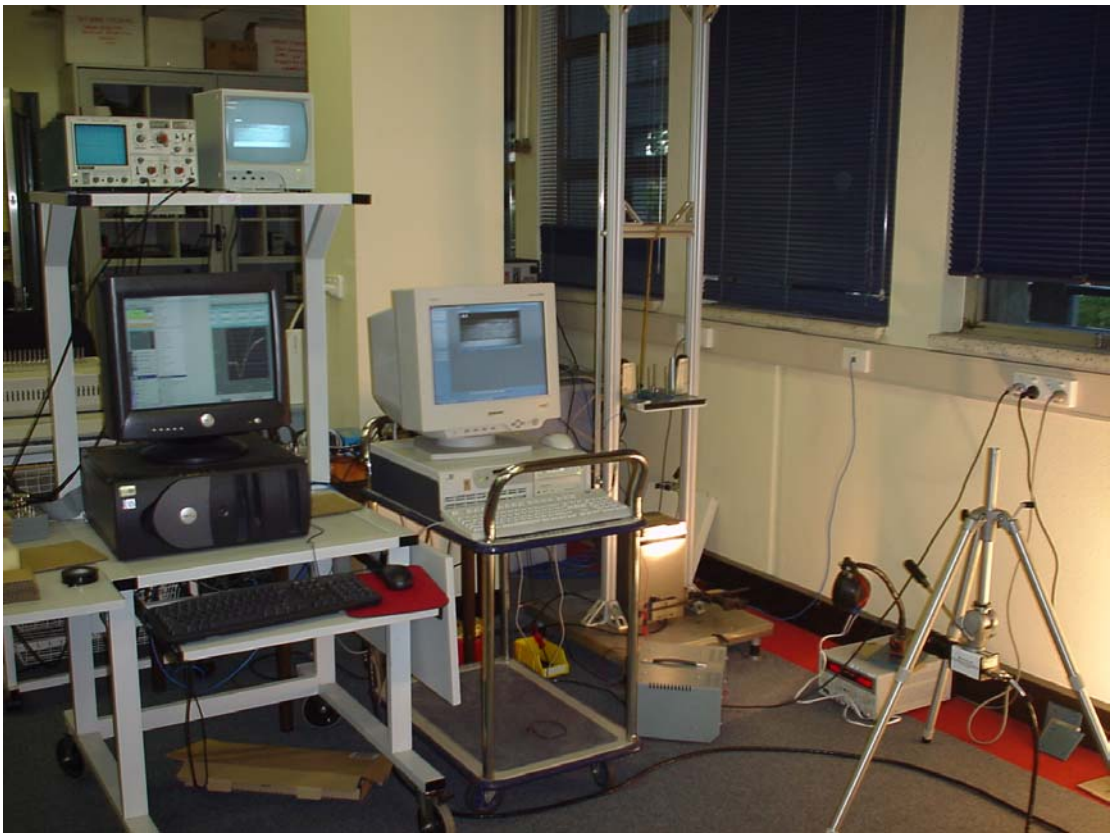

Figure 6.3 Experimental setup for measuring accelerations and cushion displacement

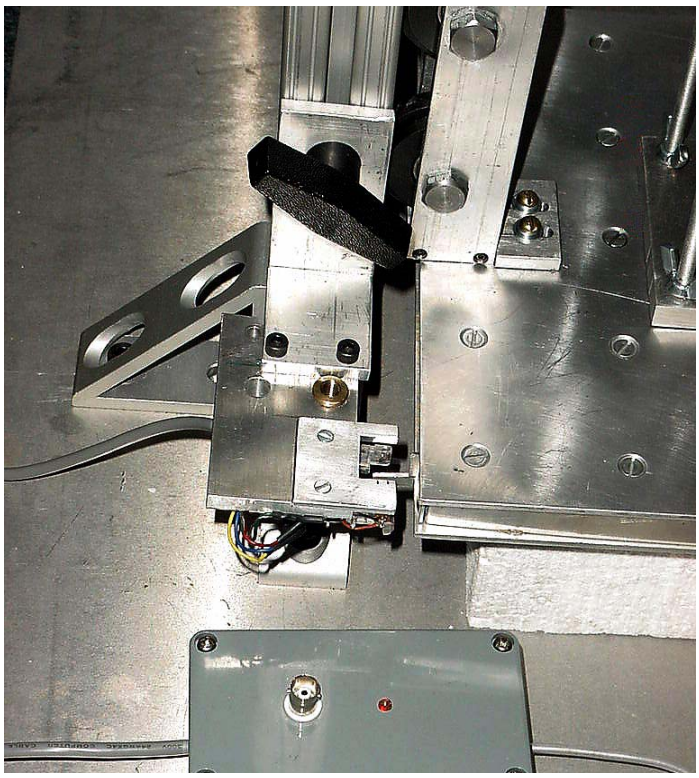

Figure 6.4 Infrared Data Acquisition Trigger

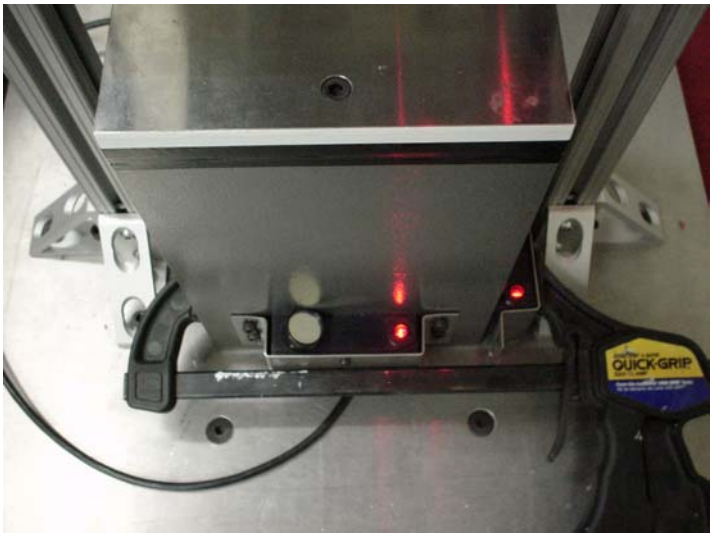

Figure 6.5 Displacement Laser Beam Set-Up

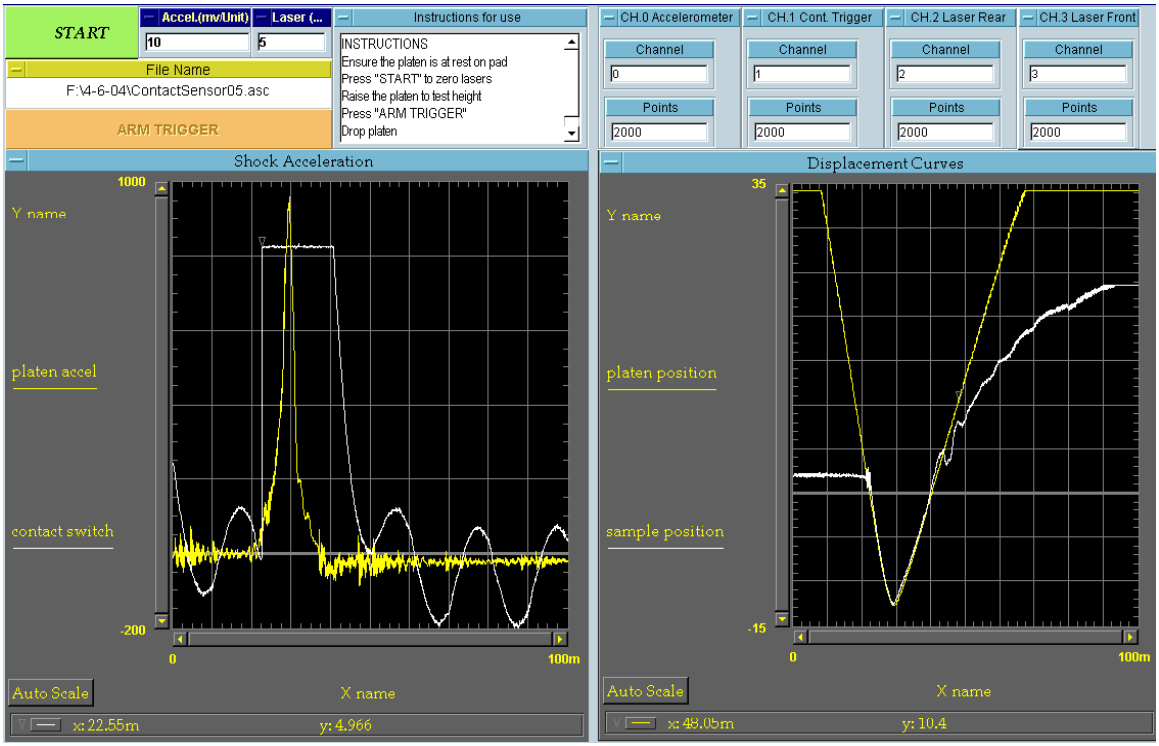

Figure 6.6 Data Capture set-up developed in DT Vee The left hand panel represents the acceleration together with the contact point and the right hand panel representing the displacement of the platen and the cushion.

6.2 Experimental Procedure for Pre-Contact Acceleration

Cushion tests were carried out on 168mm square samples of multi-layered fibreboard consisting of 11 layers, 10 pre-compressed layers and one virgin or stiff layer, the latter for the laser measuring system to measure cushion displacement measurement. Two tests were carried out at drop height of 200mm and subsequent drops at 300 and 400mm respectively, with a platen mass of 2.514 kg. Although this study is centred on the behaviour of pre-compressed multi-layered fibreboard cushions it was thought the previous procedure should be repeated for virgin cushions of the same configuration as pre-contact acceleration may be of larger values. Cushion tests were also carried out on in a similar vein to the pre-compressed tests on square cushions with the same specifications but virgin not pre-compressed to attempt to explore this phenomenon for stiffer materials. The experimental results are compared with simulations carried out using the model representing trapped air or throttled flow of air above square cushions, as the platen approaches developed in chapter 5 is re-stated here for clarity.

$$\ddot{h}_{i+1} = k\frac{\rho L^4}{2hm}\left[\frac{1}{h}\left(\dot{h}_i\right)^2 + \frac{1}{2}\left(\ddot{h}_i\right)\right] \times IF$$

where

i=1, 2, 3.....n

m = platen mass

L = cushion length

ρ = air density (6.1)

h = platen-cushion air space

$\dot{h}$ = platen velocity

$\ddot{h}$ = platen acceleration

k = dimensionless experimental factor

IF = impact factor

Software written in Matlab® together with a Simulink® to analyse the experimental data was written and is presented in appendix B.

6.2.1. Experimental Results and Simulations for Pre-Contact

The following results are from the tests described in the experimental procedure from section 6.2 to determine the pre-contact acceleration. Firstly, the experimental data is followed by the theoretical representation and lastly a comparison between simulated and experimental pre-contact acceleration. Typical graphs are shown Figure 6.7 through to Figure 6.12 together with a tabulation of results in Table 6.1. The results clearly show the pre-Contact acceleration exists and can be simulated using equation (6.1). Also shown are pictures of the process filmed with the high speed camera, they also reveal the tendency of the cushion to depress just prior to contact which suggests that there is pre-contact acceleration and equation (6.1) can be applied.

From the results there is a tendency for the pre-acceleration level to increase with the increase of drop height. This seems normal, as the platen velocity prior to impact would be higher thus producing a sharper increase in pressure build up.

Figure 6.13 illustrates the tendency for the cushion to deflect prior to the contact point (black vertical line). Figure 6.2 to Figure 6.17 display the filmed sequences, which show the positions of the platen and the cushion top relative to each other. As there is no contact up to this point the only explanation can be that there is a build up of air pressure (throttling of the flow). This verifies both what is postulated in chapter 4 and defined by the model developed in chapter 5.

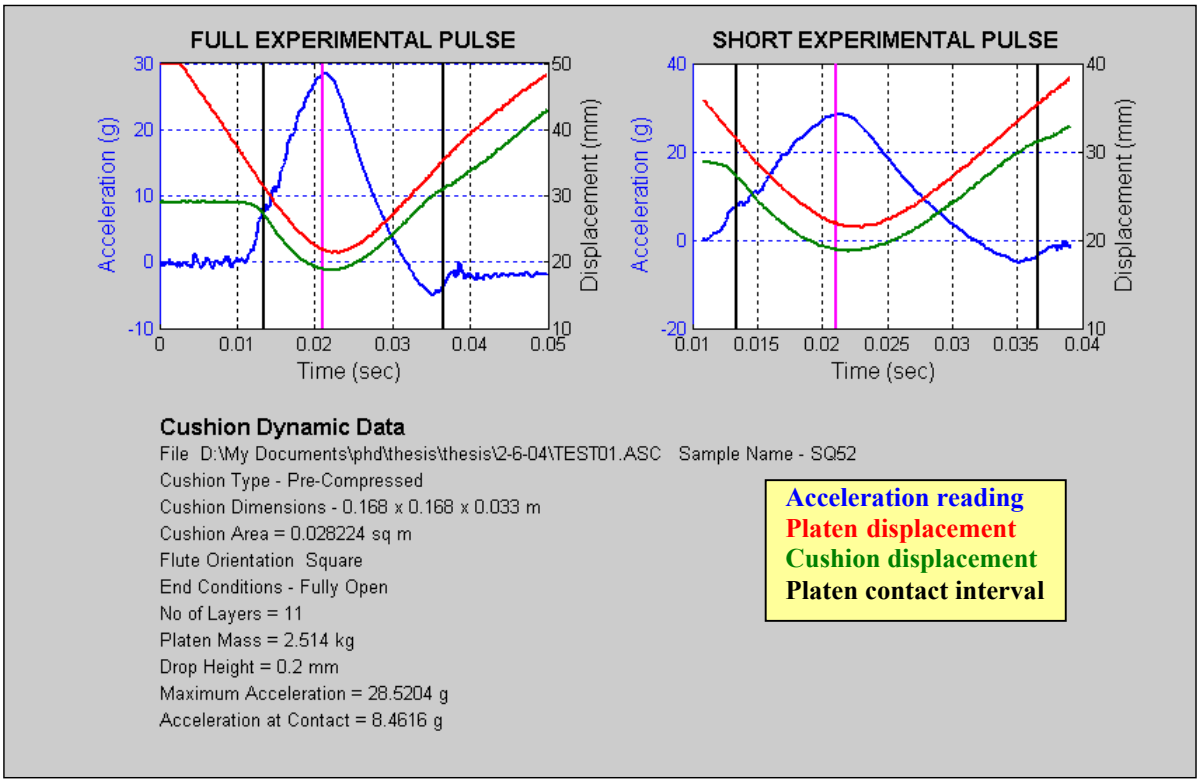

Figure 6.7 Typical Experimental Results showing Pre-Contact Acceleration, Platen Displacement and Cushion Displacement for Mutli-Layered Pre-Compressed Corrugated Fibreboard

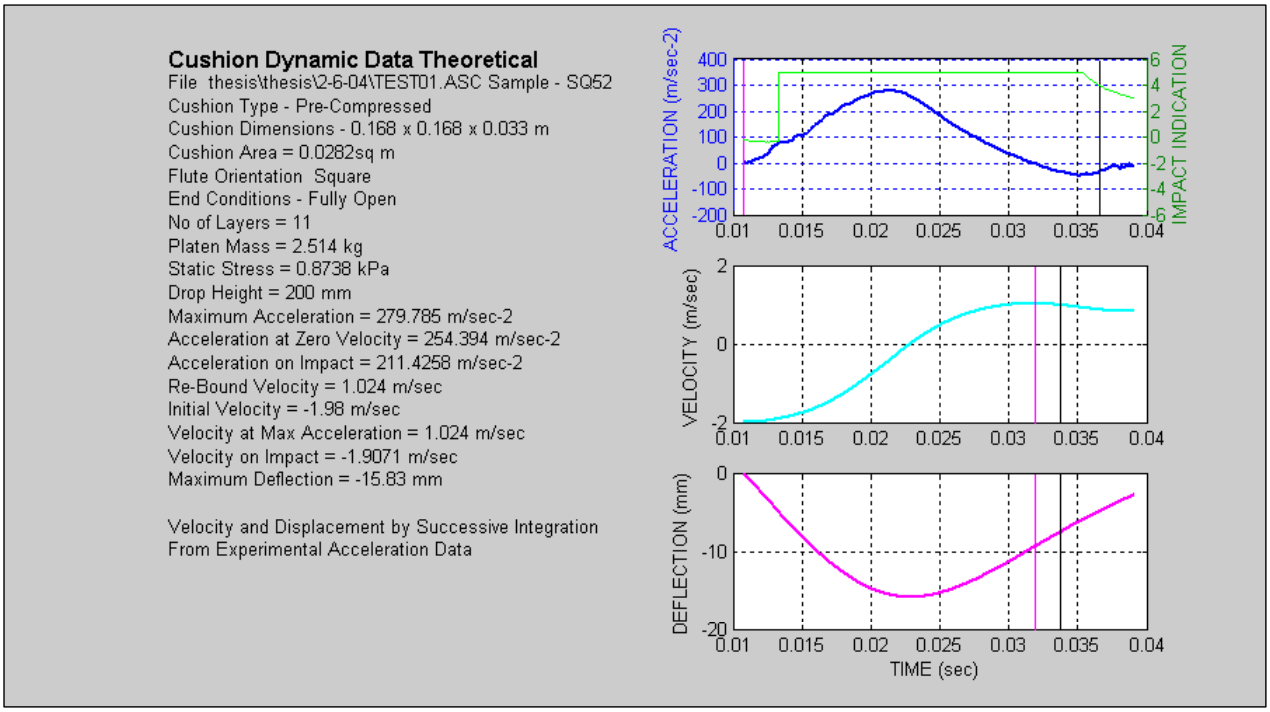

Figure 6.8 Typical Theoretical Results by Successive Integration to determine Velocity and Cushion displacement for Multi-layered Pre-Compressed Corrugated Fibreboard

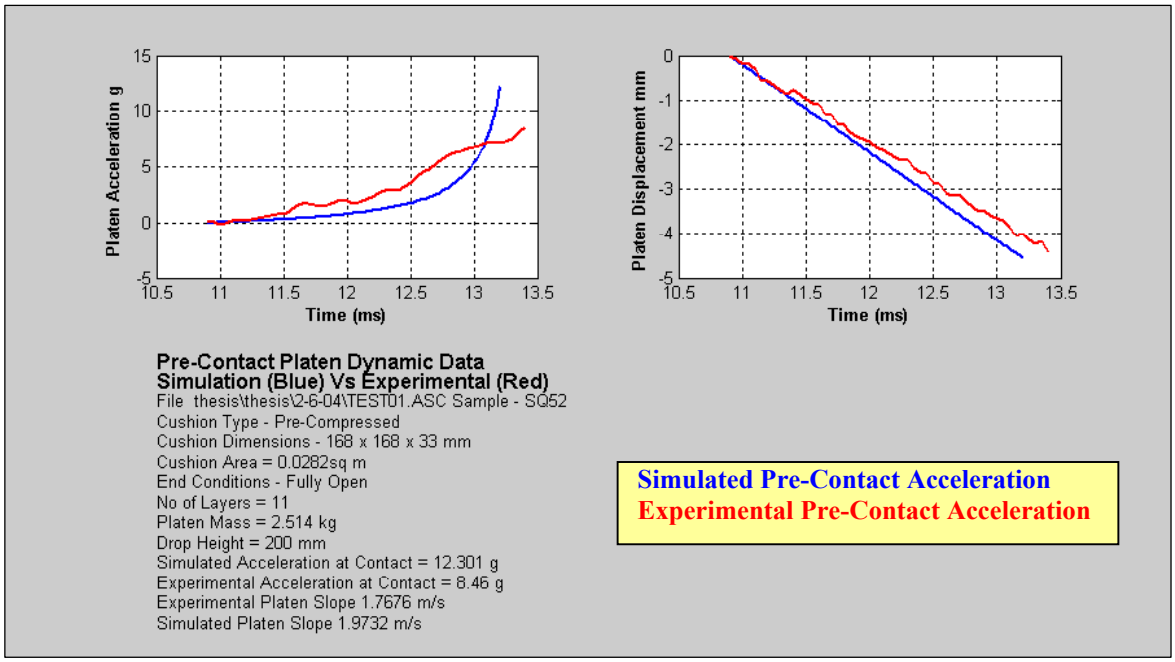

Figure 6.9 Typical Comparison between Experimental and Simulated Pre-Contact Acceleration for Multi-layered Pre-Compressed Corrugated Fibreboard.

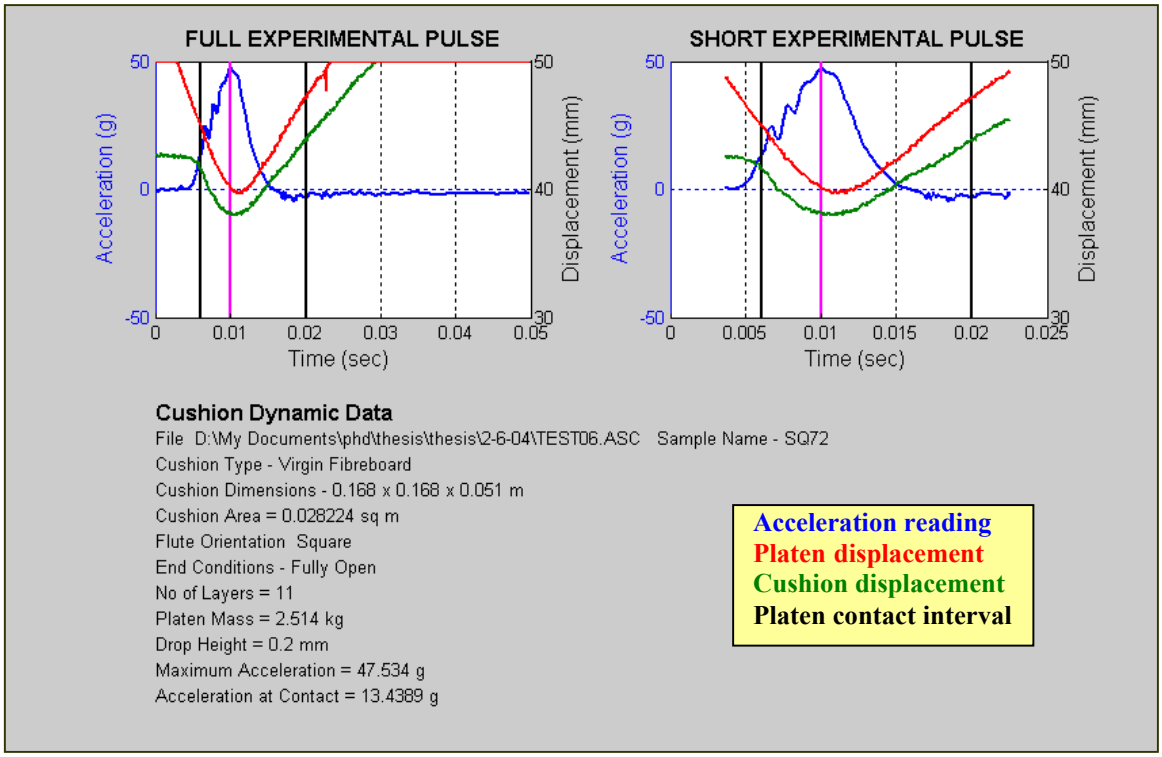

Figure 6.10 Typical Experimental Results showing Pre-Contact Acceleration, Platen Displacement and Cushion Displacement for Mutli-Layered Virgin Corrugated Fibreboard

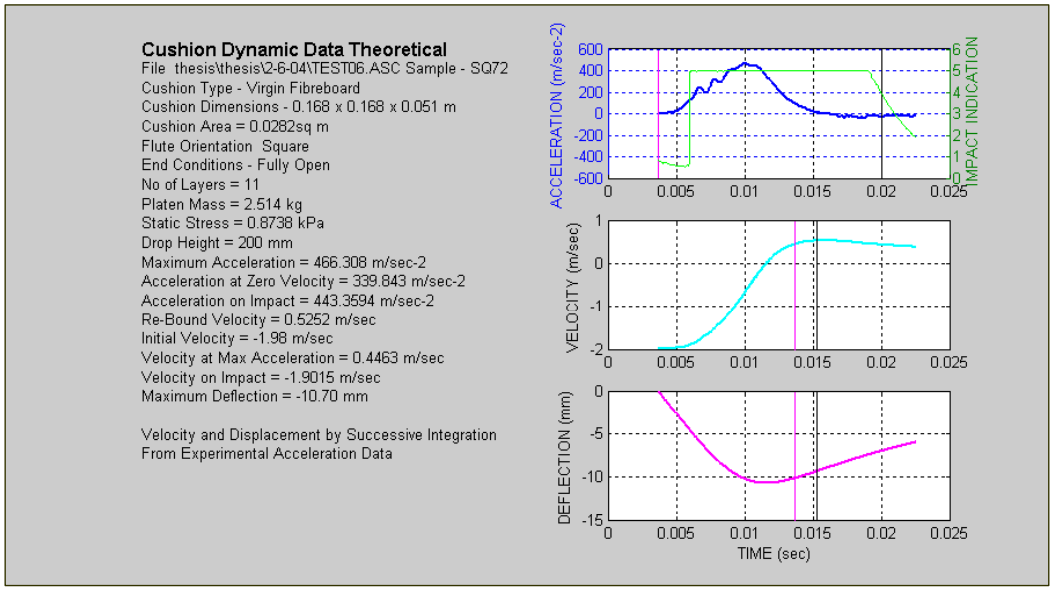

Figure 6.11 Typical Theoretical Results by Successive Integration to determine Velocity and Cushion displacement from Multi-layered Virgin Corrugated Fibreboard

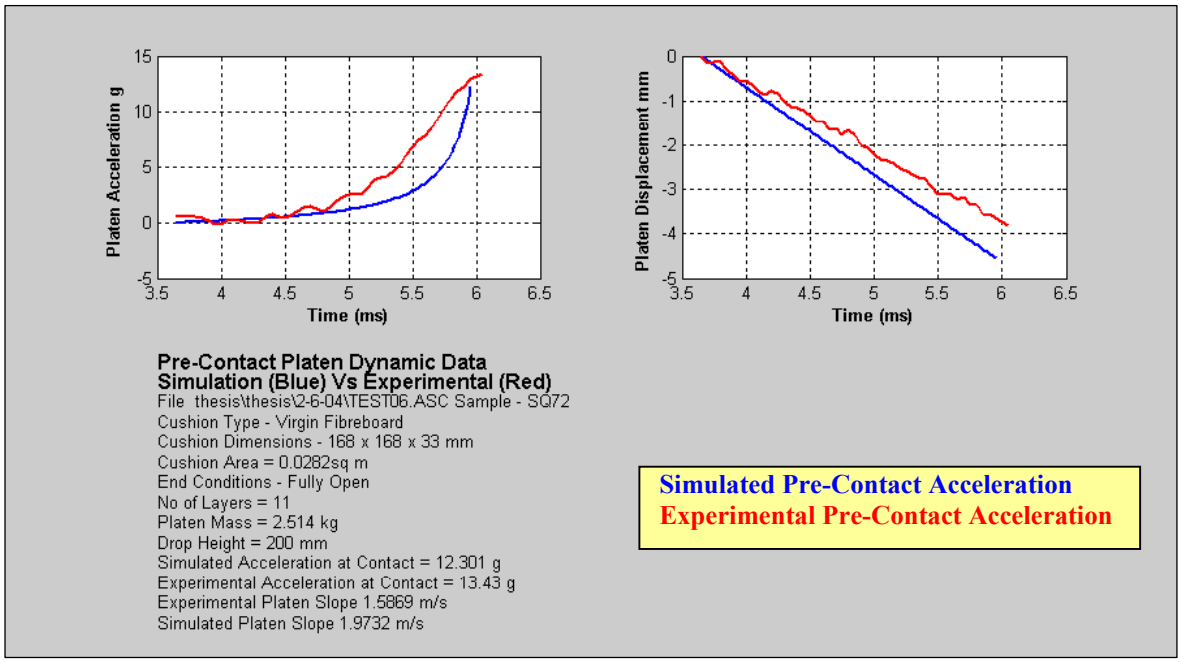

Figure 6.12 Typical Comparison between Experimental and Simulated Pre-Contact Acceleration for Multi-layered Virgin Corrugated Fibreboard.

Table 6.1 Tabulation of Typical Experimental Results for Maximum and Contact Acceleration for pre-compressed and virgin multi-layerd corrugated fibreboard.

Testing of Corrugated Fibreboard Cushions June 13·

Sample Number	SQ52
Size (mm)	168 x 168 x 31
No of Layers	10 Pre-Compressed + I Stiff
Flute Configuration	Square
Drop Height (mm)	200
Platen Mass (kg)	2.514
Static Load (kPa)	0.873
End Condition	Fully Open
File Path	\2-6-04\TEST__.ASC

File	Drop Height (mm)	Exp Max Acc (g)	Exp Contact Acc (g)	Sim Contact Acc (g)
1	200.000	28.520	8.460	12.303
2	200.000	28.223	6.023	12.301
3	300.000	36.683	9.258	22.1
4	400.000	59.830	11.096	33.475

Testing of Corrugated Fibreboard Cushions June 13·

Sample Number	SQ72
Size (mm)	168 x 168 x 31
No of Layers	10 Virgin + I Stiff
Flute Configuration	Square
Drop Height (mm)	200
Platen Mass (kg)	2.514
Static Load (kPa)	0.873
End Condition	Fully Open
File Path	\2-6-04\TEST__.ASC

File	Drop Height (mm)	Exp Max Acc (g)	Exp Contact Acc (g)	Sim Contact Acc (g)
5	200.000	44.896	14.882	5.3
6	200.000	47.543	13.430	12.301
7	300.000	80.484	18.914	22.098
8	500.000	96.263	6.172	11.696
9	500.000	101.887	0.846	2.038

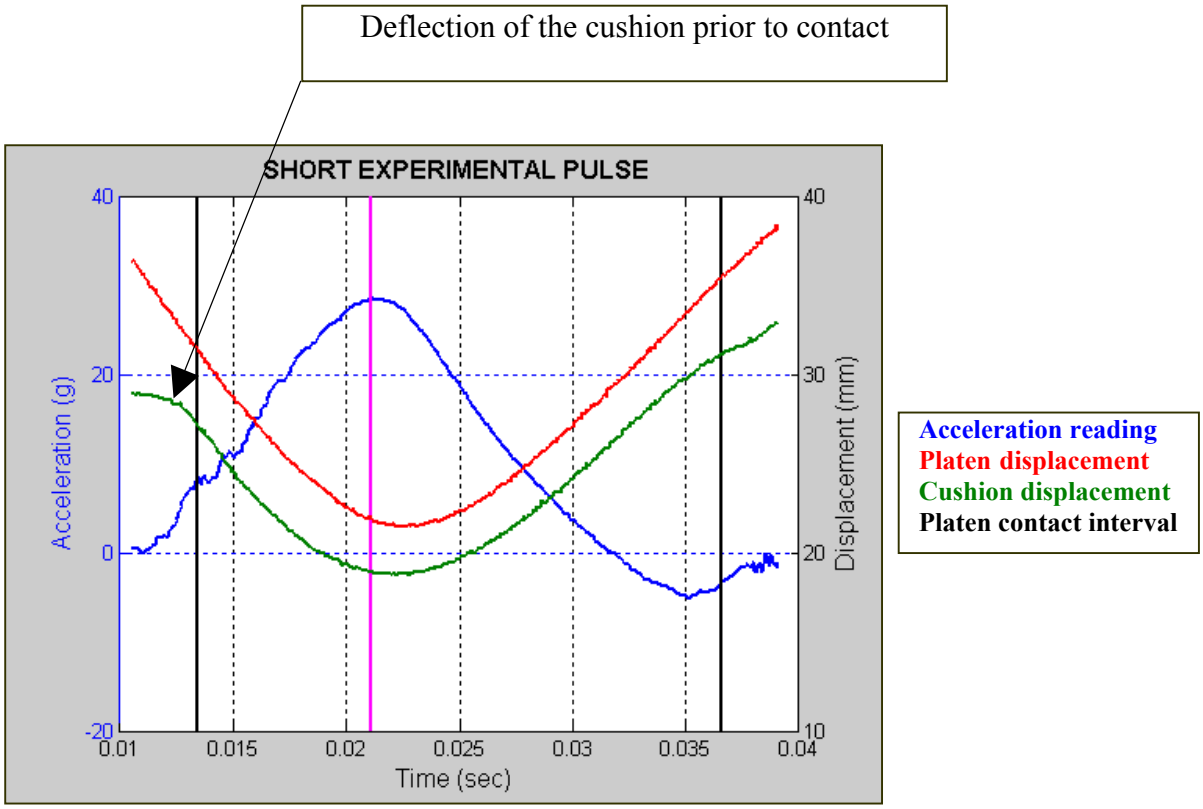

Figure 6.13 Typical Experimental Results from Figure 6.7 (Pre-Compressed) using the short pulse

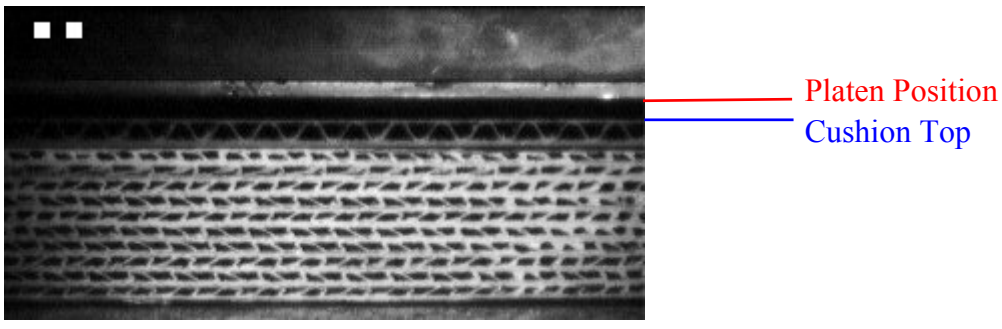

Figure 6.14 Platen and Cushion filmed at 13ms

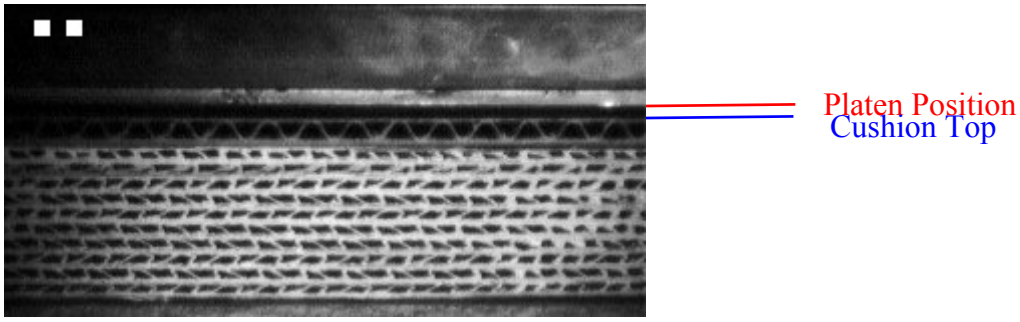

Figure 6.15 Platen and Cushion filmed at 14ms

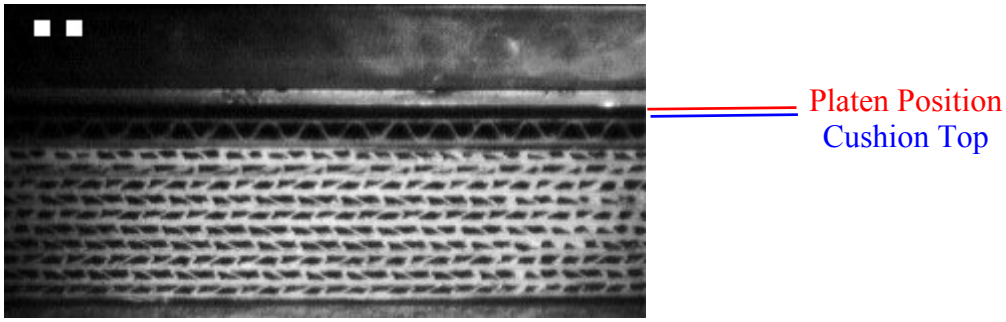

Figure 6.16 Platen and Cushion filmed at 15ms

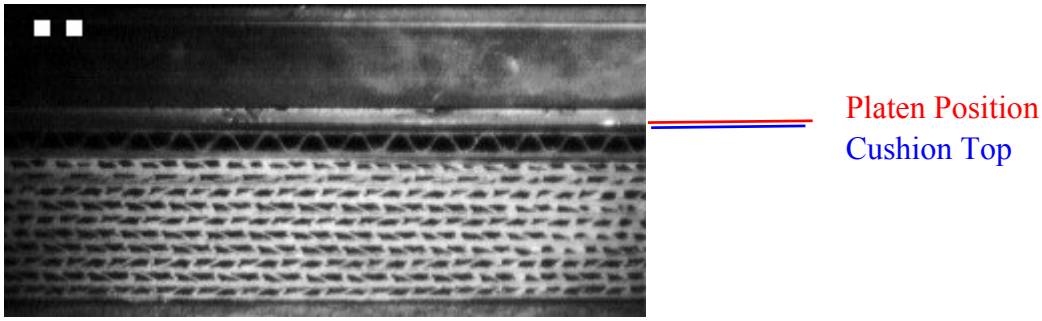

Figure 6.17 Platen and Cushion filmed at 16ms

Chapter 7 Conclusions and Discussion

7.1 Discussion

The questions posed in chapter 2 and 4 were as follows:

(a) How does corrugated fibreboard react when pre-compressed, and what is the resulting stiffness?

(b) When precisely does the acceleration pulse begin?

(c) What effect does the airflow and pressure within the flutes has on the acceleration pulse and deformation velocity under testing?

(d) What effect do the end conditions, namely pressure conditions, and flute configuration, will have on the acceleration pulse and deformation velocity?

(e) Can these effects be modelled mathematically?

(f) Is there build up of air pressure just prior to impact and how does it affect the acceleration pulse, and the deformation velocity?

This investigation was an attempt to answer these questions in terms of testing conditions and not as in actual operating conditions.

During impact of a mass on a protective cushion the resistance is basically influenced by, the applied force, the structural resistance and the damping characteristics. The resistive force or acceleration when applying Newton's Second Law of Motion is a measure of the cushion's performance and was discussed thoroughly in chapter 2. For pre-compressed corrugated fibreboard structural stiffness plays a greatly reduced role in the resistive force, as a majority of the stiffness has been removed. It is in fact similar to a spring in its behaviour. However an understanding of the stiffness or more correctly the static stiffness is required for the pre-compressing mechanism.

In chapter 3 a model for the pre-compressing mechanism was developed and repeated here. This mechanism is basically the static behaviour under slow compression.

The pre-compressing model equation (7.1) has some correlation with experimental data and is shown in Figure 7.1. However more investigation on how the layers progressively crush is recommended. Minett and Sek (2000) suggested a process for how layers progressively crush to which more investigation could lead to the refining of equation (7.1).

After pre-compressing the static behaviour of this material becomes a simple straight-line relationship up to the point of squashing described by equation (7.2). At the point of squashing there is a large increase in resistive force for little deflection.

$$P1 = F_m\left(1 - e^{-a\varepsilon}\right) \qquad \text{Phase 1 Elastic}$$

$$P2 = SF\left(\frac{1}{(\varepsilon_0 - \varepsilon)} - \frac{1}{\varepsilon_0}\right) \qquad \text{Phase 2 Visco-Elastic}$$

$$P3 = F_a \cos\left(2N\pi y / b\right) \qquad \text{Periodic Phase}$$

$$F = P1 + P2 + P3$$

Therefore

$$F = F_m\left(1 - e^{-a\varepsilon}\right) + SF\left(\frac{1}{(\varepsilon_0 - \varepsilon)} - \frac{1}{\varepsilon_0}\right) + F_a \cos\left(2N\pi y / b\right)$$

where

F = the instantaneous force

F_m = the mean force

F_a = the alternating force

SF = the slope factor

N = the number of cushion layers

y = the displacement record

ε = the strain - the ratio of deflection to unloaded thickness

ε_0 = the maximum strain

b is a multiplier

(7.1)

$$\text{Static Stress} = \frac{F}{A} = \frac{k\delta}{A}$$

where

F = the applied force (7.2)

δ = deflection

k = cushion stiffness

A = the cushion area

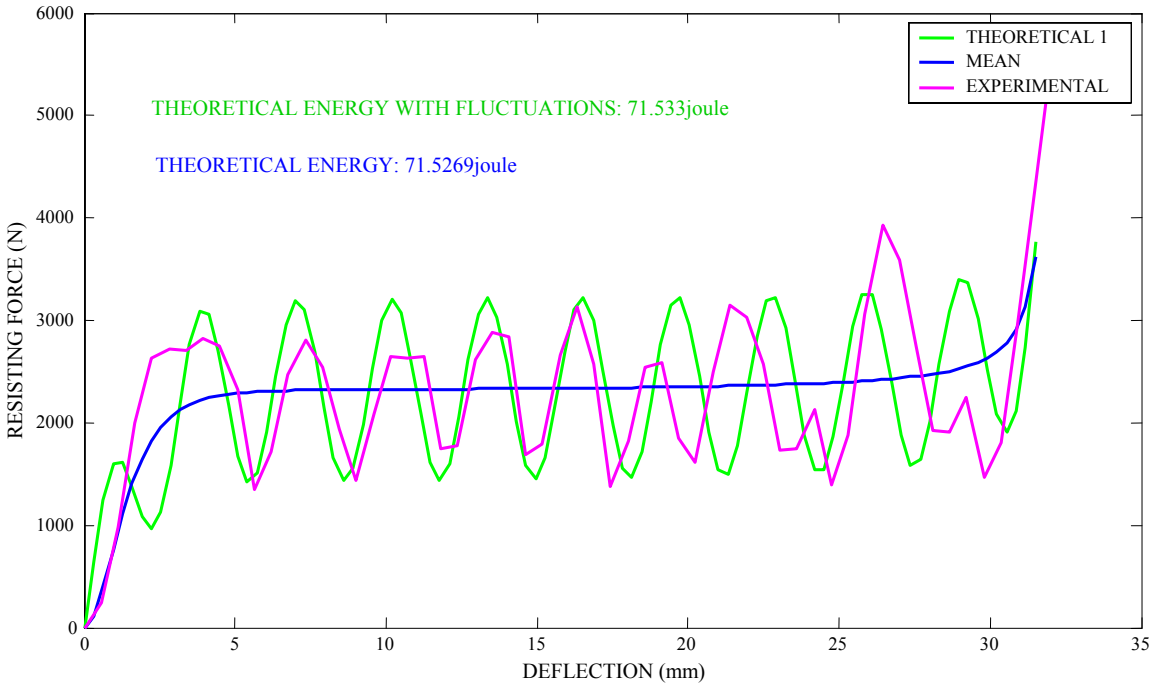

Figure 7.1 Typical Force-Deflection curve of Pre-Compressing Model Compared with Experimental Data

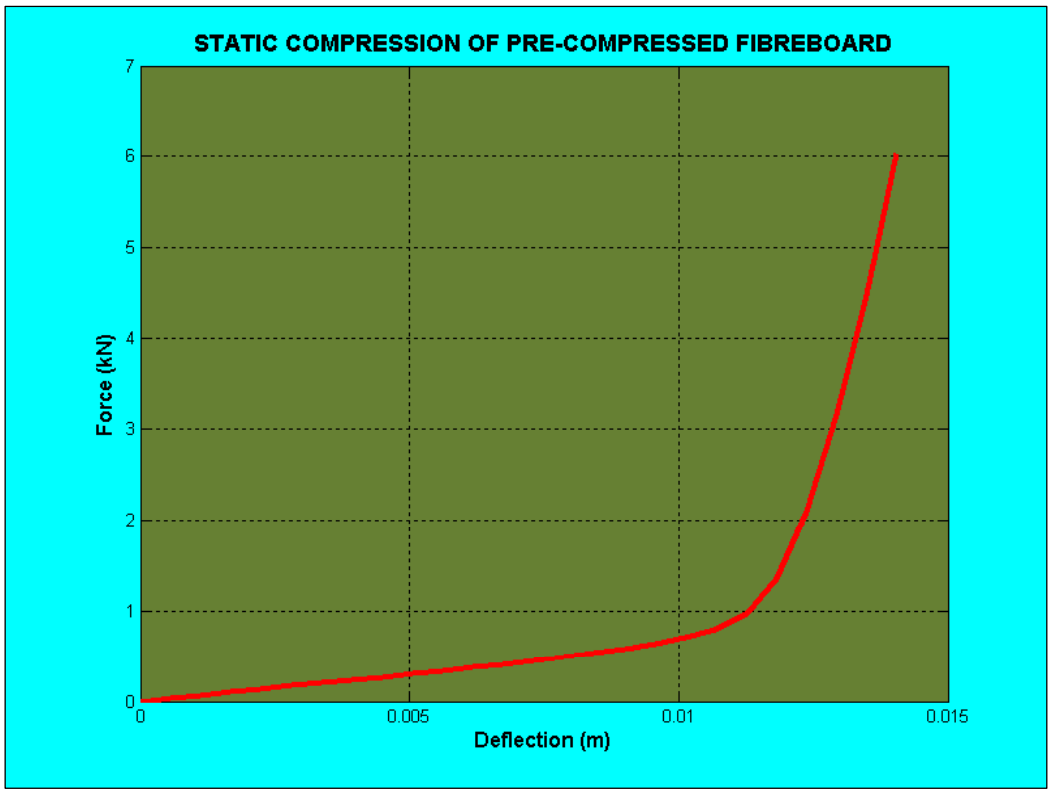

Figure 7.2 Typical Force Deflection Curve of Pre-Compressed Corrugated Fibreboard

The impact on a multi-layered corrugated fibreboard cushion can be thought of as the well-known mass-spring damper system where the components of the system are the mass spring and a damper. It was postulated that the airflow effects, or under some circumstances trapped air, play the damping role during dynamic compression.

A model was developed to describe the dynamics for cushion testing of multi-layered corrugated fibreboard cushions refer to in equation 3.23 and is repeated here as the differential equation (7.3). The extreme right term of the equation describes the damping due to flow of air.

$$a = \left(\frac{F \times IF}{m}\right) - \left(\frac{k\,\Delta h}{m}\right) - 2\left[\frac{A_t\left(P_0 - P_x\right) - F_f}{\rho\, DL^2} - \frac{1}{h_t}\left(\dot{h}\right)^2\right] \tag{7.3}$$

where

a = platen total acceleration

F = forcing function

IF = impact factor

k = cushion static stiffness

m = platen mass

D = cushion width

L = the flute length

$\dot{h}$ = platen or load velocity due to air effects

h_t = cushion height at any point in time

A_t = exit area of cushion cross section at any point in time

F_f = frictional resisting force

P_0 = average air pressure

P_x = air pressure at point x

ρ = air density

This equation was replicated in Simulink. The Simulink model can be viewed in chapter 3, together with software to compare with experimental testing for different end

conditions on square multi-layered corrugated fibreboard. Experimentally the ends were progressively taped in an attempt to vary the end conditions. Earlier testing found that by blocking the cushion ends tended to lower the acceleration levels. The differing end conditions alter the pressure term in the equation (7.3) to the point that depending on the percentage blocked the pressure term has to be split between straight compression and no flow of air to flow of air.

Typical results from this simulation to the experimental tests are shown in Figure 7.3. They show that as the multi-layered pre-compressed fibreboard flute ends are progressively blocked the end pressures are basically increased and as a subsequence the acceleration levels are reduced. In a qualitative way the simulations coincide with experimental results whereby gradually closing the ends, the acceleration levels were reduced and verify the equations developed in chapter three.

It should be pointed out that the friction term F_f is difficult to find. For this study the friction term was determined by iterating the model until a friction value produced appropriate peak acceleration for fully opened ends. Then the model was allowed to recalculate for the progressive closing of the ends. This gave reasonable correlation with experimental values and a typical comparison is shown in Figure 7.4. The simulations have shown that accelerations can be predicted using the models described with the proviso that a record of one experimental cushion test is available. Further research into the determination of the friction component could serve this process well as it would allow this simulation to be tried for combinations of different flute sizes and configurations.

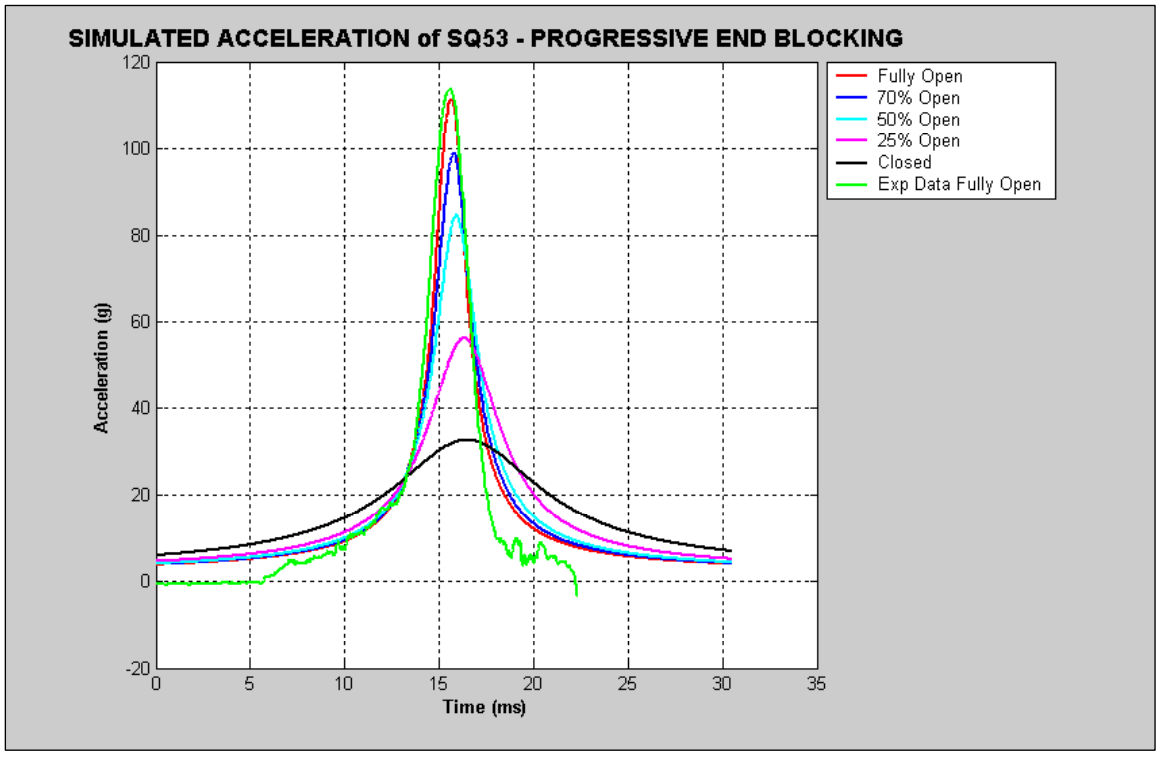

Figure 7.3 Typical Experimental – Simulated Results from Cushion Testing on Multi-layered Corrugated Fibreboard

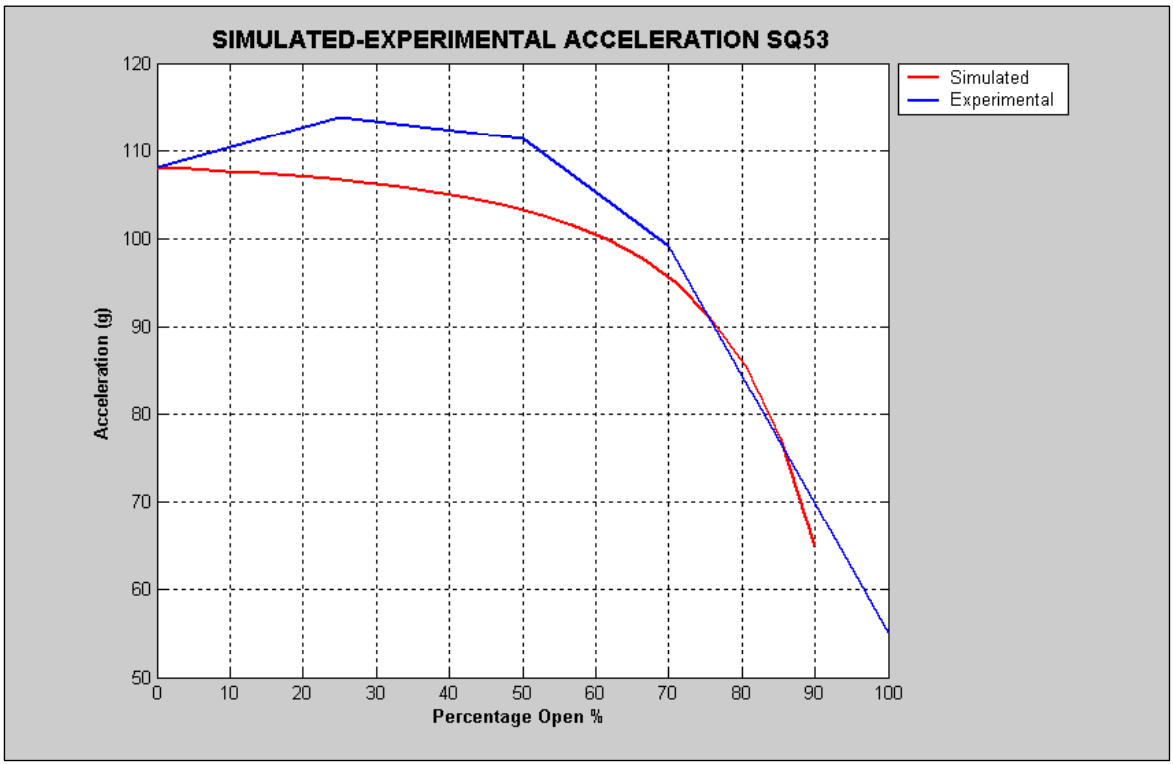

Figure 7.4 Typical Comparison of Experimental to Simulated Cushion Tests for Progressively Closing of the Cushion ends

For rectangular cushions the configuration of the flutes is somewhat important in that, if they coincide with the long direction the acceleration tends to be slightly lower. Simulations on rectangular cushions using the same model but swapping the flute configuration produced less definite results. Flutes configured in the short direction tended to only have slight increases in acceleration, which was not expected. More investigation should be carried out on large length to width ratios to determine if this can be proven more convincingly.

During preliminary testing for the previous discussion there was some difficulty determining the precise contact velocity. After some investigations it was discovered that for cushion testing there is an element of pre-contact acceleration. This can be explained as a build up of air just prior to the platen contacting the cushion. Chapter 5 describes an experimental procedure to determine the significance of this action.
In chapter 4 a model was developed to attempt to predict this pre-acceleration refer to equation 5.24. This model is repeated here as equation (7.4)

$$\ddot{h}_{i+1} = k\frac{\rho L^4}{2hm}\left[\frac{1}{h}\left(\dot{h}_i\right)^2 + \frac{1}{2}\left(\ddot{h}_i\right)\right] \times IF \qquad (7.4)$$

where
i=1, 2, 3.....n
n = differential iteration number
m = platen mass
L = cushion length
ρ = air density
h = platen-cushion air space
$\dot{h}$ = platen velocity
$\ddot{h}$ = platen acceleration
k = dimensionless experimental factor
IF = impact factor

The experimental procedure from chapter 6 allowed for the measurement of the platen displacement, the cushion displacement, the acceleration and the point when the platen makes contact refer to Figure 7.5. Software and a simulink model were developed for equation (7.4) and comparisons are made in Figure 7.6.

It has been shown, both numerically and experimentally, that the air-cushion formed between the platen of a cushion tester and the sample, and the resulting pressure build-up, have a significant effect on the shock pulse. The effect produces a substantial acceleration and deflection of a cushion prior to the platen making contact and verifies the hypothesis first voiced in chapter 4. Awareness of this effect should assist in the interpretations of experimental results.

Table 6.1 shows a comparison of experimental and simulated acceleration results for both maximum, or peak acceleration and the contact acceleration of pre-compressed together with virgin multi-layered corrugated fibreboard cushions. It can be seen that there is a tendency for the case of pre-compressed cushions to experience higher contact acceleration increases as the drop height increases. Contrary to that, in the case of the virgin cushion, the contact acceleration seems to rise, then drop away as the drop height increases. This can be attributed to the cushion not yielding as quickly as the pre-compressed, however the air exhaustion rate is faster at higher drop height with the pre-contact acceleration having less influence.

As would be expected the maximum acceleration on both types of cushion increased as the drop height was increased with those for the virgin cushions having higher values, approximately double.

By comparing the time position from Figure 6.13 and the high speed photographs it can be seen, that the air-cushion formed between the platen of a cushion tester and the sample, and the resulting pressure build-up, has an effect on the shock pulse. The effect produces a

substantial acceleration and deflection of a cushion prior to the platen making contact. Awareness of this effect should assist in the interpretations of experimental results.

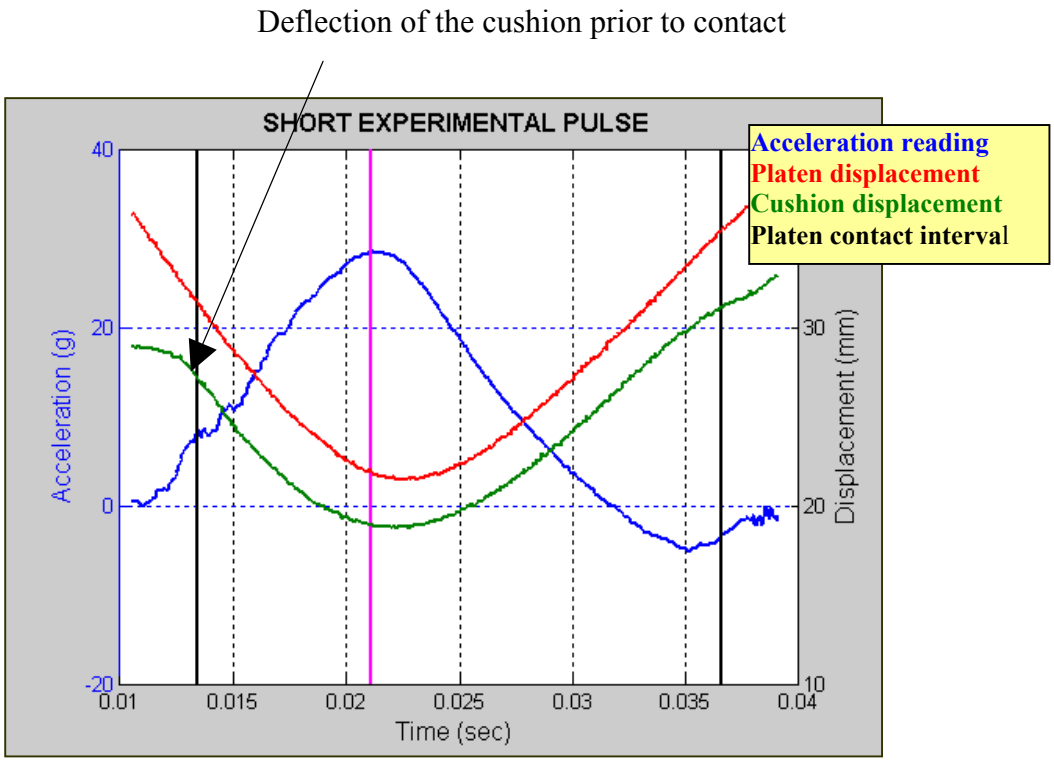

Figure 7.5 Typical Experimental Results from using an abbreviated pulse

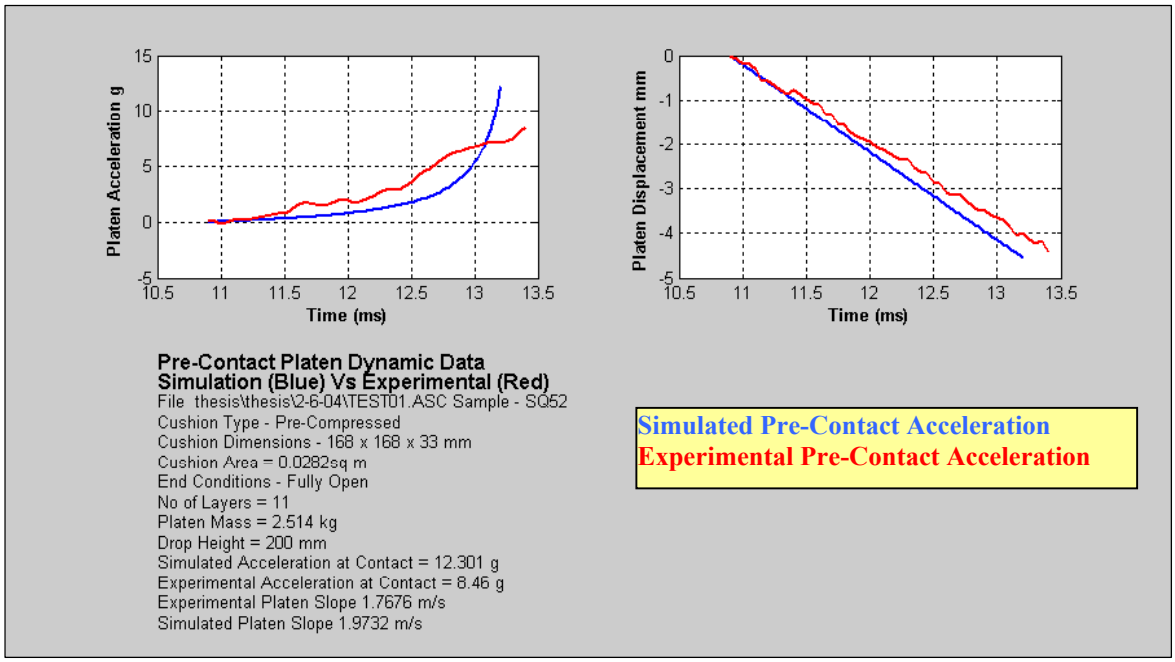

Figure 7.6 Typical Comparison between Experimental and Simulated Pre-Contact Acceleration for Multi-layered Pre-Compressed Corrugated Fibreboard.

7.2 Conclusions

The principal conclusions that have arisen from this investigation are as follows:

Multi-layered Corrugated fibreboard when compressed has properties similar to polymeric materials. It behaves in a similar manner to a compression spring. It has up to the point of squashing a linear relationship between load and deflection according to the following relationship.

$$\text{Load} = k\delta$$

The pre-compressing mechanism for pre-compressed multi-layered corrugated fibreboard, can be described by the mathematical model:

$$F = F_m\left(1 - e^{-a\varepsilon}\right) + SF\left(\frac{1}{\left(\varepsilon_0 - \varepsilon\right)} - \frac{1}{\varepsilon_0}\right) + F_a\cos\left(2N\pi y / b\right)$$

Due to air pressure build up prior to platen contact there is some difficulty in determining precisely where the acceleration begins. The air pressure creates a pre-contact acceleration component that can be described by the following mathematical model:

$$\ddot{h}_{i+1} = k\frac{\rho L^4}{2hm}\left[\frac{1}{h}\left(\dot{h}_i\right)^2 + \frac{1}{2}\left(\ddot{h}_i\right)\right] \times IF$$

where

i=1, 2, 3.....n

The flow of air through pre-compressed corrugated fibreboard flutes, during impact, plays an important role in the damping characteristics of protective cushions made of this material. The flow air is controlled by the flute configurations and by the cushion end conditions. Rectangular cushions with the flutes configured in the longer direction tend to experience slightly lower acceleration and deformation levels. In cushions where ends are partially of fully closed tend to experience varying degrees of lower acceleration and deformation velocity levels compared with fully opened ends. The following model describes this process.

$$a = \left(\frac{F \times IF}{m}\right) - \left(\frac{k\,\Delta h}{m}\right) - 2\left[\frac{A_t\left(P_0 - P_x\right) - F_f}{\rho\, DL^2} - \frac{1}{h_t}\left(\dot{h}\right)^2\right]$$

7.3 Summarising Remarks

This study has presented models to allow for the prediction of the behaviour of multi-layered corrugated fibreboard for the use as protective cushions. The main thrust has been the behaviour of the airflow during impact whilst testing. The models have good correlation to the experimental work carried out. It is envisaged that the models developed for both pre and post contact, will assist in the design of protective packaging and produce predictive tools for the use in the packaging industry.

Chapter 8 References

Soper W. G., Dove R. C., *Data Presentation for Cushioning Material,* Technical Papers of the Seventeenth Annual Technical Conference of the Society of Plastics Engineers, Inc., Volume VII, Paper 27-4, January 1961.

Woolam W. E., 1968, *A Study of the Dynamics of Low Energy Cushioning Materials Using Scale Models,* Journal of Cellular Plastics.

Brandenburg R.K., Lee, J.J., 1985, *Fundamentals of Packaging Dynamics*, MTS Systems Corporation.

Wenger E.C., 1994, *Corrugated Board as a Package Cushioning Material*, Masters Thesis, school of Packaging, Michigan state University, USA

ASTM D1596, *Standard Test Method for Shock Absorbing Characteristics of Package Cushioning Materials.*

Teragashi Y., et al, 1993, *Study of static cushioning properties: automated data input and reliability testing of static cushioning properties*, International Journal, Packaging Technology and Science, Vol 6, pp.221-233.

Burgess G., 1994 *Generation of cushion curves from one shock pulse*, Packaging Technology and Science, Vol 7, pp.169-173.

Henriksson J., 1994, *Measuring system for cushioning properties*, Packforsk, Kista, Sweden.

Ge C., (1994), *Design Method of the Corrugated Board Cushion*, Proceedings of the 18th IAPRI Symposium , Reims, France, Vol 6, 1-5

Naganathan P., Marcondes J., 1995 *Effect of Specimen Size on Test Results to Determine Cushioning Characteristics of Corrugated Fibreboard*, Packaging Technology and Science, Vol 8, pp 85-95.

Sek M. *et al.,* 1996, *Cushioning properties of Corrugated Cardboard: Test Methods*, Proceedings of the 18th IAPRI Symposium, Hanasaari Cultural Centre, Helsinki, Finland.

Sek M., Kirkpatrick, J., 1996, *Prediction of cushioning properties of corrugated fibreboard from statistical and quasi-dynamic compression data*, Proceedings of the 18th IAPRI Symposium, Hanasaari Cultural Centre, Helsinki, Finland.

Thakur K.P., McDougall A., 1996, *Mechanics of Foam*, Proceedings of the First Australasian Congress on Applied Mechanics, Vol 2, pp 677-681.

Sek M., Kirkpatrick J., 1997, *Prediction of Cushioning Properties of Corrugated Fibreboard from Static and Quasi-dynamic Compression Data*, Packaging Technology and Science, Vol 10, pp 87-94.

Ansorge T., Nendel K., 1998, *Calculation of Cushion Diagrams Using a Physical Model,* Packaging Technology and Science, Vol 11, pp 1-8.

Hsiao H., Daniel I., and Cordes R., 1998, *Dynamic Compressive Behaviour of Thick Composite Material,* Journal of Experimental Mechanics, Vol 38, No 3, pp 172-180.

Sek M., *et al,.* 1999*, Performance characteristics of paper based recyclable material Corrupad™ for cushioning applications,* Proceeding of the 11th IAPRI World Conference on Packaging, Singapore, pp 403-415.

Minett M, Sek M., 1999, *Behaviour of corrugated fibreboard as a cushioning material*, Proceedings of the 11th IAPRI World Conference on Packaging, Singapore, pp 591-601.

Sasaki. H., Kaku Saito., and Kaname Abe., 1999, *The Development of an Air Cushioning Material Based on a Novel Idea,* Packaging Technology and Science, Vol 12, pp 143-150.

Naganathan P., He J., Kirkpatrick J., 1999, *The Effect of Compression of enclosed Air on the Cushioning Properties of Corrugated Fibreboard*, Packaging Technology and Science, Vol 12, pp 81-91.

Sek M., et al., 2000, *A New Method for the Determination of Cushion Curves*, Packaging Technology and Science, Vol 13, pp 249-255.

Sek M., Kirkpatrick J., 2002, *Handbook for the Effective Use of Corrugated Fibreboard as a Cushioning Medium in Protective Packaging,* Collaboration between Victoria University, Melbourne, Australia and Amcor Research and Technology, Australia.

Singh R., et al, 2002, *Transient response evaluation of a Hydraulic Engine Mount*, Journal of Sound and Vibration , pp 30-35

Minett, M. and Sek, M. (2002) *The Significance of Air Flow within Corrugated Fibreboard Cushion Pads*. Proceedings of the 13th IAPRI World Conference on Packaging, Worldpak 2002, Michigan, USA, Book 2, pp 788-796.

Wyskida, R. M. *Modelling of Cushioning Systems, Gordon and Breach*, Scientific Publishers

White, Frank. M. *Fluid Mechanics. Fourth Edition*. (1999) WCB McGraw-Hill.

Hornebeck, R. W. (1975) *Numerical* Methods, Prentice-Hall

Juvinall, R. C. and Marshek, K. M (2000*) Fundamentals of Machine Component Design.* Chapter 7, Impact Loading, John Wiley and Sons.

Sek, M, and Minett, M. (2004) *Pre-Contact Effect on Acceleration Pulses during Cushion Testing of Protective Packaging,* Proceedings of the 14th IAPRI World Conference on Packaging, Stockholm, Sweden

Lee M., and Park J., 2004, *Flexural Stiffness of Selected Corrugated Structures.* Packaging Technology and Science, Vol 17, pp 275-286.

Appendix A

The following programs are written to read and analyse data for the pre-contact airflow analysis. These programs are written in Matlab m files and also call the Simulink models referred to in the main body of work.

File : contact.m

```
%This is the main program that analyses and simulates pre-contact dynamics
%for multi-layered fibreboard cushions.
%Written by M Minett


clear all;
global G filte cushArea platenMass dropHeight cushLength cushWidth cushThickness
numLayers fOrder cutOff ec samp stest pg cushdes rho fo

G = 9.81065;

%Input of data
answer = inputdlg({'CUSHION DESCRIPTION','CUSHION THICKNESS mm','CUSHION
WIDTH mm', 'CUSHION LENGTH mm',...
      'NUMBER OF LAYERS','FLUE ORIENTATION','DROP HEIGHT mm','PLATEN
MASS kg','SAMPLE NAME','END CONDITIONS','END PRESSURE', 'FILTER
DYNAMIC DATA',...
      'SAMPLING RATE Hz','USE STATIC DATA'},'CUSHION INFORMATION',1,...
      {'Virgin Fibreboard','33  ','168.00','168.00','11','Square', '200','2.514', 'SQ52','Fully
Open','101e-3','no','20000', 'yes'});
answer = cell2struct(answer,{'cushdes','thick', 'wid', 'le', 'nlay', 'fo', 'dh', 'pm','samp','ec',
'ep','filte', 'sr','stest'});
cushdes = answer.cushdes;
cushThickness = (str2num(answer.thick))/1000;
cushWidth = (str2num(answer.wid))/1000;
cushLength = (str2num(answer.le))/1000;
numLayers = str2num(answer.nlay);
dropHeight = (str2num(answer.dh))/1000;
platenMass = str2num(answer.pm);
sr = str2num(answer.sr);
ec = answer.ec;
filte = answer.filte;
samp = answer.samp;
stest = answer.stest;

endPress = str2num(answer.ep);
fo = answer.fo;
```

```
cushArea = cushLength * cushWidth;
if strcmp(stest, 'yes')==1
   %Read static testing files
   [ys, fs, staticStiffness, statDeflect, index, sthresh, sComment, sFilePath, sFile] =
read_static;
   %staticStiffness N/m
else
   staticStiffness = 0;
end

%Reads cushion testing files
[fullTime, fullData, accFilter, index, channels, aFilePath, aFile, dummyFile] =
read_dynamic_acc_ascii(sr);
%Index has element numbers for ShortPulseStart VoltStart, MaxAccel, VlotFinish,
ShortPulseFinish

%Smooths data and theoretically determine velocity and displacement for
%display
[expPlatVel, expPlatVelTime, expPlatVelAcc, expPlatDispSmooth, staticStress]=
PlatenAccVelExperimental(fullTime, fullData, index);


%Display of Experimental data
y = expDataDisplay(fullTime, fullData, expPlatVel, expPlatVelTime, expPlatVelAcc,
expPlatDispSmooth, index, aFilePath, aFile);
%y = expDataDisplay2Chan(fullTime, fullData, index, aFilePath, aFile);


%Package Dynamics Theoretical - experimental acc to calculated Velocity and Displacement
[calcV0, calcV, calcY,index] = AccVelContactTheoretical(fullTime, fullData, index,
staticStress, aFilePath, aFile);

%Simulates pre-impact dynamics
[simPlatenAccPre, simPlatenVelPre, simPlatenDispPre, stim] = freeFallVelocity(fullTime,
fullData, calcY, calcV, index, staticStiffness, aFilePath, aFile);
```

File read_dynamic_acc_ascii.m

```
%Usage: This macro reads acceleration data from cushion test taken from a Cushion Tester
%Recorded with DTVee. The measurements are acceleration and a voltage pulse
%that determine when the plate contacts the cushion. Sorts out the true
%acceleration pulse.  Sampling rate 10k
%Written by M Minett

function [timeRaw, data, accf, index, chan, cFilePath, cFile, dFile] = fa(sr)

   global filte fOrder cutOff tag
```

```
cFilePath = uigetdir('D:\My Documents\phd\thesis\thesis', 'FIND DIRECTORY FOR
CUSHION FILES');
cFilePath = [cFilePath,'\'];
cFile = uigetfile([cFilePath,'*.*'],'Cushion File from VU Cushion Tester');
answer = inputdlg({'NUMBER OF DATA CHANNELS'}, '', 1,{'4'});
answer = cell2struct(answer,{'chan'});
chan = (str2num(answer.chan));

%Read the data file
data = load([cFilePath,cFile]);

%Reading dummy file for data offset check
idx=find(cFile == '.');
dFile = [cFile(1:idx-1),'dummy', cFile(idx:end)];

%[cFilePath,dFile]
%pause;

%dummydata = load([cFilePath,dFile]);

%Reshape the data for appropriate properties
data = reshape(data, length(data)/chan, chan);

%Assign volts and acceleration for temporary plotting
accRaw = data(:,1);
volts = data(:,2);

%Create time vector against sampling rate
timeRaw = 0:1/sr:(length(accRaw)-1)*1/sr;
timeRaw = timeRaw';


%Determine the short pulse start and finish

figure(1);
plot(timeRaw, accRaw);
[x,thresh]=ginput(2);
idx1 = find(timeRaw >= x(1));
idx2 = find(timeRaw >= x(2));
x = min(timeRaw(idx1:idx2));
delete(1);

%Determine the short pulse indexes
idx = find(timeRaw >= x);
idxss = idx(1);  %Start short pulse

%Find the maximum acceleration index
idx = find(accRaw >= max(accRaw));
idxm = idx(1);
%idxss
```

```
   %Determine where the platen contacts the cushion is equal to where
   %voltage measurement peaks.
   idx = find(volts(idxss:end) >= 4);



   idxvs = idx(1)+idxss;
   idx = find(volts(idxvs:end) <= 4);
   idxvf = idx(1)+idxvs;
   clear idx;


   %Find the finsh of the short pulse
   %idx = find(accRaw(idxm:end) <= accRaw(idxss));
   idxsf = idxvf + 50;  %Finish short pulse


   %Assign index array [start short pulse, platen contact, maximum acc, platen disengages,
finish short pulse]
   index = [idxss, idxvs, idxm, idxvf, idxsf];


   %Performs filtering if required
   if strcmp(filte,'YES')==1
      accf = zeros(length(acc));
      dt = mean(diff(time));
      [b,a] = butter(fOrder, 2 * cutOff * dt);
            accf = fliplr(filter(b,a,fliplr(filter(b,a,acc))));
  else
     accf = 0;
  end
```

File platenAccVelExperimental.m

```
%This macro uses the experimental acceleration and displacement data - integrates and
%differentiates for velocity and smooths the data
%Written by M Minett

function [fexpVel, fexpVelTim, fexpVelA, pdssf, statStress] = f(Time, Data, index)

   global G filte cushArea platenMass dropHeight cushLength cushWidth cushThickness
numLayers fo ec samp tag sd stest pg kg cushdes



   %Determine the static stress and place in structure
   statStress = platenMass * G /(cushArea * 1000);
```

```
%Platen Dynamics over the Short Pulse
%Find the platen displacement over the short pulse
timShort = Time(index(1):index(5));
platDispShort = Data(index(1):index(5),4);
%timShortFine = linspace(timShort(1), timShort(end), 5000);

%Smooth the platen displacement over full data
[coef, S, mu] = polyfit(Time(1:index(5)), Data(1:index(5),4), 10);
[pdssf, delta] = polyval(coef, Time(1:index(5)), S, mu);
%pdss = pdssf(index(1):index(5));
dh = mean(diff(timShort));

%Determine the experinmental platen velocity by differentiating
%displacement with Central Differences Higher Order
fexpVel = (-pdssf(5:end) + 8*pdssf(4:end-1) - 8*pdssf(2:end-3) + pdssf(1:end-4))/(12*dh);
fexpVel = fexpVel/1000;  %m/sec
fexpVelTim = Time(3:index(5)-2);
%Diplacement with Central Differences Lower order
%fexpVel = (pdssf(3:end) - pdssf(1:end-2))/(2*dh);
%fexpVelTim = Time(2:index(5)-1);


%determine the experimental platen velocity by integrating acceleration
fexpVelA = cumtrapz(Time(1:index(5)), Data(1:index(5),1));
v0 = min(fexpVel)/1000;
fexpVelA = fexpVelA + v0;
fexpVelA = fexpVel/1000;   %m/sec
```

File expDataDisplay.m

```
%This macro displays experimental data
%Written by M Minett

function y = f(Time, Data, fexpVel, fexpVelTim, fexpVelA, pdssf, index, filePath, file)

   global G cushArea platenMass dropHeight cushLength cushWidth cushThickness
numLayers fo ec samp sd stest pg cushdes


   y = 0;

   fname = ['FILE ', filePath, file];


    %Graphing Displacement Data
```

```
pname = ['CUSHION TEST DATA'];
figure(21);

set(gcf, 'position', [50,50,850,550]);
%set(gcf, 'color', 'c');
set(gcf, 'name', pname);
set(gcf, 'numbertitle', 'off');
set(gcf, 'PaperOrientation', 'landscape');
set(gcf, 'PaperUnits', 'centimeters');
set(gcf, 'PaperType', 'A4');
set(gcf, 'PaperPositionMode', 'manual');
set(gcf, 'PaperPosition', [1.0 1.0,  28.5 18.5]);

dog1 = [Data(:,1)/9.81];
dog2 = [Data(:,3), Data(:,4)];
dog3 = Time(index(2));
dog4 = Time(index(4));
dog5 = Time(index(3));




subplot(2,2,1);


[ax, pyy1, pyy2] = plotyy(Time, dog1, Time, dog2);
v = axis;
hold on;
pv1 = plot([dog3, dog3], [v(3), v(4)], 'k', [dog4, dog4], [v(3), v(4)], 'k',[dog5, dog5], [v(3),
v(4)], 'm' );
set(pv1, 'linewidth', 1.5);
set(pyy1, 'linewidth', 2);
set(pyy2, 'linewidth', 2);
t1 = title('FULL EXPERIMENTAL PULSE');
set(t1, 'fontsize', 12);
set(t1, 'fontweight', 'bold');
set(get(ax(1),'Ylabel'),'string','Acceleration (g)');
set(get(ax(1), 'Ylabel'),'fontsize', 12);
set(get(ax(2),'Ylabel'),'string','Displacement (mm)');
set(get(ax(2), 'Ylabel'),'fontsize', 12);
Lx1 = xlabel('Time (sec) ');
set(Lx1, 'fontsize', 12);
grid;



dog1 = [Data(index(1):index(5),1)/9.81];
dog2 = [Data(index(1):index(5),3), Data(index(1):index(5),4)];
```

```
    subplot(2,2,2);
    [ax, pyy1, pyy2] = plotyy(Time(index(1):index(5)), dog1, Time(index(1):index(5)), dog2);
    set(pyy1, 'linewidth', 2);
    set(pyy2, 'linewidth', 2);
    v = axis;
    hold on;
    pv1 = plot([dog3, dog3], [v(3), v(4)], 'k', [dog4, dog4], [v(3), v(4)], 'k',[dog5, dog5], [v(3),
v(4)], 'm' );
    set(pv1, 'linewidth', 1.5);

    t1 = title('SHORT EXPERIMENTAL PULSE');
    set(t1, 'fontsize', 12);
    set(t1, 'fontweight', 'bold');

    set(get(ax(1),'Ylabel'),'string','Acceleration (g)');
    set(get(ax(1), 'Ylabel'),'fontsize', 12);
    set(get(ax(2),'Ylabel'),'string','Displacement (mm)');
    set(get(ax(2), 'Ylabel'),'fontsize', 12);
    Lx1 = xlabel('Time (sec) ');
    set(Lx1, 'fontsize', 12);
    grid;




    k = 1;
    subplot(2,2,3);
    set(gca,'Visible','Off');
    set(gca,'FontSize',10);
    inc = 0.10;

    t2 = text(0,1-(k-1)*inc, ['Cushion Dynamic Data']);
    set(t2, 'fontsize', 12);
    set(t2, 'fontweight', 'bold');

    k = k + 1;
    pname = ['File  ', filePath, file, '   Sample Name - ',samp];
    t1 = text(0,1-(k-1)*inc, pname);
    k = k + 1;
    pname = ['Cushion Type - ', cushdes];
    t1 = text(0,1-(k-1)*inc, pname);
    k = k + 1;
    pname = ['Cushion Dimensions - ', num2str(cushLength),' x ', num2str(cushWidth),' x ',
num2str(cushThickness), ' m'];
    t1 = text(0,1-(k-1)*inc, pname);
    k = k + 1;
    pname = ['Cushion Area = ', num2str(cushLength*cushWidth), ' sq m'];
    t1 = text(0,1-(k-1)*inc, pname);
    k = k + 1;
    pname = ['Flute Orientation  ', fo];
```

```
t1 = text(0,1-(k-1)*inc, pname);
k = k + 1;
pname = ['End Conditions - ', ec];
t1 = text(0,1-(k-1)*inc, pname);
k = k + 1;
pname = ['No of Layers = ', num2str(numLayers)];
t1 = text(0,1-(k-1)*inc, pname);
k = k + 1;
pname = ['Platen Mass = ', num2str(platenMass), ' kg'];
t1 = text(0,1-(k-1)*inc, pname);
k = k + 1;
pname = ['Drop Height = ', num2str(dropHeight), ' mm'];
t1 = text(0,1-(k-1)*inc, pname);
k = k + 1;
pname = ['Maximum Acceleration = ', num2str(max(Data(:,1))/9.81),' g'];
t1 = text(0,1-(k-1)*inc, pname);
k = k + 1;
pname = ['Acceleration at Contact = ',  num2str(Data(index(2),1)/9.81),' g'];
t1 = text(0,1-(k-1)*inc, pname);
%k = k + 1;
%pname = ['Acceleration on Impact = ', dynamic_init_acc,' m/sec-2'];
%t1 = text(0,1-(k-1)*inc, pname);
%k = k + 1;
%pname = ['Re-Bound Velocity = ', rebound_vel,' m/sec'];
%t1 = text(0,1-(k-1)*inc, pname);



figure(500)
[ax, pyy1, pyy2] = plotyy(Time(index(1):index(5)), dog1, Time(index(1):index(5)), dog2);
set(pyy1, 'linewidth', 2);
set(pyy2, 'linewidth', 2);
v = axis;
hold on;
pv1 = plot([dog3, dog3], [v(3), v(4)], 'k', [dog4, dog4], [v(3), v(4)], 'k',[dog5, dog5], [v(3),
v(4)], 'm' );
set(pv1, 'linewidth', 1.5);

t1 = title('SHORT EXPERIMENTAL PULSE');
set(t1, 'fontsize', 12);
set(t1, 'fontweight', 'bold');

set(get(ax(1),'Ylabel'),'string','Acceleration (g)');
set(get(ax(1), 'Ylabel'),'fontsize', 12);
set(get(ax(2),'Ylabel'),'string','Displacement (mm)');
set(get(ax(2), 'Ylabel'),'fontsize', 12);
Lx1 = xlabel('Time (sec) ');
set(Lx1, 'fontsize', 12);
grid;
```

File freeFallVelocity.m

```
%This macro solves for free fall velocity and displacement displacement analysis
%and calls the pre-contact simulink model
%Written by M Minett

%clear all;
function [sPlatenAcc, sPlatenVel, sPlatenDisp, stim] = f(td, data, theorDisp, theorVel, index,
statStiff, fpath, fname)


global G filte cushArea platenMass dropHeight cushLength cushWidth cushThickness
numLayers fOrder cutOff ec samp stest pg kg stiffness cushdes rho fo


%Index has element numbers for ShortPulseStart VoltStart, MaxAccel,
   %VoltFinish, ShortPulseFinish zeroVel, reboundVel

expDispP = data(:,4)/1000;
test = expDispP(index(2));
%expDispC = fullData(:,3);
y = 0;
%platenMass = 2.494;
%platenArea = 0.168 * 0.168;
rho = 101.235 / (0.287 * (273 + 20));
%g = 9.8065;
%dropHeight = 0.2;
Cd = 1.0;
%len = 0.168;

tim = [td(index(1)),td(index(2))];


%Simulation before impact

if statStiff == 0

   sim('preCompressNoStatic', tim);
else
   sim('preCompressStatic', tim);
end

sPlatenAcc = sPlatenAcc - sPlatenAcc(1);

stim = tout(end);

platDispSlopeExp = (data(index(1), 4) - data(index(2),4))/(tim(end)- tim(1))/1000;
platDispSlopeSim = (sPlatenDisp(end)-sPlatenDisp(1))/(tout(1) - tout(end));
```

```
%Graphing of Simulation Data Prior to Impact
%sPlatenDisp = sPlatenDisp - sPlatenDisp(1);
pname = 'Pre-Contact dynamics - Simulated';
figure(30);
set(30, 'position', [100,100,900,500]);
%set(gcf, 'color', 'c');
set(30, 'name', pname);
set(30, 'numbertitle', 'off');
set(30, 'PaperOrientation', 'landscape');
set(30, 'PaperUnits', 'centimeters');
set(30, 'PaperType', 'A4');
set(30, 'PaperPositionMode', 'manual');
set(30, 'PaperPosition', [1.0 1.0,  28.5 18.5]);

subplot(2,2,1);
p1 = plot(tout*1000, sPlatenAcc/G, 'b');
set(p1, 'linewidth', 1.5);
lx1 = xlabel('Time (ms)');
set(lx1, 'fontweight', 'bold');
ly1 = ylabel('Simulated Platen Acceleration g');
set(ly1, 'fontweight', 'bold');
grid;

subplot(2,2,2);
p2 = plot(tout*1000, sPlatenVel, 'm');
lx2 = xlabel('Time (ms)');
set(lx2, 'fontweight', 'bold');
set(p2, 'linewidth', 1.5);
ly2 = ylabel('Simulated Platen Velocity m/sec');
set(ly2, 'fontweight', 'bold');
grid;

subplot(2,2,3);
p3 = plot(tout*1000, sPlatenDisp*1000,  'r');
set(p3, 'linewidth', 1.5);
lx3 = xlabel('Time (ms)');
set(lx3, 'fontweight', 'bold');
ly3 = ylabel('Platen Displacement mm');
set(ly3, 'fontweight', 'bold');
grid;

drop_h = [num2str(dropHeight*1000)];
simAccContact = [num2str(sPlatenAcc(end)/G)];
simAccContact(end) = [];
cush_area = [num2str(cushArea)];
cush_area(7:end) = [];
cush_width = [num2str(cushWidth*1000)];
cush_length = [num2str(cushLength*1000)];
```

```
cush_thick = [num2str(cushThickness*1000)];
test_mass = [num2str(platenMass)];
num_layers = [num2str(numLayers)];

 k = 1;
 subplot(2,2,4);
    set(gca,'Visible','Off');
    set(gca,'FontSize',10);
    inc = 0.09;

    t2 = text(0,1-(k-1)*inc, ['Pre-Contact Simulated Platen Dynamic Data']);
    set(t2, 'fontsize', 12);
    set(t2, 'fontweight', 'bold');
    k = k + 1;

    pname = ['File  ', fpath(21:end), fname, ' Sample - ',samp];
    t1 = text(0,1-(k-1)*inc, pname);
    k = k + 1;
    pname = ['Cushion Type - ', cushdes];
    t1 = text(0,1-(k-1)*inc, pname);
    k = k + 1;
    pname = ['Cushion Dimensions - ', cush_length,' x ', cush_width,' x ', cush_thick, ' mm'];
    t1 = text(0,1-(k-1)*inc, pname);
    k = k + 1;
    pname = ['Cushion Area = ', cush_area, 'sq m'];
    t1 = text(0,1-(k-1)*inc, pname);
    k = k + 1;
    if cushLength ~= cushWidth
        pname = ['Flute Orientation  ', fo];
        t1 = text(0,1-(k-1)*inc, pname);
        k = k + 1;
    end
    pname = ['End Conditions - ', ec];
    t1 = text(0,1-(k-1)*inc, pname);
    k = k + 1;
    pname = ['No of Layers = ', num_layers];
    t1 = text(0,1-(k-1)*inc, pname);
    k = k + 1;
    pname = ['Platen Mass = ', test_mass, ' kg'];
    t1 = text(0,1-(k-1)*inc, pname);
    k = k + 1;
    pname = ['Drop Height = ', drop_h, ' mm'];
    t1 = text(0,1-(k-1)*inc, pname);
    k = k + 2;
    pname = ['Simulated Acceleration at Contact = ', simAccContact, ' g'];
    t1 = text(0,1-(k-1)*inc, pname);
```

```
%Graphing of Simulation and Experimental Data Prior to Impact
sPlatenDisp = sPlatenDisp - sPlatenDisp(1);
pname = 'Pre-Contact dynamics - Experimental  and Simulated';
figure(31);
set(31, 'position', [100,100,900,500]);
%set(gcf, 'color', 'c');
set(31, 'name', pname);
set(31, 'numbertitle', 'off');
set(31, 'PaperOrientation', 'landscape');
set(31, 'PaperUnits', 'centimeters');
set(31, 'PaperType', 'A4');
set(31, 'PaperPositionMode', 'manual');
set(31, 'PaperPosition', [1.0 1.0,  28.5 18.5]);

subplot(2,2,1);
p1 = plot(tout*1000, sPlatenAcc/G, td(index(1):index(2))*1000, data(index(1):index(2),1)/G,
'r');
set(p1, 'linewidth', 1.5);
lx1 = xlabel('Time (ms)');
set(lx1, 'fontweight', 'bold');
ly1 = ylabel('Platen Acceleration g');
set(ly1, 'fontweight', 'bold');
grid;

%subplot(2,2,4);
%p2 = plot(tout*1000, sPlatenVel, td(1:index(2))*1000, theorVel(1:index(2)), 'r');
%lx2 = xlabel('Time (ms)');
%set(lx2, 'fontweight', 'bold');
%set(p2, 'linewidth', 1.5);
%ly2 = ylabel('Platen Velocity m/sec');
%set(ly2, 'fontweight', 'bold');

subplot(2,2,2);
p3 = plot(tout*1000, sPlatenDisp*1000, td(index(1):index(2))*1000,...
(expDispP(index(1):index(2))- expDispP(index(1)))*1000, 'r');
%td(1:index(2))*1000, yd(1:index(2)), ':g');
set(p3, 'linewidth', 1.5);
lx3 = xlabel('Time (ms)');
set(lx3, 'fontweight', 'bold');
ly3 = ylabel('Platen Displacement mm');
set(ly3, 'fontweight', 'bold');
grid;



 %Display data
```

```
drop_h = [num2str(dropHeight*1000)];

%contact_vel = [num2str(v0)];
 %   calc_init_vel(end) = [];
  %  contact_deflect = [num2str(ydmin*1000)];
 %   max_deflect(end-1:end) = [];
 simAccContact = [num2str(sPlatenAcc(end)/G)];
 simAccContact(end) = [];
 expAccContact = [num2str(data(index(2),1)/G)];
 expAccContact(end) = [];
 %   vel_max_acc(end) = [];
 %   static_stress = [num2str(statstress)];
 %   static_stress(end) = [];
 %   dynamic_init_vel = [num2str(vd(index(2)))];
 cush_area = [num2str(cushArea)];
 cush_area(7:end) = [];
 cush_width = [num2str(cushWidth*1000)];
 cush_length = [num2str(cushLength*1000)];
 cush_thick = [num2str(cushThickness*1000)];
 test_mass = [num2str(platenMass)];
 %dynamic_init_acc = [num2str(ad(index(2)))];
 num_layers = [num2str(numLayers)];

 k = 1;
 subplot(2,2,3);
    set(gca,'Visible','Off');
    set(gca,'FontSize',10);
    inc = 0.09;

    t2 = text(0,1-(k-1)*inc, ['Pre-Contact Platen Dynamic Data']);
    set(t2, 'fontsize', 12);
    set(t2, 'fontweight', 'bold');
    k = k + 1;
    t2 = text(0,1-(k-1)*inc, ['Simulation (Blue) Vs Experimental (Red)']);
    set(t2, 'fontsize', 12);
    set(t2, 'fontweight', 'bold');
    k = k + 1;
    pname = ['File  ', fpath(21:end), fname, ' Sample - ',samp];
    t1 = text(0,1-(k-1)*inc, pname);
    k = k + 1;
    pname = ['Cushion Type - ', cushdes];
    t1 = text(0,1-(k-1)*inc, pname);
    k = k + 1;
    pname = ['Cushion Dimensions - ', cush_length,' x ', cush_width,' x ', cush_thick, ' mm'];
    t1 = text(0,1-(k-1)*inc, pname);
    k = k + 1;
    pname = ['Cushion Area = ', cush_area, 'sq m'];
    t1 = text(0,1-(k-1)*inc, pname);
    k = k + 1;
    if cushLength ~= cushWidth
```

```
    pname = ['Flute Orientation  ', fo];
    t1 = text(0,1-(k-1)*inc, pname);
    k = k + 1;
end
pname = ['End Conditions - ', ec];
t1 = text(0,1-(k-1)*inc, pname);
k = k + 1;
pname = ['No of Layers = ', num_layers];
t1 = text(0,1-(k-1)*inc, pname);
k = k + 1;
pname = ['Platen Mass = ', test_mass, ' kg'];
t1 = text(0,1-(k-1)*inc, pname);
k = k + 1;
pname = ['Drop Height = ', drop_h, ' mm'];
t1 = text(0,1-(k-1)*inc, pname);
k = k + 1;
pname = ['Simulated Acceleration at Contact = ', simAccContact, ' g'];
t1 = text(0,1-(k-1)*inc, pname);
k = k + 1;
pname = ['Experimental Acceleration at Contact = ', expAccContact, ' g'];
t1 = text(0,1-(k-1)*inc, pname);
k = k+1;
pname = ['Experimental Platen Slope ', num2str(platDispSlopeExp), ' m/s'];
t1 = text(0,1-(k-1)*inc, pname);
k = k+1;
pname = ['Simulated Platen Slope ', num2str(platDispSlopeSim),' m/s'];
t1 = text(0,1-(k-1)*inc, pname);
```

Appendix B

The following programs are written to read and analyse data for the pre-contact air-flow analsys. These programs are written in Matlab m files and also call the simulink models referred to in the main body of work.

File : contact.m

```
%This is the main progam that analyses and simulates pre-contact dynamics
%for mult-layered fibreboard cushions.
%Written by M Minett


clear all;
global G filte cushArea platenMass dropHeight cushLength cushWidth cushThickness
numLayers fOrder cutOff ec samp stest pg cushdes rho fo

G = 9.81065;

%Input of data
answer = inputdlg({'CUSHION DESCRIPTION','CUSHION THICKNESS mm','CUSHION
WIDTH mm', 'CUSHION LENGTH mm',...
      'NUMBER OF LAYERS','FLUE ORIENTATION','DROP HEIGHT mm','PLATEN
MASS kg','SAMPLE NAME','END CONDITIONS','END PRESSURE', 'FILTER
DYNAMIC DATA',...
      'SAMPLING RATE Hz','USE STATIC DATA'},'CUSHION INFORMATION',1,...
      {'Virgin Fibreboard','33  ','168.00','168.00','11','Square', '200','2.514', 'SQ52','Fully
Open','101e-3','no','20000', 'yes'});
answer = cell2struct(answer,{'cushdes','thick', 'wid', 'le', 'nlay', 'fo', 'dh', 'pm','samp','ec',
'ep','filte', 'sr','stest'});
cushdes = answer.cushdes;
cushThickness = (str2num(answer.thick))/1000;
cushWidth = (str2num(answer.wid))/1000;
cushLength = (str2num(answer.le))/1000;
numLayers = str2num(answer.nlay);
dropHeight = (str2num(answer.dh))/1000;
platenMass = str2num(answer.pm);
sr = str2num(answer.sr);
ec = answer.ec;
filte = answer.filte;
samp = answer.samp;
stest = answer.stest;

endPress = str2num(answer.ep);
fo = answer.fo;
```

```
cushArea = cushLength * cushWidth;
if strcmp(stest, 'yes')==1
   %Read static testing files
   [ys, fs, staticStiffness, statDeflect, index, sthresh, sComment, sFilePath, sFile] =
read_static;
   %staticStiffness N/m
else
   staticStiffness = 0;
end

%Reads cushion testing files
[fullTime, fullData, accFilter, index, channels, aFilePath, aFile, dummyFile] =
read_dynamic_acc_ascii(sr);
%Index has element numbers for ShortPulseStart VoltStart, MaxAccel, VlotFinish,
ShortPulseFinish

%Smooths data and theoretically determine velocity and displacement for
%display
[expPlatVel, expPlatVelTime, expPlatVelAcc, expPlatDispSmooth, staticStress]=
PlatenAccVelExperimental(fullTime, fullData, index);


%Display of Experimental data
y = expDataDisplay(fullTime, fullData, expPlatVel, expPlatVelTime, expPlatVelAcc,
expPlatDispSmooth, index, aFilePath, aFile);
%y = expDataDisplay2Chan(fullTime, fullData, index, aFilePath, aFile);


%Package Dynamics Theoretical - experimental acc to calculated Velocity and Displacement
[calcV0, calcV, calcY,index] = AccVelContactTheoretical(fullTime, fullData, index,
staticStress, aFilePath, aFile);

%Simulates pre-impact dynamics
[simPlatenAccPre, simPlatenVelPre, simPlatenDispPre, stim] = freeFallVelocity(fullTime,
fullData, calcY, calcV, index, staticStiffness, aFilePath, aFile);
```

File read_dynamic_acc_ascii.m

```
%Usage: This macro reads acceleration data from cushion test taken from a Cushion Tester
%Recorded with DTVee. The measurements are acceleration and a voltage pulse
%that determine when the plate contacts the cushion. Sorts out the true
%acceleration pulse.  Sampling rate 10k
%Written by M Minett

function [timeRaw, data, accf, index, chan, cFilePath, cFile, dFile] = fa(sr)

   global filte fOrder cutOff tag
```

```
cFilePath = uigetdir('D:\My Documents\phd\thesis\thesis', 'FIND DIRECTORY FOR
CUSHION FILES');
cFilePath = [cFilePath,'\'];
cFile = uigetfile([cFilePath,'*.*'],'Cushion File from VU Cushion Tester');
answer = inputdlg({'NUMBER OF DATA CHANNELS'}, '', 1,{'4'});
answer = cell2struct(answer,{'chan'});
chan = (str2num(answer.chan));

%Read the data file
data = load([cFilePath,cFile]);

%Reading dummy file for data offset check
idx=find(cFile == '.');
dFile = [cFile(1:idx-1),'dummy', cFile(idx:end)];

%[cFilePath,dFile]
%pause;

%dummydata = load([cFilePath,dFile]);

%Reshape the data for appropriate properties
data = reshape(data, length(data)/chan, chan);

%Assign volts and acceleration for temporary plotting
accRaw = data(:,1);
volts = data(:,2);

%Create time vector against sampling rate
timeRaw = 0:1/sr:(length(accRaw)-1)*1/sr;
timeRaw = timeRaw';


%Determine the short pulse start and finish

figure(1);
plot(timeRaw, accRaw);
[x,thresh]=ginput(2);
idx1 = find(timeRaw >= x(1));
idx2 = find(timeRaw >= x(2));
x = min(timeRaw(idx1:idx2));
delete(1);

%Determine the short pulse indexes
idx = find(timeRaw >= x);
idxss = idx(1);  %Start short pulse

%Find the maximum acceleration index
idx = find(accRaw >= max(accRaw));
idxm = idx(1);
%idxss
```

```
   %Determine where the platen contacts the cushion is equal to where
   %voltage measurement peaks.
   idx = find(volts(idxss:end) >= 4);



   idxvs = idx(1)+idxss;
   idx = find(volts(idxvs:end) <= 4);
   idxvf = idx(1)+idxvs;
   clear idx;


   %Find the finsh of the short pulse
   %idx = find(accRaw(idxm:end) <= accRaw(idxss));
   idxsf = idxvf + 50;  %Finish short pulse


   %Assign index array [start short pulse, platen contact, maximum acc, platen disengages,
finish short pulse]
   index = [idxss, idxvs, idxm, idxvf, idxsf];


   %Performs filtering if required
   if strcmp(filte,'YES')==1
      accf = zeros(length(acc));
      dt = mean(diff(time));
      [b,a] = butter(fOrder, 2 * cutOff * dt);
            accf = fliplr(filter(b,a,fliplr(filter(b,a,acc))));
  else
     accf = 0;
  end
```

File platenAccVelExperimental.m

```
%This macro uses the experimental acceleration and displacement data - integrates and
%differentiates for velocity and smooths the data
%Written by M Minett

function [fexpVel, fexpVelTim, fexpVelA, pdssf, statStress] = f(Time, Data, index)

   global G filte cushArea platenMass dropHeight cushLength cushWidth cushThickness
numLayers fo ec samp tag sd stest pg kg cushdes



   %Determine the static stress and place in structure
   statStress = platenMass * G /(cushArea * 1000);
```

```
%Platen Dynamics over the Short Pulse
%Find the platen displacement over the short pulse
timShort = Time(index(1):index(5));
platDispShort = Data(index(1):index(5),4);
%timShortFine = linspace(timShort(1), timShort(end), 5000);

%Smooth the platen displacement over full data
[coef, S, mu] = polyfit(Time(1:index(5)), Data(1:index(5),4), 10);
[pdssf, delta] = polyval(coef, Time(1:index(5)), S, mu);
%pdss = pdssf(index(1):index(5));
dh = mean(diff(timShort));

%Determine the experinmental platen velocity by differentiating
%displacement with Central Differences Higher Order
fexpVel = (-pdssf(5:end) + 8*pdssf(4:end-1) - 8*pdssf(2:end-3) + pdssf(1:end-4))/(12*dh);
fexpVel = fexpVel/1000;  %m/sec
fexpVelTim = Time(3:index(5)-2);
%Diplacement with Central Differences Lower order
%fexpVel = (pdssf(3:end) - pdssf(1:end-2))/(2*dh);
%fexpVelTim = Time(2:index(5)-1);


%determine the experimental platen velocity by integrating acceleration
fexpVelA = cumtrapz(Time(1:index(5)), Data(1:index(5),1));
v0 = min(fexpVel)/1000;
fexpVelA = fexpVelA + v0;
fexpVelA = fexpVel/1000;   %m/sec
```

File expDataDisplay.m

```
%This macro displays experimental data
%Written by M Minett

function y = f(Time, Data, fexpVel, fexpVelTim, fexpVelA, pdssf, index, filePath, file)

   global G cushArea platenMass dropHeight cushLength cushWidth cushThickness
numLayers fo ec samp sd stest pg cushdes


   y = 0;

   fname = ['FILE ', filePath, file];


    %Graphing Displacement Data
```

```
pname = ['CUSHION TEST DATA'];
figure(21);

set(gcf, 'position', [50,50,850,550]);
%set(gcf, 'color', 'c');
set(gcf, 'name', pname);
set(gcf, 'numbertitle', 'off');
set(gcf, 'PaperOrientation', 'landscape');
set(gcf, 'PaperUnits', 'centimeters');
set(gcf, 'PaperType', 'A4');
set(gcf, 'PaperPositionMode', 'manual');
set(gcf, 'PaperPosition', [1.0 1.0,  28.5 18.5]);

dog1 = [Data(:,1)/9.81];
dog2 = [Data(:,3), Data(:,4)];
dog3 = Time(index(2));
dog4 = Time(index(4));
dog5 = Time(index(3));




subplot(2,2,1);


[ax, pyy1, pyy2] = plotyy(Time, dog1, Time, dog2);
v = axis;
hold on;
pv1 = plot([dog3, dog3], [v(3), v(4)], 'k', [dog4, dog4], [v(3), v(4)], 'k',[dog5, dog5], [v(3),
v(4)], 'm' );
set(pv1, 'linewidth', 1.5);
set(pyy1, 'linewidth', 2);
set(pyy2, 'linewidth', 2);
t1 = title('FULL EXPERIMENTAL PULSE');
set(t1, 'fontsize', 12);
set(t1, 'fontweight', 'bold');
set(get(ax(1),'Ylabel'),'string','Acceleration (g)');
set(get(ax(1), 'Ylabel'),'fontsize', 12);
set(get(ax(2),'Ylabel'),'string','Displacement (mm)');
set(get(ax(2), 'Ylabel'),'fontsize', 12);
Lx1 = xlabel('Time (sec) ');
set(Lx1, 'fontsize', 12);
grid;



dog1 = [Data(index(1):index(5),1)/9.81];
dog2 = [Data(index(1):index(5),3), Data(index(1):index(5),4)];
```

```
    subplot(2,2,2);
    [ax, pyy1, pyy2] = plotyy(Time(index(1):index(5)), dog1, Time(index(1):index(5)), dog2);
    set(pyy1, 'linewidth', 2);
    set(pyy2, 'linewidth', 2);
    v = axis;
    hold on;
    pv1 = plot([dog3, dog3], [v(3), v(4)], 'k', [dog4, dog4], [v(3), v(4)], 'k',[dog5, dog5], [v(3),
v(4)], 'm' );
    set(pv1, 'linewidth', 1.5);

    t1 = title('SHORT EXPERIMENTAL PULSE');
    set(t1, 'fontsize', 12);
    set(t1, 'fontweight', 'bold');

    set(get(ax(1),'Ylabel'),'string','Acceleration (g)');
    set(get(ax(1), 'Ylabel'),'fontsize', 12);
    set(get(ax(2),'Ylabel'),'string','Displacement (mm)');
    set(get(ax(2), 'Ylabel'),'fontsize', 12);
    Lx1 = xlabel('Time (sec) ');
    set(Lx1, 'fontsize', 12);
    grid;




    k = 1;
    subplot(2,2,3);
    set(gca,'Visible','Off');
    set(gca,'FontSize',10);
    inc = 0.10;

    t2 = text(0,1-(k-1)*inc, ['Cushion Dynamic Data']);
    set(t2, 'fontsize', 12);
    set(t2, 'fontweight', 'bold');

    k = k + 1;
    pname = ['File  ', filePath, file, '   Sample Name - ',samp];
    t1 = text(0,1-(k-1)*inc, pname);
    k = k + 1;
    pname = ['Cushion Type - ', cushdes];
    t1 = text(0,1-(k-1)*inc, pname);
    k = k + 1;
    pname = ['Cushion Dimensions - ', num2str(cushLength),' x ', num2str(cushWidth),' x ',
num2str(cushThickness), ' m'];
    t1 = text(0,1-(k-1)*inc, pname);
    k = k + 1;
    pname = ['Cushion Area = ', num2str(cushLength*cushWidth), ' sq m'];
    t1 = text(0,1-(k-1)*inc, pname);
    k = k + 1;
    pname = ['Flute Orientation  ', fo];
```

```
t1 = text(0,1-(k-1)*inc, pname);
k = k + 1;
pname = ['End Conditions - ', ec];
t1 = text(0,1-(k-1)*inc, pname);
k = k + 1;
pname = ['No of Layers = ', num2str(numLayers)];
t1 = text(0,1-(k-1)*inc, pname);
k = k + 1;
pname = ['Platen Mass = ', num2str(platenMass), ' kg'];
t1 = text(0,1-(k-1)*inc, pname);
k = k + 1;
pname = ['Drop Height = ', num2str(dropHeight), ' mm'];
t1 = text(0,1-(k-1)*inc, pname);
k = k + 1;
pname = ['Maximum Acceleration = ', num2str(max(Data(:,1))/9.81),' g'];
t1 = text(0,1-(k-1)*inc, pname);
k = k + 1;
pname = ['Acceleration at Contact = ',  num2str(Data(index(2),1)/9.81),' g'];
t1 = text(0,1-(k-1)*inc, pname);
%k = k + 1;
%pname = ['Acceleration on Impact = ', dynamic_init_acc,' m/sec-2'];
%t1 = text(0,1-(k-1)*inc, pname);
%k = k + 1;
%pname = ['Re-Bound Velocity = ', rebound_vel,' m/sec'];
%t1 = text(0,1-(k-1)*inc, pname);



figure(500)
[ax, pyy1, pyy2] = plotyy(Time(index(1):index(5)), dog1, Time(index(1):index(5)), dog2);
set(pyy1, 'linewidth', 2);
set(pyy2, 'linewidth', 2);
v = axis;
hold on;
pv1 = plot([dog3, dog3], [v(3), v(4)], 'k', [dog4, dog4], [v(3), v(4)], 'k',[dog5, dog5], [v(3),
v(4)], 'm' );
set(pv1, 'linewidth', 1.5);

t1 = title('SHORT EXPERIMENTAL PULSE');
set(t1, 'fontsize', 12);
set(t1, 'fontweight', 'bold');

set(get(ax(1),'Ylabel'),'string','Acceleration (g)');
set(get(ax(1), 'Ylabel'),'fontsize', 12);
set(get(ax(2),'Ylabel'),'string','Displacement (mm)');
set(get(ax(2), 'Ylabel'),'fontsize', 12);
Lx1 = xlabel('Time (sec) ');
set(Lx1, 'fontsize', 12);
grid;
```

File freeFallVelocity.m

```
%This macro solves for free fall velocity and displacement displacement analysis
%and calls the pre-contact simulink model
%Written by M Minett

%clear all;
function [sPlatenAcc, sPlatenVel, sPlatenDisp, stim] = f(td, data, theorDisp, theorVel, index,
statStiff, fpath, fname)


global G filte cushArea platenMass dropHeight cushLength cushWidth cushThickness
numLayers fOrder cutOff ec samp stest pg kg stiffness cushdes rho fo


%Index has element numbers for ShortPulseStart VoltStart, MaxAccel,
   %VoltFinish, ShortPulseFinish zeroVel, reboundVel

expDispP = data(:,4)/1000;
test = expDispP(index(2));
%expDispC = fullData(:,3);
y = 0;
%platenMass = 2.494;
%platenArea = 0.168 * 0.168;
rho = 101.235 / (0.287 * (273 + 20));
%g = 9.8065;
%dropHeight = 0.2;
Cd = 1.0;
%len = 0.168;

tim = [td(index(1)),td(index(2))];


%Simulation before impact

if statStiff == 0

   sim('preCompressNoStatic', tim);
else
   sim('preCompressStatic', tim);
end

sPlatenAcc = sPlatenAcc - sPlatenAcc(1);

stim = tout(end);

platDispSlopeExp = (data(index(1), 4) - data(index(2),4))/(tim(end)- tim(1))/1000;
platDispSlopeSim = (sPlatenDisp(end)-sPlatenDisp(1))/(tout(1) - tout(end));
```

```
%Graphing of Simulation Data Prior to Impact
%sPlatenDisp = sPlatenDisp - sPlatenDisp(1);
pname = 'Pre-Contact dynamics - Simulated';
figure(30);
set(30, 'position', [100,100,900,500]);
%set(gcf, 'color', 'c');
set(30, 'name', pname);
set(30, 'numbertitle', 'off');
set(30, 'PaperOrientation', 'landscape');
set(30, 'PaperUnits', 'centimeters');
set(30, 'PaperType', 'A4');
set(30, 'PaperPositionMode', 'manual');
set(30, 'PaperPosition', [1.0 1.0,  28.5 18.5]);

subplot(2,2,1);
p1 = plot(tout*1000, sPlatenAcc/G, 'b');
set(p1, 'linewidth', 1.5);
lx1 = xlabel('Time (ms)');
set(lx1, 'fontweight', 'bold');
ly1 = ylabel('Simulated Platen Acceleration g');
set(ly1, 'fontweight', 'bold');
grid;

subplot(2,2,2);
p2 = plot(tout*1000, sPlatenVel, 'm');
lx2 = xlabel('Time (ms)');
set(lx2, 'fontweight', 'bold');
set(p2, 'linewidth', 1.5);
ly2 = ylabel('Simulated Platen Velocity m/sec');
set(ly2, 'fontweight', 'bold');
grid;

subplot(2,2,3);
p3 = plot(tout*1000, sPlatenDisp*1000,  'r');
set(p3, 'linewidth', 1.5);
lx3 = xlabel('Time (ms)');
set(lx3, 'fontweight', 'bold');
ly3 = ylabel('Platen Displacement mm');
set(ly3, 'fontweight', 'bold');
grid;

drop_h = [num2str(dropHeight*1000)];
simAccContact = [num2str(sPlatenAcc(end)/G)];
simAccContact(end) = [];
cush_area = [num2str(cushArea)];
cush_area(7:end) = [];
cush_width = [num2str(cushWidth*1000)];
cush_length = [num2str(cushLength*1000)];
```

```
cush_thick = [num2str(cushThickness*1000)];
test_mass = [num2str(platenMass)];
num_layers = [num2str(numLayers)];

 k = 1;
 subplot(2,2,4);
    set(gca,'Visible','Off');
    set(gca,'FontSize',10);
    inc = 0.09;

    t2 = text(0,1-(k-1)*inc, ['Pre-Contact Simulated Platen Dynamic Data']);
    set(t2, 'fontsize', 12);
    set(t2, 'fontweight', 'bold');
    k = k + 1;

    pname = ['File  ', fpath(21:end), fname, ' Sample - ',samp];
    t1 = text(0,1-(k-1)*inc, pname);
    k = k + 1;
    pname = ['Cushion Type - ', cushdes];
    t1 = text(0,1-(k-1)*inc, pname);
    k = k + 1;
    pname = ['Cushion Dimensions - ', cush_length,' x ', cush_width,' x ', cush_thick, ' mm'];
    t1 = text(0,1-(k-1)*inc, pname);
    k = k + 1;
    pname = ['Cushion Area = ', cush_area, 'sq m'];
    t1 = text(0,1-(k-1)*inc, pname);
    k = k + 1;
    if cushLength ~= cushWidth
        pname = ['Flute Orientation  ', fo];
        t1 = text(0,1-(k-1)*inc, pname);
        k = k + 1;
    end
    pname = ['End Conditions - ', ec];
    t1 = text(0,1-(k-1)*inc, pname);
    k = k + 1;
    pname = ['No of Layers = ', num_layers];
    t1 = text(0,1-(k-1)*inc, pname);
    k = k + 1;
    pname = ['Platen Mass = ', test_mass, ' kg'];
    t1 = text(0,1-(k-1)*inc, pname);
    k = k + 1;
    pname = ['Drop Height = ', drop_h, ' mm'];
    t1 = text(0,1-(k-1)*inc, pname);
    k = k + 2;
    pname = ['Simulated Acceleration at Contact = ', simAccContact, ' g'];
    t1 = text(0,1-(k-1)*inc, pname);
```

```
%Graphing of Simulation and Experimental Data Prior to Impact
sPlatenDisp = sPlatenDisp - sPlatenDisp(1);
pname = 'Pre-Contact dynamics - Experimental  and Simulated';
figure(31);
set(31, 'position', [100,100,900,500]);
%set(gcf, 'color', 'c');
set(31, 'name', pname);
set(31, 'numbertitle', 'off');
set(31, 'PaperOrientation', 'landscape');
set(31, 'PaperUnits', 'centimeters');
set(31, 'PaperType', 'A4');
set(31, 'PaperPositionMode', 'manual');
set(31, 'PaperPosition', [1.0 1.0,  28.5 18.5]);

subplot(2,2,1);
p1 = plot(tout*1000, sPlatenAcc/G, td(index(1):index(2))*1000, data(index(1):index(2),1)/G,
'r');
set(p1, 'linewidth', 1.5);
lx1 = xlabel('Time (ms)');
set(lx1, 'fontweight', 'bold');
ly1 = ylabel('Platen Acceleration g');
set(ly1, 'fontweight', 'bold');
grid;

%subplot(2,2,4);
%p2 = plot(tout*1000, sPlatenVel, td(1:index(2))*1000, theorVel(1:index(2)), 'r');
%lx2 = xlabel('Time (ms)');
%set(lx2, 'fontweight', 'bold');
%set(p2, 'linewidth', 1.5);
%ly2 = ylabel('Platen Velocity m/sec');
%set(ly2, 'fontweight', 'bold');

subplot(2,2,2);
p3 = plot(tout*1000, sPlatenDisp*1000, td(index(1):index(2))*1000,...
(expDispP(index(1):index(2))- expDispP(index(1)))*1000, 'r');
%td(1:index(2))*1000, yd(1:index(2)), ':g');
set(p3, 'linewidth', 1.5);
lx3 = xlabel('Time (ms)');
set(lx3, 'fontweight', 'bold');
ly3 = ylabel('Platen Displacement mm');
set(ly3, 'fontweight', 'bold');
grid;



 %Display data
```

```
drop_h = [num2str(dropHeight*1000)];

%contact_vel = [num2str(v0)];
 %   calc_init_vel(end) = [];
  %  contact_deflect = [num2str(ydmin*1000)];
 %   max_deflect(end-1:end) = [];
 simAccContact = [num2str(sPlatenAcc(end)/G)];
 simAccContact(end) = [];
 expAccContact = [num2str(data(index(2),1)/G)];
 expAccContact(end) = [];
 %   vel_max_acc(end) = [];
 %   static_stress = [num2str(statstress)];
 %   static_stress(end) = [];
 %   dynamic_init_vel = [num2str(vd(index(2)))];
 cush_area = [num2str(cushArea)];
 cush_area(7:end) = [];
 cush_width = [num2str(cushWidth*1000)];
 cush_length = [num2str(cushLength*1000)];
 cush_thick = [num2str(cushThickness*1000)];
 test_mass = [num2str(platenMass)];
 %dynamic_init_acc = [num2str(ad(index(2)))];
 num_layers = [num2str(numLayers)];

 k = 1;
 subplot(2,2,3);
    set(gca,'Visible','Off');
    set(gca,'FontSize',10);
    inc = 0.09;

    t2 = text(0,1-(k-1)*inc, ['Pre-Contact Platen Dynamic Data']);
    set(t2, 'fontsize', 12);
    set(t2, 'fontweight', 'bold');
    k = k + 1;
    t2 = text(0,1-(k-1)*inc, ['Simulation (Blue) Vs Experimental (Red)']);
    set(t2, 'fontsize', 12);
    set(t2, 'fontweight', 'bold');
    k = k + 1;
    pname = ['File  ', fpath(21:end), fname, ' Sample - ',samp];
    t1 = text(0,1-(k-1)*inc, pname);
    k = k + 1;
    pname = ['Cushion Type - ', cushdes];
    t1 = text(0,1-(k-1)*inc, pname);
    k = k + 1;
    pname = ['Cushion Dimensions - ', cush_length,' x ', cush_width,' x ', cush_thick, ' mm'];
    t1 = text(0,1-(k-1)*inc, pname);
    k = k + 1;
    pname = ['Cushion Area = ', cush_area, 'sq m'];
    t1 = text(0,1-(k-1)*inc, pname);
    k = k + 1;
    if cushLength ~= cushWidth
```

```
    pname = ['Flute Orientation  ', fo];
    t1 = text(0,1-(k-1)*inc, pname);
    k = k + 1;
end
pname = ['End Conditions - ', ec];
t1 = text(0,1-(k-1)*inc, pname);
k = k + 1;
pname = ['No of Layers = ', num_layers];
t1 = text(0,1-(k-1)*inc, pname);
k = k + 1;
pname = ['Platen Mass = ', test_mass, ' kg'];
t1 = text(0,1-(k-1)*inc, pname);
k = k + 1;
pname = ['Drop Height = ', drop_h, ' mm'];
t1 = text(0,1-(k-1)*inc, pname);
k = k + 1;
pname = ['Simulated Acceleration at Contact = ', simAccContact, ' g'];
t1 = text(0,1-(k-1)*inc, pname);
k = k + 1;
pname = ['Experimental Acceleration at Contact = ', expAccContact, ' g'];
t1 = text(0,1-(k-1)*inc, pname);
k = k+1;
pname = ['Experimental Platen Slope ', num2str(platDispSlopeExp), ' m/s'];
t1 = text(0,1-(k-1)*inc, pname);
k = k+1;
pname = ['Simulated Platen Slope ', num2str(platDispSlopeSim),' m/s'];
t1 = text(0,1-(k-1)*inc, pname);
```

Software Graphics User Interface